RI/RD79-278

NASA

FINAL REPORT

HIGH-PRESSURE LOX/CH_4 INJECTOR PROGRAM

by

D. B. Wheeler and F. M. Kirby

Rockwell International

Rocketdyne Division

Prepared for

NATIONAL AERONAUTICS AND SPACE ADMINISTRATION

SEPTEMBER 1979

George C. Marshall Space Flight Center

Contract NAS8-33206

FOREWORD

The High-Pressure LOX/CH_4 Injector Program was conducted at the Rocketdyne Division of Rockwell International under Contract NAS8-33206. Mr. Rex Bailey, NASA-Marshall Space Flight Center, was the Project Manager. At Rocketdyne, Mr. Frank Kirby was Program Manager and Mr. David Wheeler was the Project Engineer.

The study effort was supported by the following team of technical specialists at Rocketdyne:

I. Kaith
V. Jaqua
W. Wang
K. Held

CONTENTS

ILLUSTRATIONS

TABLES

INTRODUCTION

Future launch vehicles may have need of high-bulk-density propellant systems. The use of high-density hydrocarbon fuels, in combination with liquid oxygen, will permit more optimized vehicle designs as a result of the smaller fuel tanks. The use of methane for this application has received considerable attention lately because of its excellent regenerative cooling characteristics, allowing high chamber pressure (3000 to 4000 psia) operation without the aid of advanced cooling enhancement techniques. Methane also has high performance relative to other hydrocarbon fuels, and is the least likely to exhibit any carbon deposition problem. These and other features such as temperature compatibility with the LOX and low carbon dioxide content in the combustion products makes CH_4 an attractive fuel for future launch vehicle applications.

Recent advanced booster engine system studies have indicated several areas where technology demonstrations are required. These areas are LOX/CH_4 injector performance, combustion stability, heat transfer, and CH_4 regenerative cooling characteristics. The injector furnished as the principal output of this program will be combined with existing chambers and facilities to form the means of accomplishing these technology demonstrations.

This program was subdivided into two major tasks plus reporting, hardware, and drawing delivery tasks. Task I was devoted to performing a preliminary design and analysis evaluation of two injector types (coaxial and impinging elements) for LOX/CH_4 high-pressure operation, and selecting one concept. with MSFC approval for fabrication. In Task II, the detailed fabrication drawings for the selected injector were produced. Supporting design analysis was conducted in the areas of heat transfer and stress. The finalized injector was fabricated, flow tested, cleaned, and delivered to MSFC for a subsequent hot-firing test program, and a recommended test matrix and procedure also was provided. The injector, four sets of seals, five complete sets of the injector fabrication drawings, the recommended test matrix, and procedures were delivered to MSFC.

TASK I - ANALYSIS AND PRELIMINARY DESIGN

The overall objective of Task I was to select, with NASA approval, an injector design concept for input to Task II.

Injector Concept Study

This portion of the task was primarily concerned with identifying the injector design configurations to be analyzed, flowrates and operating conditions, and basic element sizes and arrangements.

This task was initiated by establishing the injector operating conditions for the planned testing. Initial tests will be conducted at approximately 1800 psia with a calorimeter chamber. The 1800-psia chamber pressure limit is imposed due to the available water coolant supply pressure. Subsequent testing with a regenerative chamber will be conducted at 3000-psia chamber pressure. The flowrates and operating conditions established for the design of the injector at these two operating points are presented in Table 1.

TABLE 1. DESIGN REQUIREMENTS

Chambe. Pressure, psia	1800	3000
Mixture Ratio	3.5	3.5
Chamber Throat Area, $in.^2$	8.60	8.60
C*, ft/sec	5918	5947
$\dot{w}$ Oxidizer, lb/sec	65.5	108.7
w Fuel, lb/sec	18.7	31.0
Oxidizer Density	70.0 lb/ft^3	
Fuel Density* at 3400 psia and 77 F	11.48 lb/ft^3	
Fuel Density* at 3000 psia and 77 F	10.13 lb/ft^3	
fuel Density* at 1800 psia and 77 F	6.05 lb/ft^3	
Oxidizer Maximum Interface Pressure	4200 psia	
Fuel Maximum Interface Pressure	3800 psia	

*Short extrapolations to other temperatures and pressures can be made by $\rho = P/0.824\ RT$

Based on the results of preliminary screening, two basic injection element configurations were proposed for in-depth evaluation during the program. The selected injection concepts were: (1) a recessed coaxial configuration and (2) an unlike impingement configuration.

Performance Analysis

Two injector concepts, an unlike triplet impingement configuration and a recessed coaxial configuration were analyzed to determine their performance potential for high-pressure LOX/CH_4 operation. An energy release efficiency of 97% or better was required. The operating conditions to be considered include a nominal chamber pressure at 3000 psia with possible operation down to 1800 psia.

Excellent success has been achieved in the past with the coaxial injector using gas-liquid propellants. Engines like the J-2 and the space shuttle main engine are the examples. Both use liquid oxygen and gaseous hydrogen or partially reacted hot gas (O_2-H_2). With the use of gaseous methane rather than hydrogen, a significant difference will be experienced in the gas density under high pressure. Previous work indicates that the coaxial injector relies on the large relative velocity difference to produce high performance. To achieve the high performance level, the injector gas flow area for the annulus must be very small due to the high methane gas density. An analytical Coaxial Injector Combustion Model (CICM) is utilized to analyze and determine the design requirements for a high-performing coaxial LOX/CH_4 injector.

The triplet element configuration also has been chosen to be a candidate representing the impinging-type injector. For the triplet, a proper balance between the flow area and the momentum can be achieved and is significant in achieving high performance. The Standardized Distributed Energy Release (SDER) model is utilized to analyze such an injector.

The two models (CICM and SDER) differ only in their formulations for the atomization process. The CICM characterizes the process by jet stripping and a drop-size correlation. The coefficients are determined based on the LOX/H_2 test

results. The SDER has a Liquid Injector Spray Pattern (LISP) subprogram that computes both the mixing and the atomization process based on previous cold flow experiments. Both models are extended to include the properties of the high density gaseous methane.

The combustion stability is analyzed after the performance evaluation. The generalized Priem's method is applied. The results are the stability index for each injector and can be used for comparison purposes. Individual combustion stability evaluation and the need for stability aids will then be based on similar established engines.

The performance of the triplet injector is discussed first, followed by the coaxial injector. The combustion stability analysis for both candidates is then presented in the following section.

Triplet Injector. The impinging-type injector has the inherent feature that the injection mechanics promote mixing as well as atomization. Figure 1 shows the spray mass flux from a single triplet injector element. The outer two jet streams impinge on the inner stream and create an inner spray fan shaped like a dumbbell, as illustrated in Fig. 1. The stream from the outer orifices will form a conventional fan as a result of the momentum exchange. Highest mixing performance is achieved when the fuel flux and the oxidizer flux are uniform within the spray fan prior to initiation of combustion. For the LOX-methane injector, the gaseous methane is assigned to the outer orifices due to its lower density and, thereby, more flow area is necessary. Both momentum and geometric balance are prerequisite for good mixing and atomization. If the outer stream's momentum is much greater than the inner stream momentum (this usually entails smaller outer orifices than the inner one), the outer streams can penetrate into the center stream. As a consequence, two heavily concentrated oxidizer mass flowfields will be produced at both ends of the fan and the mixing is therefore degraded. Conversely, if the outer stream's momentum is less than the center one, a spray fan will be formed but not as wide. As a result, the mass flux will be more concentrated and the mixing is also poor.

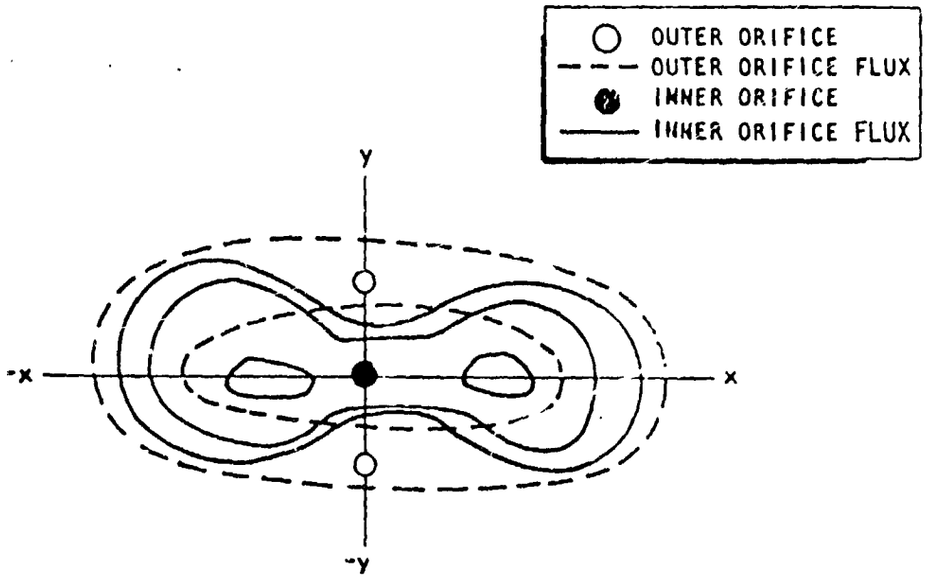

Figure 1. Spray Mass Flux From Single Triplet Injector Element

These mixing studies are based on cold-flow injection element test data. At present, there is no gas-liquid cold flow data available for the triplet injector; therefore, the performance analysis conducted in this study is based on liquid-liquid cold flow data. Since the methane is actually a very dense gas and the fluid continum equations hold for both the liquid and the gas before the impingement, the analysis is considered valid. The fluid properties influence on the equations of motion is limited by the viscosity alone.

After the impingement and spray mixing phase, the liquid jet is deformed and becomes a spray fan. The processes important to the spray fan involve the momentum exchange and the stability of the resulting flow. For the gas, similar processes will occur except that there are no droplets formed. However, they can be viewed as a low-density, noncontinuum spray. The momentum exchange will force the gas flow to change direction and form a fan, as in the case for the liquid.

The error incurred in this formulation extrapolation is small if the spray properties are the actual gas properties, i.e., low gas density and viscosity, and zero surface tension. To carry a step further, the extrapolation correlates well with a gas-solid-gas triplet injection element in Rocketdyne's pulverized coal cold-flow experiments. This provides some credibility to the technique used for analyzing the gas-liquid mixing.

The spray mixing model formulation is essentially the Liquid Injector Spray Pattern (LISP) subprogram from the Standardized Distributed Energy Release (SDER) program. The methane gas properties are inputs to the model. The technique uses a standard JANNAF collection plane. Radial and angular mesh points are established as the collection points which sum up each propellant flux. The mixing efficiency is then computed by the following equation:

$$\eta c^* \text{ mx} = \frac{\sum_i c^* (MR_i)\ \dot{w}_i}{c^* (\text{mr})\ \dot{w}_T}$$

where

MR = mixture ratio

$\dot{w}$ = flowrate

The summation is over all the mesh points which form a representative chamber section.

It is a well-established fact that, for a given total flow, the mixing efficiency is proportional to the number of elements. In general, the design also is limited by the manufacturing ability, the chamber compatibility, and the combustion stability. For the current injector design effort, achieving the high performance is primary, and approximately 104 elements are believed to be the maximum number for the 5.66-inch chamber. The element sizing can then be determined by the injector pressure drop which is expressed as $\Delta P/P_c$. Certain minimum values have been determined based on the past experiences to avoid the feed system-coupled combustion instability. In this study, it is assumed that upstream orifices can be provided to meet the necessary pressure drop requirements. The performance analysis is conducted with various injection velocities and the corresponding orifice diameters.

Figure 2 shows the c* mixing efficiency as a function of the fuel-to-oxidizer injection velocity head ratio. It was discovered during previous cold-flow testing in company-funded programs and related contracts that the ratio of fuel to oxidizer velocity would be the most significant factor. From the analysis, the LOX injection velocity also is a significant factor, as the velocity obviously determines the orifice diameter and the geometric imbalance.

Three LOX injection velocities are chosen in Fig. 2. The results indicate that the optimum mixing (99.3%) can be achieved with a LOX velocity of 127 ft/sec and a fuel velocity of 446 ft/sec. It then becomes the nominal design point for the LOX-methane triplet injector.

There are other distinct features evident from the analytical results:

1. The maximum mixing efficiency points for the lower LOX injection velocity occur at a higher velocity head ratio. It indicates the mixing efficiency will not be significantly reduced at the lower pressure level at which the gas injection velocity will remain constant but the liquid velocity is reduced. A 98.2% mixing efficiency is predicted for the low chamber pressure case.

2. Both the momentum and the geometric effects are reflected in the curves. On the left side of the maximum efficiency points, the drop can be attributed to the momentum effect, and the right side the geometric imbalance.

3. The curvature is much more pronounced for the high LOX injection velocity, indicating a narrow region of operations. Both the momentum and the geometric balances have less freedom to vary because the diameter changes at the square root of the flow area, while the velocity changes linearly.

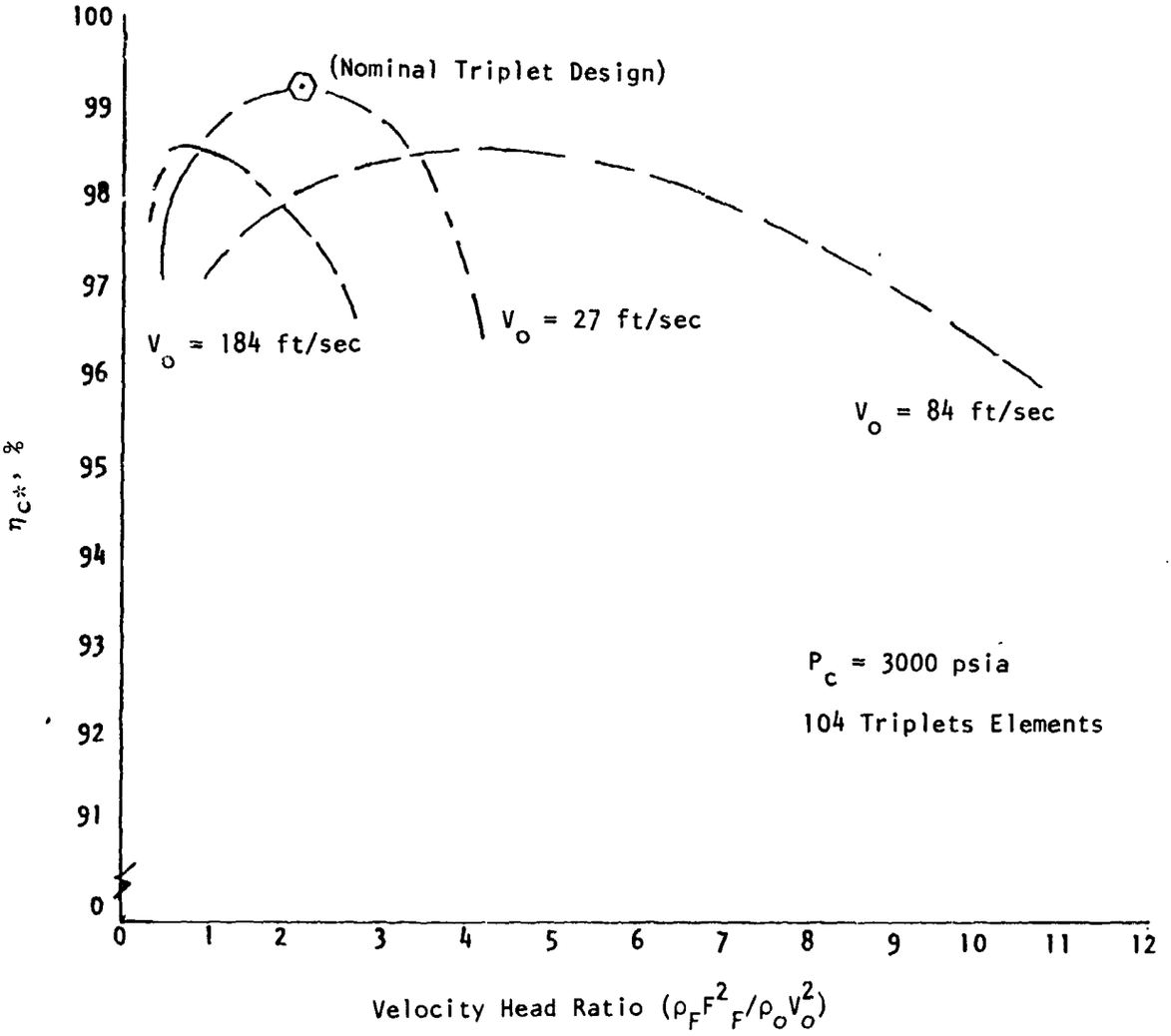

Figure 2. Mixing Efficiency of the Triplet Injector

The LOX droplets formed for all the cases studied thus far have the mass median dropsize ($\overline{D}$) at less than 0.005 inch. A rapid and complete vaporization is inevitable. Figure 3 is a plot of the vaporization efficiency versus $\overline{D}$ in a 14-inch chamber. The Rosin-Rammler distribution is assumed in each case and a 100% combustion (ηc^* VAP = 100%) is achieved in a matter of 0.5 inch from the impingement point. Therefore, Fig. 2 can be regarded as the η_{c^*} overall since η_{c^*} overall is a product of the mixing and the vaporization efficiency. A complete combustion also is expected for the lower chamber pressure.

Coaxial Injector. While the unlike, impinging-type injector for a gas-liquid propellant combination suffers from the geometric and momentum imbalance, the concentric axial injector takes advantage of that condition since high gas injection velocity results in maximizing the atomization and promotes mixing in the shear layer. However, the coaxial element analytical model (CICM) used for performance analysis does not include the mixing description.

The CICM model does not include a mixing analysis since the process is rather complex; specific cold-flow tests have been performed to obtain the mixing efficiencies. The CICM is used to analyze the combustion processes assuming 100% mixing efficiency. More discussion on mixing will be presented after the discussion on the combustion analysis.

As mentioned above, the CICM describes the injector and recessed element effects and assuming 100% mixing, the subsequent droplet atomization, burning, and the flow dynamics of gas-liquid coaxial elements. At the end of the potential core of the liquid jet, the program reverts to the standard stream tube combustion subprogram for the continued vaporization process in the combustion chamber. In the stream tube combustion subprogram, the improved droplet heating model includes real gas effects.

In the injector, the model analyzes the cup region which is formed by recessing the liquid injection post. The phenomenon inside the cup is like a confined jet if the flow is allowed to develop fully. The recessed cup has been found to enhance both mixing and atomization. During the study, the cup burning effect

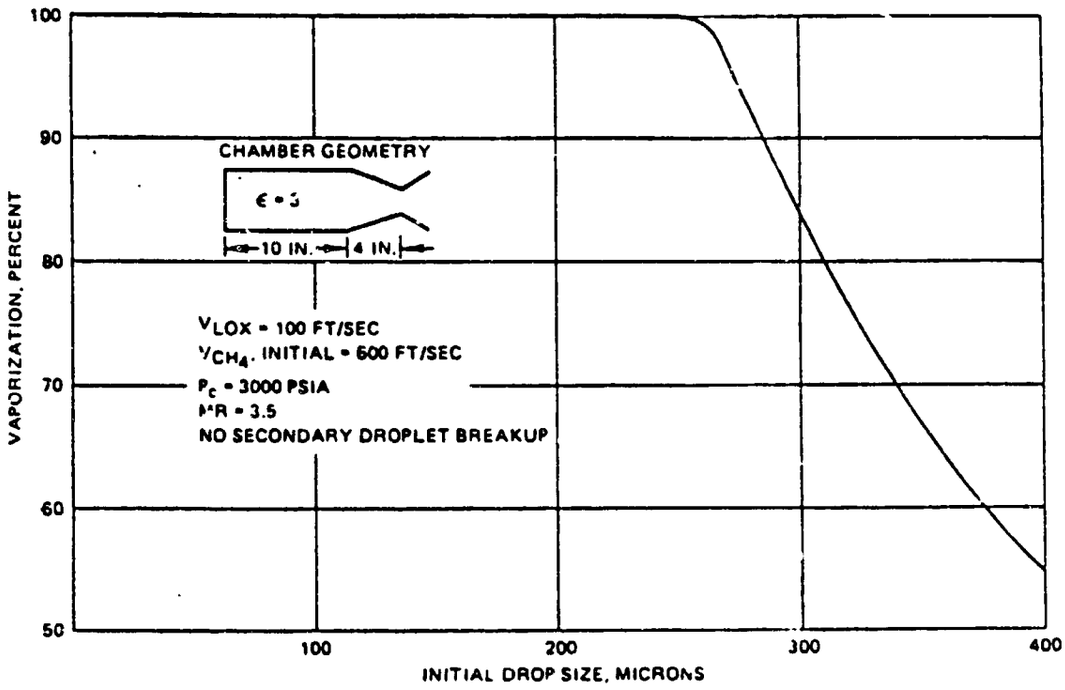

Figure 3. Percent Vaporization of LOX Droplets vs Initial Size

as well as the number of elements, the element configuration and the injection velocity are investigated. Figure 4 shows the results for two injectors with the same element configuration which has a cup recess of one liquid injection post ID. The lower LOX injection velocity is for 100 elements and the other for 89 elements. In each case, the efficiency increases linearly with the methane injection velocity.

The slope of each curve is different as the efficiency is actually a function of the velocity ratio. For the same velocity ratio, the higher LOX velocity will have a larger differential from the gas velocity but the effect on the performance is small for the cases studied. For instance, for the same efficiency at 97%, the methane injection velocity is 470 ft/sec and the LOX injection velocity is 112 ft/sec. The ratio is computed to be 4.2. It only increases to 4.3 for the case with fewer elements. Therefore, reducing the number of elements or their size does not affect the vaporization efficiency as long as the velocity ratio is maintained. From the design point of view, fewer number of elements, with the same total flow area, results in better tolerance for the concentric annular gap, but may result in a decrease in mixing efficiency. Conversely, more elements with reduced size improve the mixing but may pose design difficulties.

The effect of post recess is shown in Fig. 5. Physically, the gaseous annular jet will maintain its velocity in the cup region prior to being admitted into the chamber. Hence, more of the kinetic energy can be utilized for the stripping process. In addition, the gas velocity will result in a high convective film coefficient. In the chamber, the gas tends to slow down to fill the chamber. The incorporation of the cup essentially sustains the momentum and energy exchange between the gas and the liquid for a longer time and, thus, improves the overall performance.

The gain realized by a recessed cup is indeed significant when the design is limited by a maximum gas velocity due to gap size; when the gas velocity is designed for 488 ft/sec and the LOX injection velocity is 112 ft/sec the η_{c*}, vaporization can be increased from 98 to 100% when the cup recess is lengthened from one to 1.3 times ID. The annular gap for the element is only 0.014 inch. Higher gas velocity is possible only if significant design tolerance problems can be resolved.

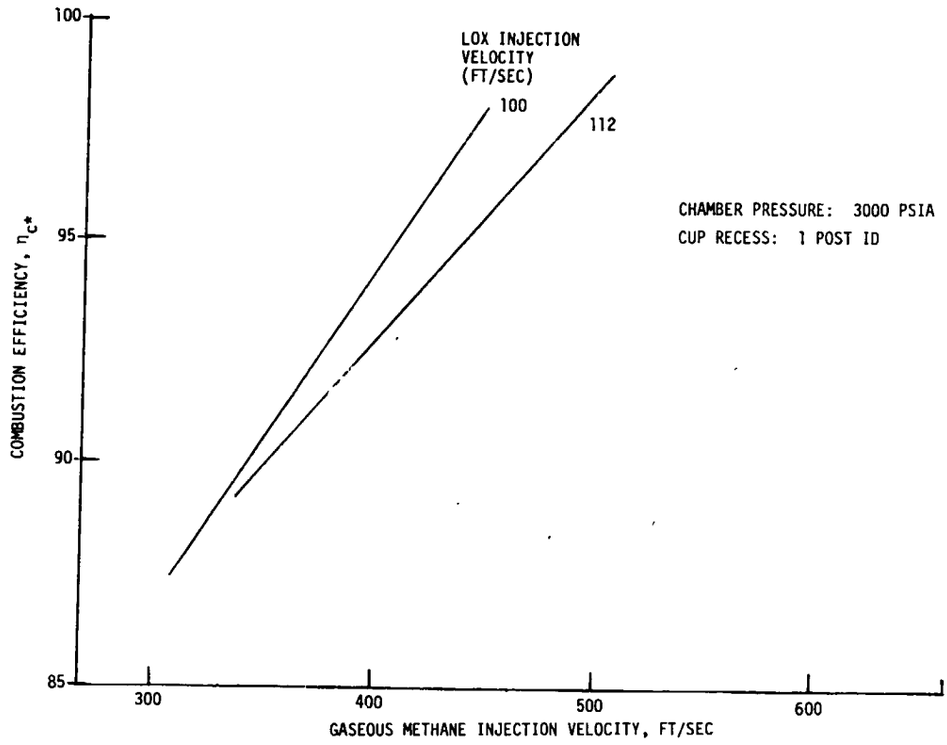

Figure 4. Vaporization Efficiency ($\eta_{c^* \text{ vap}}$) vs Gaseous Methane and Liquid Oxygen Injection

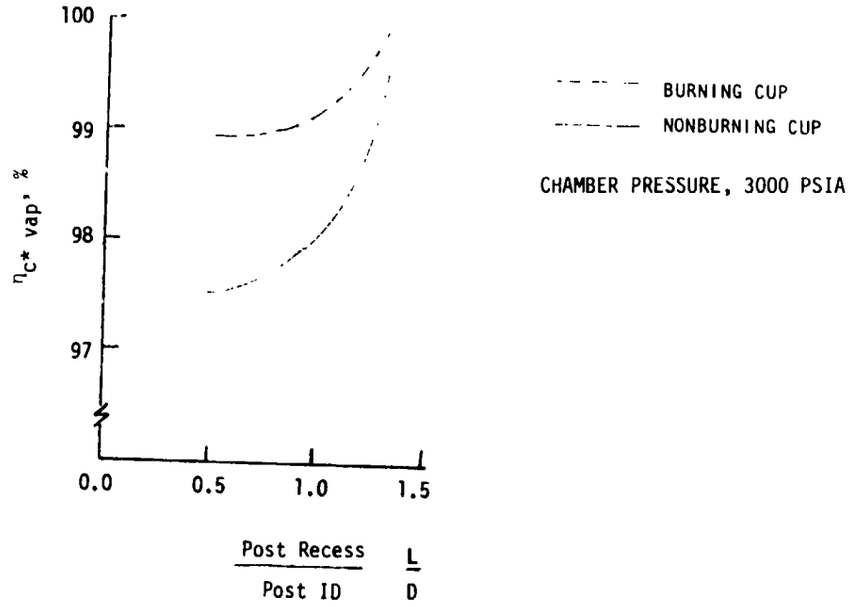

Figure 5. Vaporization Efficiency ($\eta_{c^* \text{ vap}}$) vs Injection Post Recess

Past experiences have shown that burning can occur in the cup recess and is classified as a burning cup. When the burning cup model is used, the performance is increased slightly. The gain is attributed to the accelerating combustion gas as a result of the energy release. It should be noted that, due to the lack of LOX-methane combustion data, it is difficult to predict the occurrence of cup burning. Furthermore, based on the Flox-Methane Injector Development Program (Ref. 1), no cup burning was ever experienced at a post recess up to 3 diameters in a single coaxial element hot-fire testing. Therefore, cup burning may not occur and, more importantly, the increase in efficiency diminishes at a post recess of 1.3 times its ID.

Coaxial Mixing. Presently, there is no proved analytical technique to predict the mixing performance for a coaxial injector. Specific cold-flow tests using air and water can be used only for mixing study in a limited scope. A major reason lies with the turbulent transport process in the shear layer for two parallel flows.

Almost all the shear layers are turbulent. The shear stress, T_{turb}, is expressed as:

$$T_{turb} = \rho\Sigma\frac{\delta\mu}{\delta r}$$

where

ρ = fluid density
Σ = kinematic eddy viscosity
μ = local velocity

It can be seen that a large velocity gradient is favorable to the mixing. The large shear generates the turbulent eddies which enhance the transport process between the two flows.

The kinematic eddy viscosity, Σ, however, is a unique quantity instead of the usual fluid properties. Up to now, it is not accurately derived. Therefore, no generalized cold-flow data can be established. Nevertheless, it is believed

that since it is a measure of the mass and momentum transport, it must depend on the mass flow and momentum of the two flows. An attempt is made to utilize previous cold-flow data to evaluate the mixing performance of the coaxial injector.

It should be noted that, based on our experiences, the cold-flow predictions are within 3% below the hot-fire results. Part of the discrepancy is attributed to the fluid properties; another is due to the far-field turbulent diffusion mixing. Unfortunately, neither one can be improved upon in the cold-flow tests. The increment can be included in the mixing analysis if the chamber geometry, the injection pattern, and the propellant properties are not drastically different. This is illustrated by comparing some experimental results from a FLOX/CH_4 program (Ref. 1) and the predicted results for the LOX/CH_4 coaxial injector design.

Table 2 lists the operating conditions and the element configurations for the flox-methane coaxial injector and a design resulting from the LOX-methane combustion analysis. Note that if the latter is allowed to operate at a chamber pressure less than 500 psia, the liquid injection velocity will be equal to the design condition for the flox-methane injector. The density of liquid oxygen is closer to the cold-flow simulant, water, than FLOX. The gas densities are the same; therefore, if the gas velocities are matched, the same mixing efficiency should be realized.

TABLE 2. COAXIAL ELEMENT CONFIGURATIONS AND OPERATING CONDITIONS FOR GASEOUS FLOW/METHANE AND GASEOUS LOX/METHANE INJECTOR

	Propellants	
	FLOX/CH_4*	LOX/CH_4*
Chamber Pressure, psia	512	500
Post Id, inch	0 136	0.17
Post OD, inch	0.146	0.19
Element Diameter, inch	0.182	0.218
Gas Density, lb/ft^3	1.8	10.3
Gas Velocity, ft/sec	290	490
Liquid Density, lb/ft^3	89	70
Liquid Velocity, ft/sec	20	113
ηc^* Mix predicted, %	97.7**	~97.7
ηc^* Hot Fire, %	98.4	TBD

*Gaseous
**Predicted from cold-flow data (water/air)

Based on the past experiences with the gas-liquid coaxial injectors, the reduction of gas to liquid injection velocity ratio will degrade the vaporization efficiency. Conversely, a higher gas velocity should increase the velocity gradient and also enhance the mixing. Figure 6 illustrates the predicted gas velocity effect on the mixing uniformity, as noted. The mixing efficiency for the LOX/CH_4 coaxial injector is predicted to be at least 97% at 500 psia chamber pressure, as shown in Table 2.

To carry at step further, the mixing efficiency always increases at the higher power level (higher operating pressure) based on all of the past experiences with the coaxial injectors. One must deduce that the mixing efficiency for the LOX-methane injector will be 97.7% or better at the two operating conditions (1800 and 3000 psia). Overall, the c* efficiency is above the required 97% if complete vaporization is achieved, which is predicted from CICM for the post recess of 1.3 times post ID for both chamber pressures. The coaxial injector will meet the contract performance requirement.

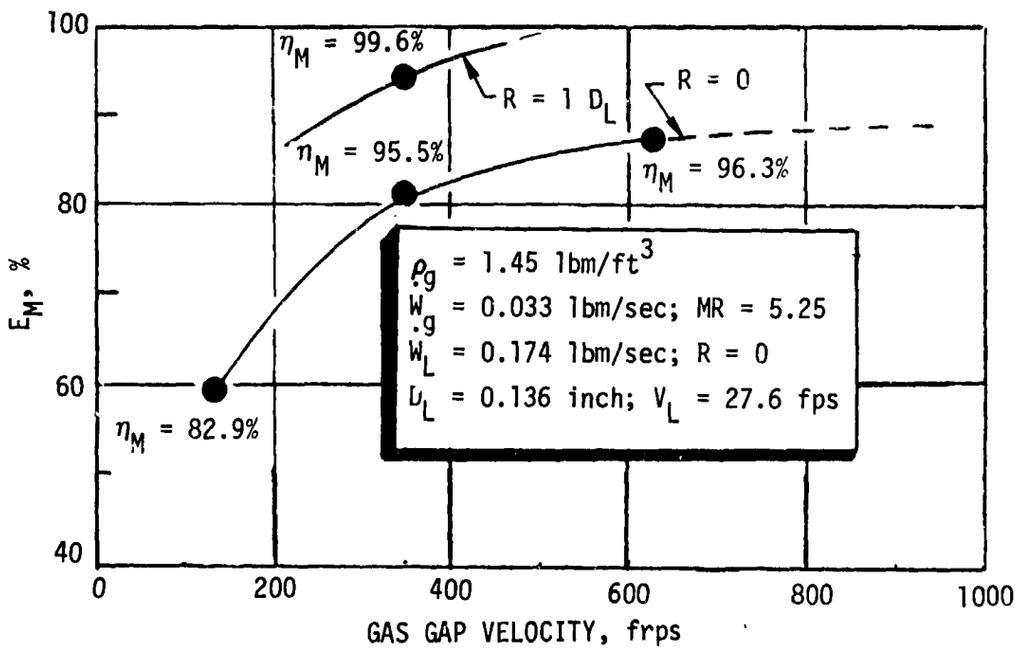

Figure 6. Effects of Gas Gap Velocity on Mixing Uniformity (E_M) for Cup Recess (R) = 0 and 1

Thus, in summarizing the performance evaluation of the coaxial element, it is noted that with a recessed cup design (recess of 1.3 times post ID) vaporization is predicted to be 100% and that overall performance will be controlled by the mixing efficiency; mixing efficiency is predicted to be 97.7% or better and, thus, overall c* efficiency should exceed 97%.

Combustion Stability

Among the various types of instability in rocket engine operation, the high frequency mode that is characterized by the chamber acoustics has always been most damaging. Combustion instability suppression will generally affect the injector design and the performance adversely. Therefore, the ability to sustain a stable combustion can influence the selection of the injector design.

The generalized Priem stability criterion is commonly used to predict the occurrence of the acoustic-coupled combustion instability in rocket combustors. The method can predict the relative merit or the trend of stability if data from similarly established engines are available for comparison.

Priem Analysis. The Priem-type combustion instability model assumes that the droplet vaporization is the rate-controlling process. A critical overpressure, A_p, is determined (using the model), which represents the amplitude of an oscillation that will neither grow nor decay. Thus, the magnitude of A_p is a measure of the stability of the engine (i.e., the larger the A_p, the more inherently stable the engine). The most important combustor parameters are the burning rate, λ, a relatively velocity term (gas to droplets), $\Delta V'$, and a mass accumulation term, MAP. These parameters are defined as follows:

$$\lambda = \frac{\Delta MR}{CR}$$

$$\Delta V' = \frac{|V_g - V_\ell|}{\alpha}$$

$$MAP = \frac{M_{vap_o}}{\dot{w}_{inj_o} \tau_w} = \frac{\dot{w}_{drop}}{\dot{w}_{gas}} \frac{\dot{w}_{gas} \, w_{gas}}{\Delta\dot{w} \, \dot{w}_{gas}} \frac{1}{\tau_w}$$

where

ΔM	=	the fraction of total propellant burned in the axial increment of chamber considered
R	=	chamber radius
CR	=	chamber contraction ratio
V_g	=	gas velocity
V_ℓ	=	droplet velocity
a	=	local acoustic velocity
τ_w	=	the period of the acoustic mode to be considered
M_{vap_o}	=	mass concentration of unburned propellants
$\dot{w}_{inj_o}$	=	product of total mass flux with ΔM

Generalized neutral stability curves, plotted as A_p versus λ, have been previously generated at Rocketdyne as a function of $\Delta V'$ and MAP. Thus, the Priem analysis, in essence, provides an estimate of the nondimensional overpressure (A_p) required for neutral stability once values of the parameters (λ, $\Delta V'$ and MAP) have been calculated from a steady-state combustion model. A_p (of a design) is then used as an index for comparison to engines of demonstrated stability characteristics.

Results. Based on the results from the combustion models, the triplet injector is predicted to be the higher performing injector. The jets, impingement produces extremely fine sprays; the burning process is fast and complete. The coaxial injector is less efficient in atomization due to the slow momentum exchange which is characterized by the stripping process in the shear flow. As a result, the vaporization process is moderated and not as vigorous as the triplet design.

The burning rate parameter directly reflects the vaporization process. Figure 7 shows the burning rate parameter for the two injectors. It rises rapidly for the triplet and diminishes as soon as all the liquid oxygen is vaporized. In comparison, the coaxial injector's burning rate profile is lower and extends further into the chamber. The burning rate has been found to be one of the major factors in determining the combustion stability. Fast burning usually involves a large energy release and tends to be more turbulent and unstable. The large gradients generated in the process may result in large pressure and temperature excursion. Hence, engines with high burning rate are more prone to incidents of combustion instability.

The relative velocity parameter and the mass accumulation parameter for the two injectors are shown in Fig. 8 and 9. A low $\Delta V'$ and a high MAP value both decrease the stability index. However, it should be noted that both parameters are themselves influenced by the burning rate. Fast burning always entails rapidly accelerating gas and smaller values for MAP near the injector as in the case for the triplet injector.

As shown in Fig. 10, the stability index for the triplet starts extremely low but rises as most of the propellants are consumed rapidly. Conversely, the coaxial injector starts out high (stable) and decreases in value, but never to values as low as that where the triplet started out. Hence, the Priem analysis indicates the coaxial injector will be more stable than the triplet. Also shown on Fig. 11 is the relative stability index for the J-2 injector and, as indicated, the coaxial injector element is similar but slightly more stable than the J-2.

Stability Aids. The coaxial element has an inherent feature conducive to acoustic combustion stability; the combustion process is resistant to transverse disturbances due to the high relative velocity of the fuel to the oxidizer. Physically, one may envision that the vaporization and atomization of the oxidizer is shielded from transverse disturbances by the gaseous outer sheath.

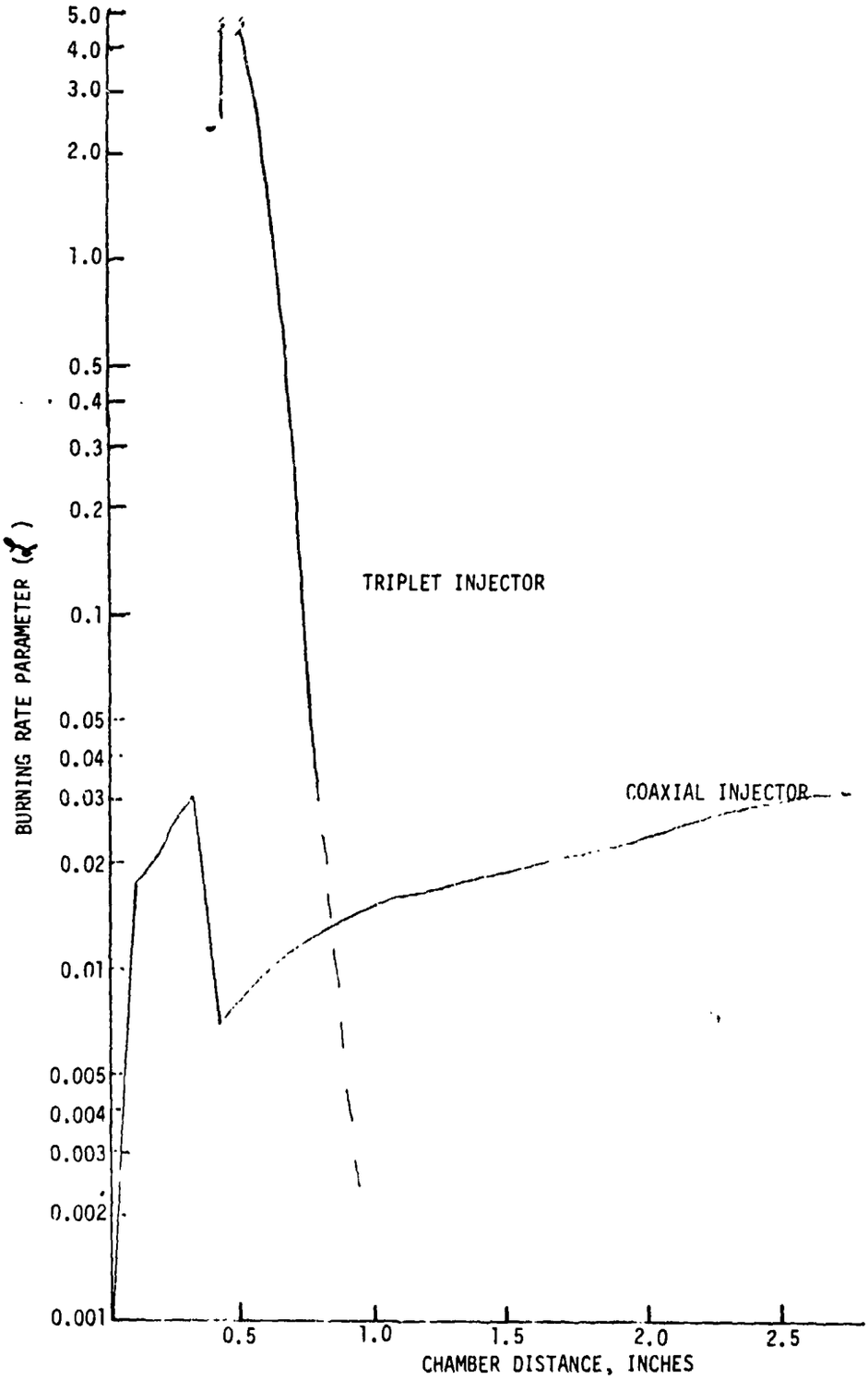

Figure 7. Burning Rate Parameter vs Chamber Distance From Injector

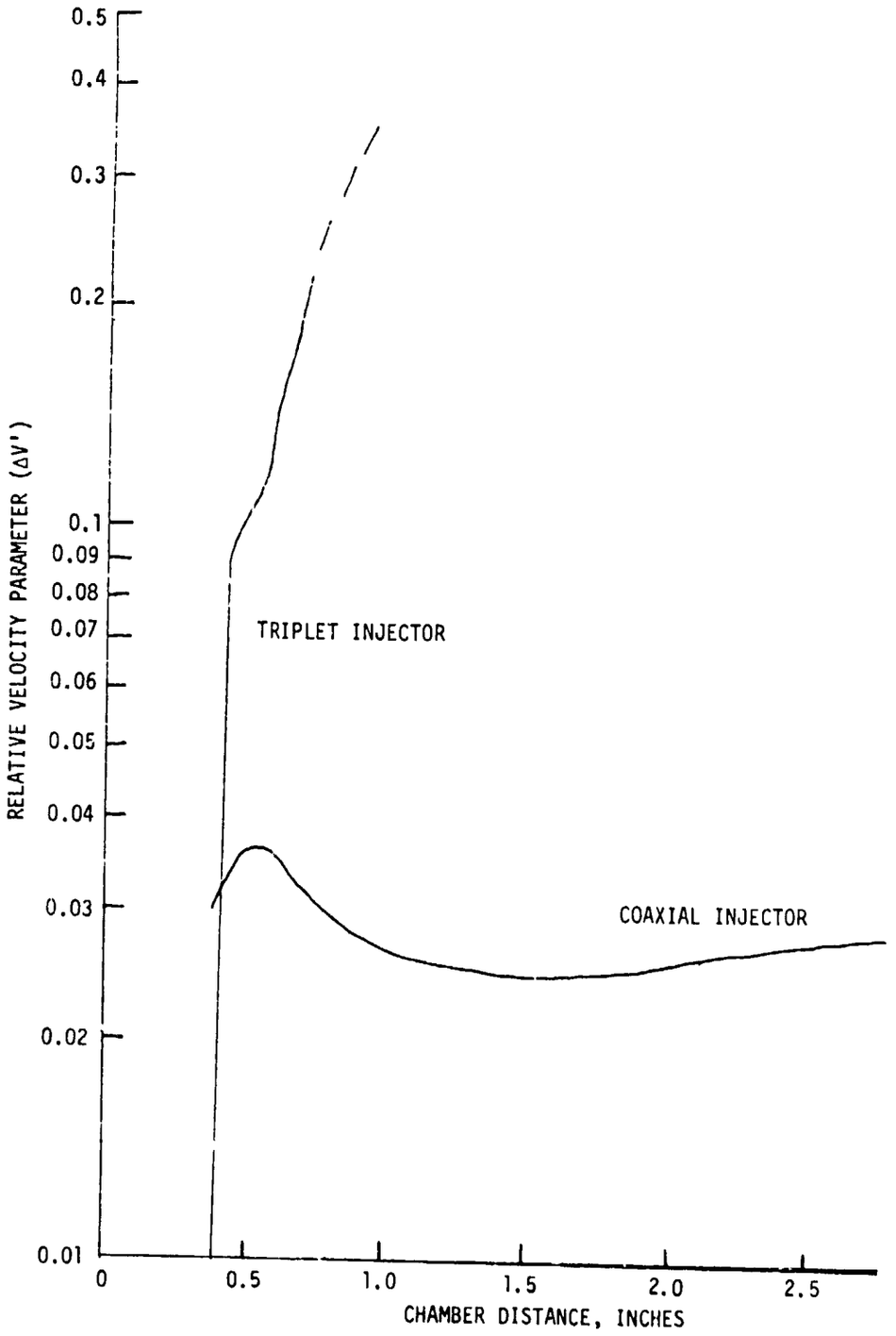

Figure 8. Relative Velocity Parameter vs Chamber Distance From Injector

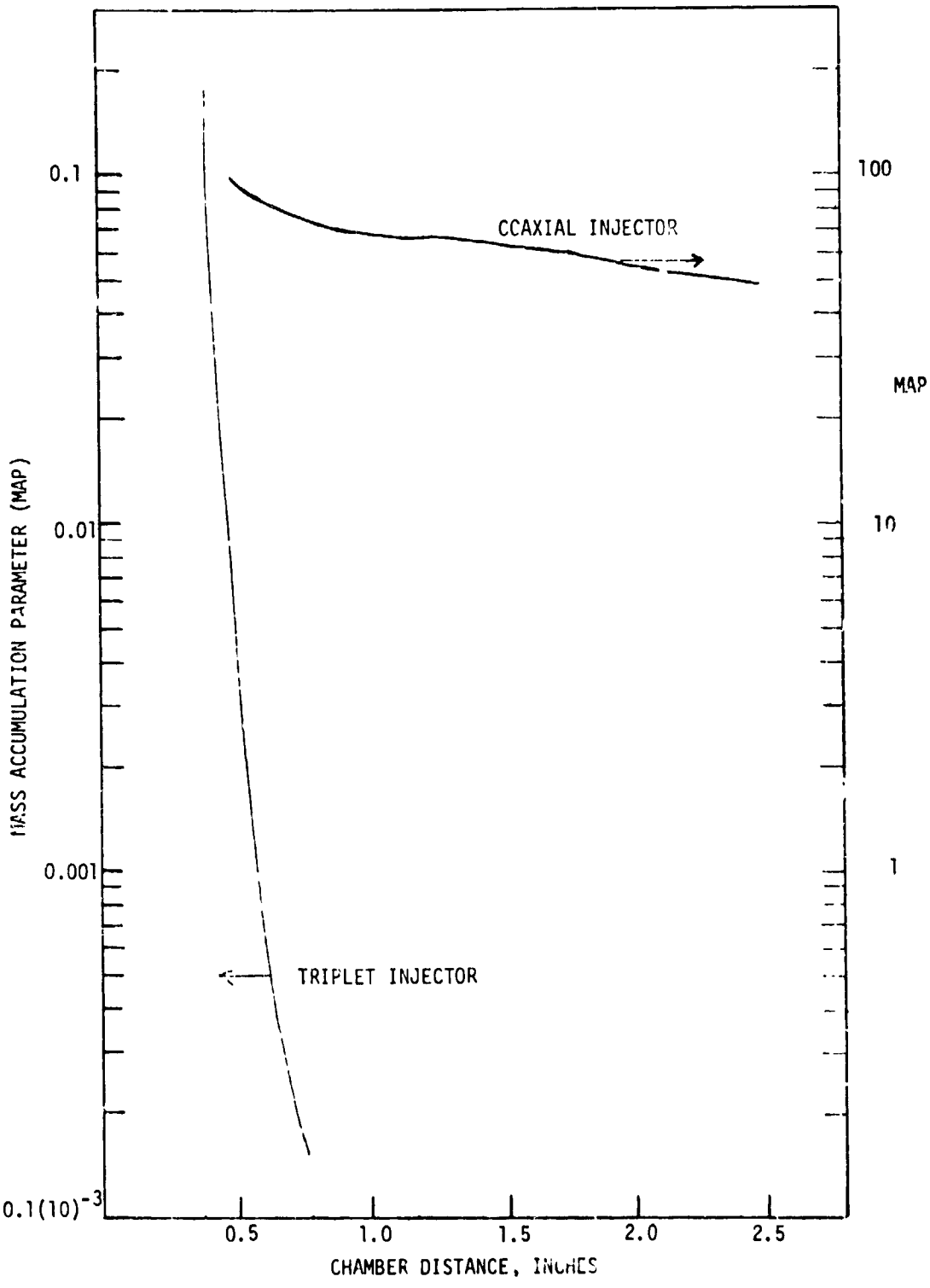

Figure 9. Mass Accumulation Parameter vs Chamber Distance From Injector

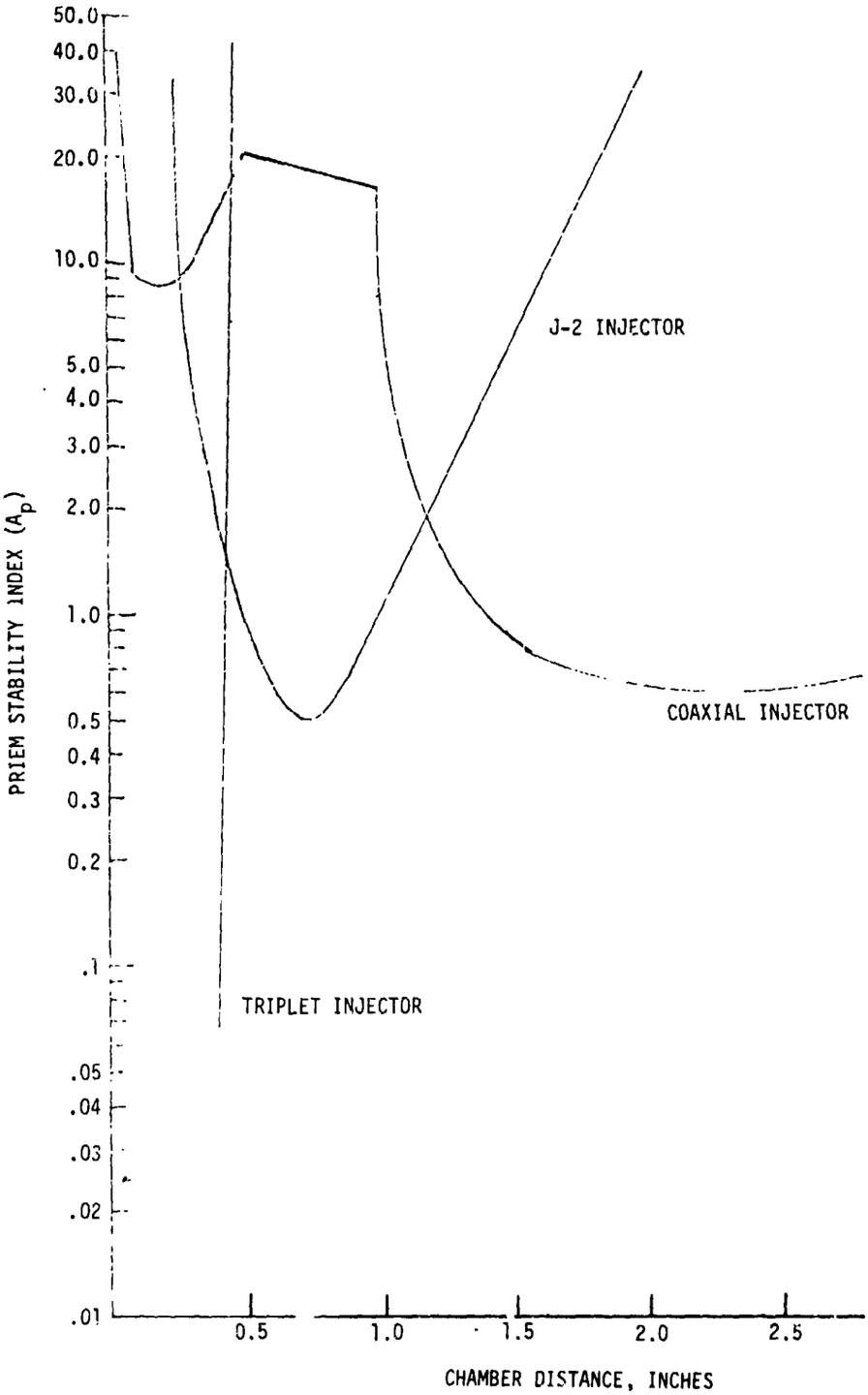

Figure 10. Priem Stability Index vs Chamber Distance From Injector

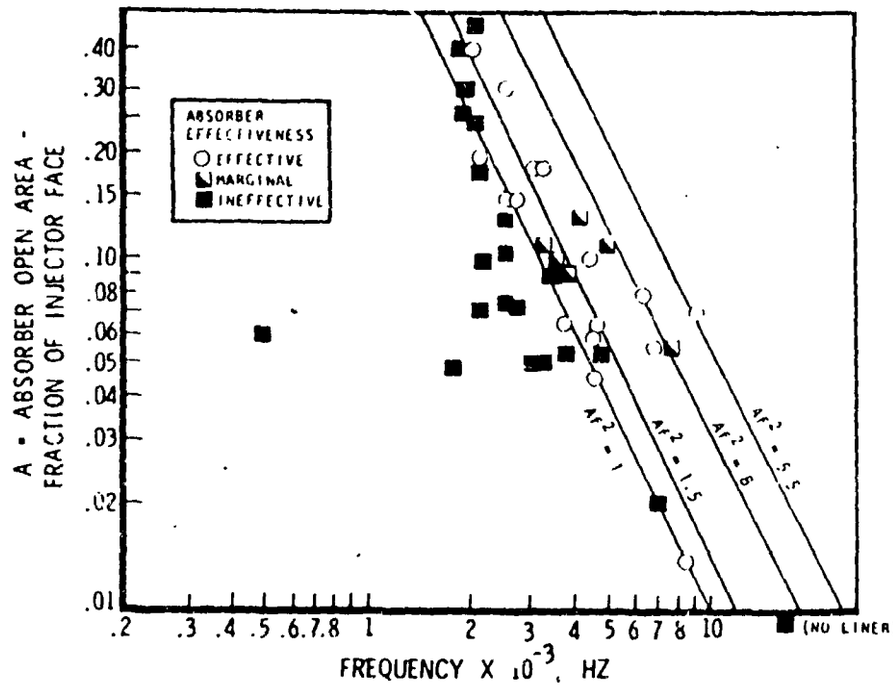

(a)

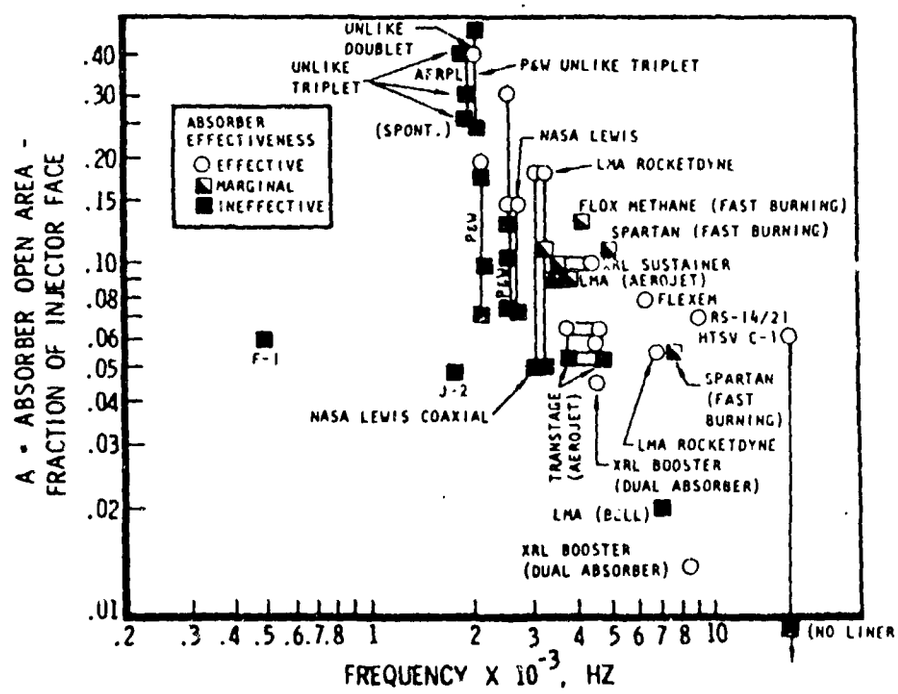

(b)

Figure 11. Absorber Experience

As evidence, the combustion stability has been demonstrated without any stability aid in the coaxial FLOX-methane injector development program as well as the LOX/GH_2 coaxial injector for the SSME subscale 40K engine. In Fig. 10 the stability index for the J-2 also is shown. Its minimum value occurs more closely to the injector and is lower than the coaxial injector candidate. It serves to indicate that the methane coaxial injector is more stable than J-2 which is rated as spontaneously stable. On rare incidents with the J-2 engine, a transition bomb test would trigger instability which persists into mainstage. Even the infrequent transition instabilities were eliminated when acoustic absorbers with an open area (that was 5% of the injector face) was incorporated. It is also reasonable that the same magnitude of absorber open area can be used for the methane absorber design if more stability margin is desired. The effect of 5% absorbers on the performance will be insignificant as long as the injector pattern does not change.

The triplet injector will probably face a large development problem to reach stable combustion and high performance due to the likely existence of combustion instability. There are two ways to circumvent the stability problem. One is to provide sufficient damping and the other is to modify the injector for a more moderate combustion, either one of which will affect the performance adversely.

As mentioned in the performance section, the triplet injector is limited by its mixing efficiency. The addition of baffles invariably degrades the mixing. The acoustic absorbers appear to be a better solution. Figure 11 is a summary of the industry's experience with the acoustic absorbers. The open area which is expressed as percentages of injector face area is plotted against the frequency. The effectiveness of the absorbers is indicated in the figure.

The chamber diameter for the LOX/methane injector is 5.66 inch. The first tangential mode will have a frequency slightly below 5000 Hz. To have effective absorbers, their total open area has to be at least 15% of the injector face. This is necessary in view of the condition for the fast burning FLOX-methane injector with 4-on-1 elements. It was rated marginal even with 12.5% open area.

The triplet pattern will be very similar to the 4 on 1 configuration in terms of the combustion process; they both are fast burning. One can infer from that experience that the acoustic absorbers must be included in the design. Presently, the injector face area is limited from the design point of view. It is impossible to include absorbers with 15% open area in the injector without eliminating and rearranging the elements. The performance will undoubtedly be degraded as fewer elements and the fuel diversion for the cavity cooling will impair the mixing efficiency.

In summary, unlike-impinging elements are highly sensitive to transverse waves and all of the impingement-type elements have high burning rates associated with high performance. Therefore, more development problems is predicted for the triplet injector.

Preliminary Design

A preliminary design study was conducted for the two injector concepts selected for comparison. The primary objectives were to develop injector element configurations, injector face patterns, and general injector design characteristics that best satisfy the basic requirements and also incorporate the results of the performance, stability, and heat transfer analysis. Some of the primary design considerations were: (1) maximum number of injector elements to provide high performance, (2) simplify manufacturing procedures, (3) provide low cost, and (4) injector flexibility or methods of modification.

Triplet Injector. The design study of the triplet injector was initiated with the study of single triplet elements. The layout of each element is depicted in Fig. 12.

The upstream face plate restraint (Fig. 12A) is integral with the body of the injector. The LOX post tube is brazed into the injector body. The face plate is supported by a face nut which threads into the face plate restraint. The integral face plate restraint requires an expensive fabrication process to produce a one-piece body. However, this design would simplify the requirement

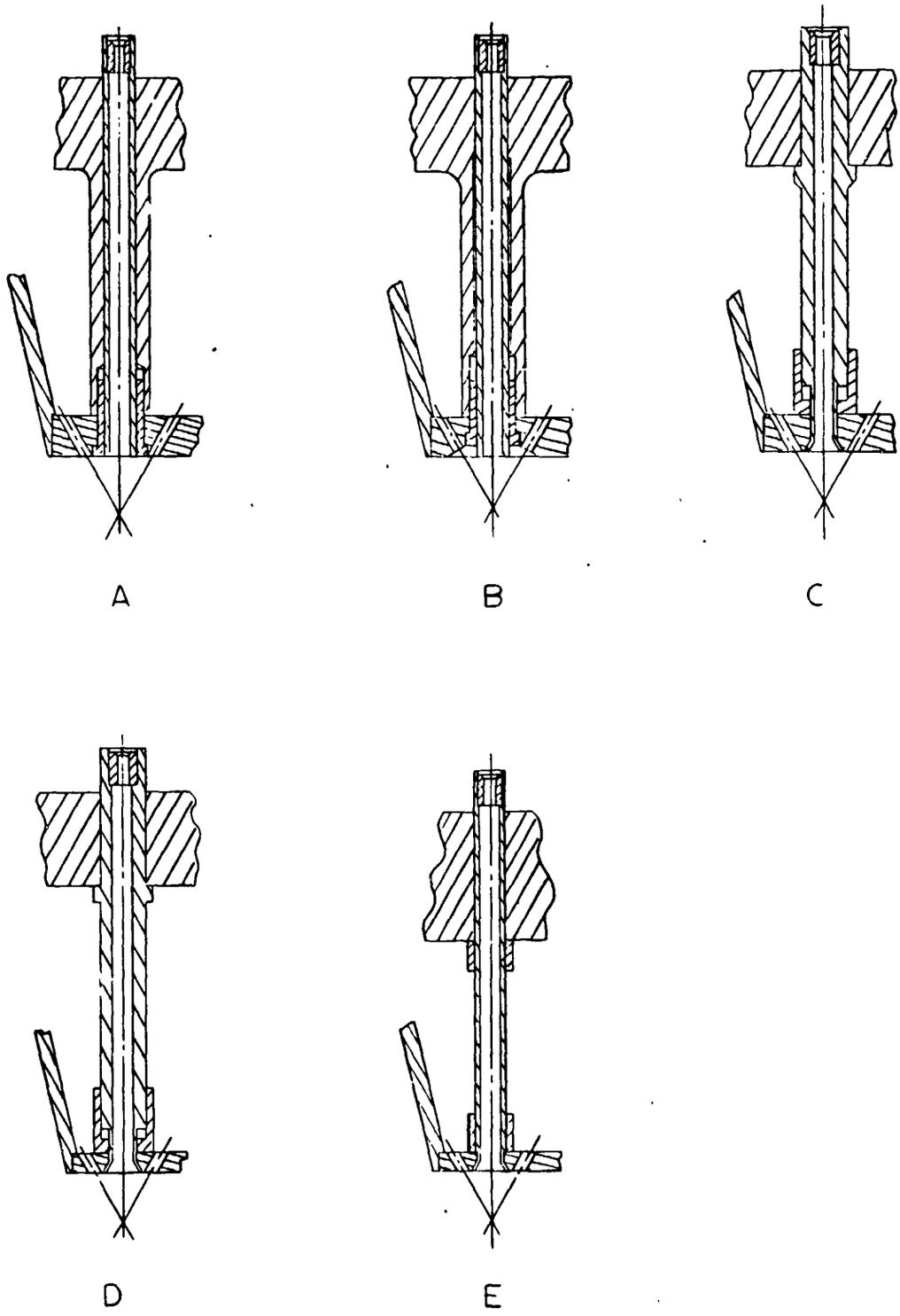

Figure 12. Triplet Elements Study

of fabricating a level restraint structure for the face plate and would eliminate a leak path between the fuel and the oxidizer.

The concept shown in Fig. 12B is the same as in Fig. 12A except the face nut recess allows an increase in the outer row element radius (i.e., more elements). The disadvantages of this concept over the Fig. concept is that a machined recess would change the flow characteristics of the Rigimesh face plate material in the machined area and that the fuel orifices would have a shorter length to diameter ratio.

The concept shown in Fig. 12C has a brazed LOX post and an adjustable face plate restraint threaded to the LOX post. The LOX post tip is swaged in place to support the face plate. This injector element concept, along with the remaining injector element concepts, has the potential of a braze joint leak path between the fuel and the oxidizer; however the fabrication of the injector body is simpler than using the Fig. 12A or 12B element concepts. The swaged tip should have a smaller diameter than the face nut, which could result in closer impingement of the propellants to the face plate and the possibility of a greater number of elements in the injector pattern. The swaging, of course, eliminates the cost of the face nuts.

The Fig. 12D concept is the same as Fig. 12C, except the use of a thinner face plate material would allow an increase in the outer row element radius (i.e., more elements). The disadvantage of this concept over the 12C concept is a reduction in the fuel orifice length-to-diameter ratio and a possible adverse shift in face plate porosity.

The concept shown in Fig. 12E would also have brazed LOX post and the swaged LOX post tip; however, no face plate restraint adjustment is provided. This should be the least expensive element to fabricate; however, care must be taken to have the posts machined as close to identical as reasonably possible to form a level face plate restraint surface.

Figure 13 depicts a Fig. 12E element in an injector face pattern of 120 elements. The pattern has maximized the number of elements without regard to propellant density distribution across the face of the injector. The usual design ratio of the outer row of elements to the first inner row of elements is 3 to 2. This pattern has a ratio of 3 to 2.4, and would result in excessive propellant density flow in the region of the second row.

The baseline triplet injector design is depicted in Fig. 14. The injector element depicted in Fig. 14 is similar to that depicted in Fig. 12. This injector element design also incorporates a replaceable oxidizer orifice. The element would be fabricated from a 0.250-inch OD tube with a 0.134-inch wall, 321 CRES. The orifice pin would be fabricated from 321 CRES bar and would be installed into the oxidizer tube, which would then be swaged over the orifice pin on final assembly. The injector body would be fabricated from 316L CRES including the grayloc fuel inlet port. The oxidizer posts have to be nickel plated (0.0004 to 0.0006-inch thick) and then brazed into the injector body. The injector face plate would be fabricated from 1/4-inch thick Rigimesh (321 CRES) which would be electron beam welded to a 316L support ring. The face plate must first be drilled to the indicated pattern and then installed on to the oxidizer posts. The end of the oxidizer posts would be swaged into the face plate counter sinks. The igniter tube is in the center of the face plate and is not to be attached to the face plate since its thermal expansion will differ from the oxidizer tubes. The injector pattern has a 10 $1/2^{o}$ cant from radial orientation. This prevents the intersection of fuel orifices on the inlet side of the face plate. It also orientates the injector fan pattern such that adjacent fans are not intersecting.

The injector face flow distribution (the face being defined out to the wall of the combustion chamber) is calculated on the annular areas defined by equal radial zones. For example, using Fig. 14 pattern, the outer radius of the element pattern is 2.34 and the next inner radius of the element pattern is 1.75 (while the combustion chamber wall radius is 2.83). The face flow rate per unit area of face is shown below for each zone in the Kg/sec CM^2 (pounds per sec $in.^2$).

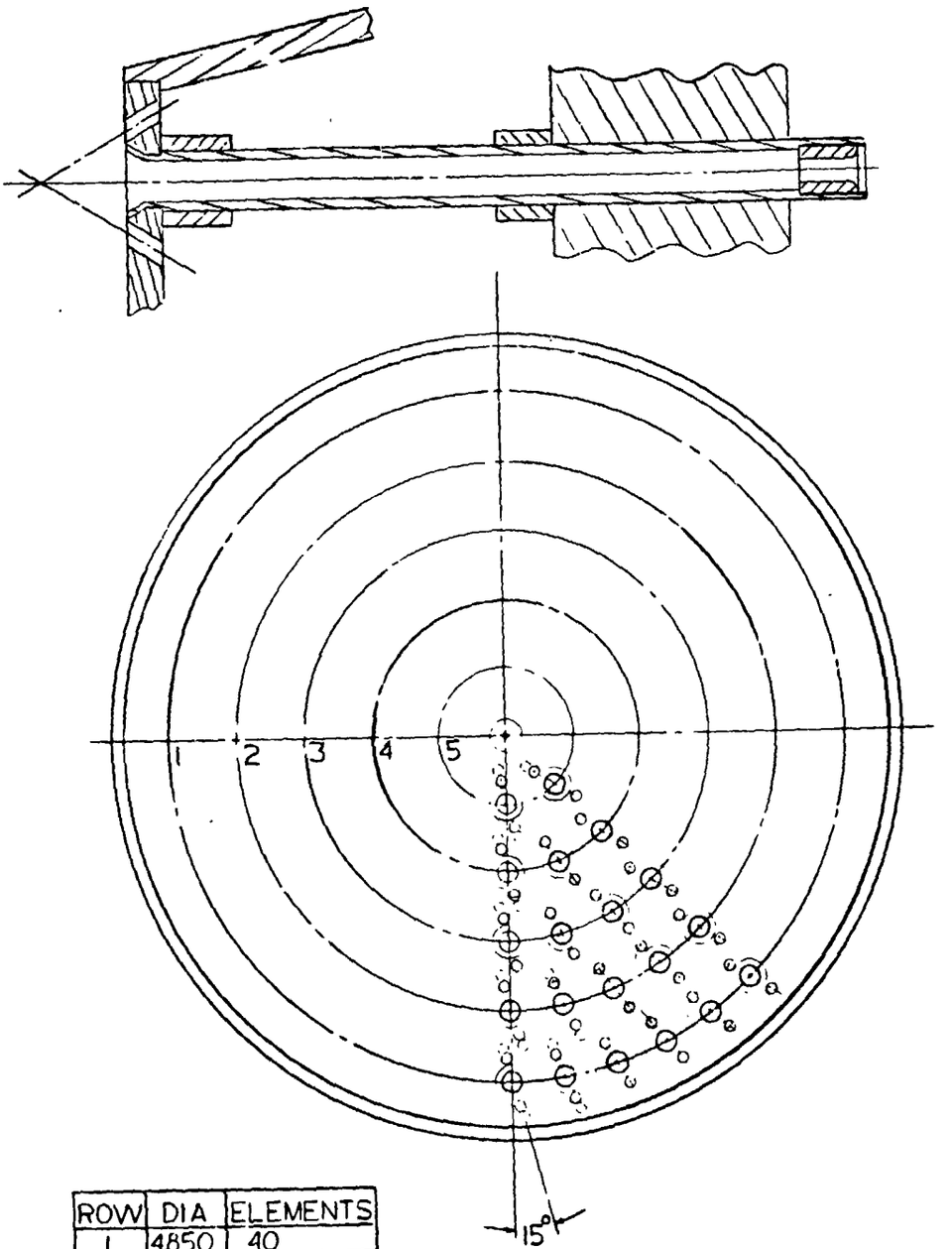

ROW	DIA	ELEMENTS
1	4.850	40
2	3.880	32
3	2.910	24
4	1.940	16
5	0.970	8
TOTAL		120

Figure 13. Injector Face Pattern

FOLDOUT FRAME

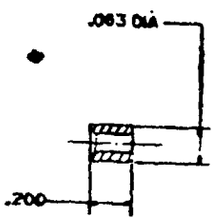

OXIDIZER ORIFICE
SCALE 4X

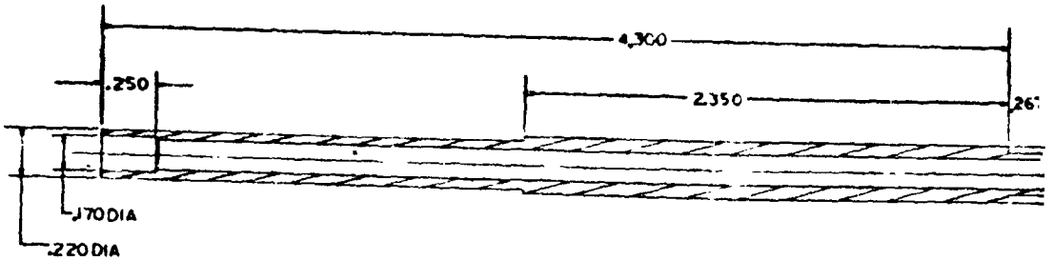

OXIDIZER POST
SCALE 4X

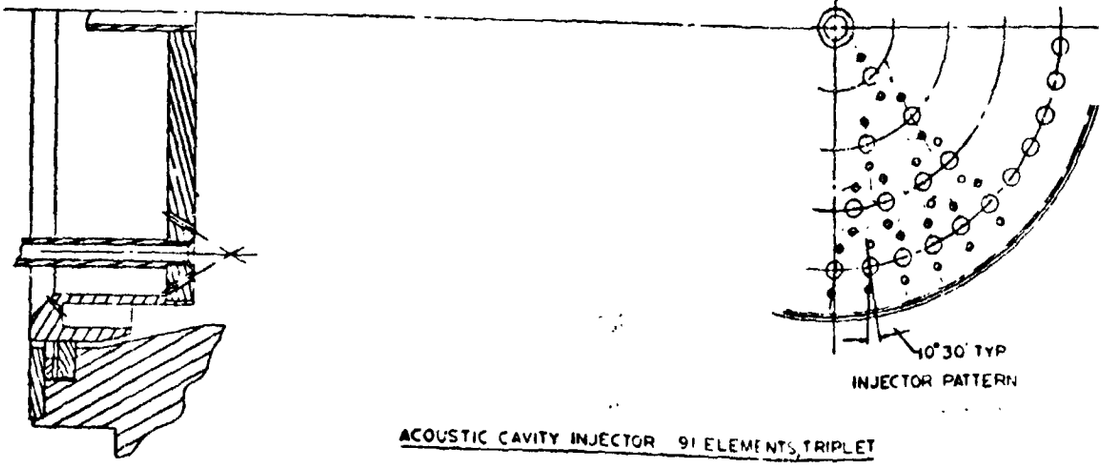

INJECTOR PATTERN

ACOUSTIC CAVITY INJECTOR 91 ELEMENTS, TRIPLET

FOLDOUT FRAME 2

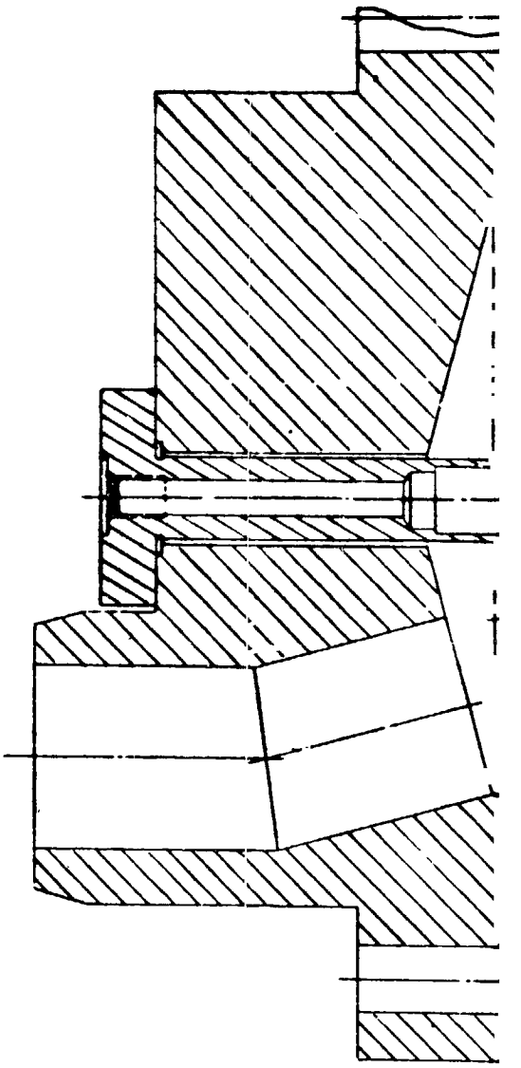

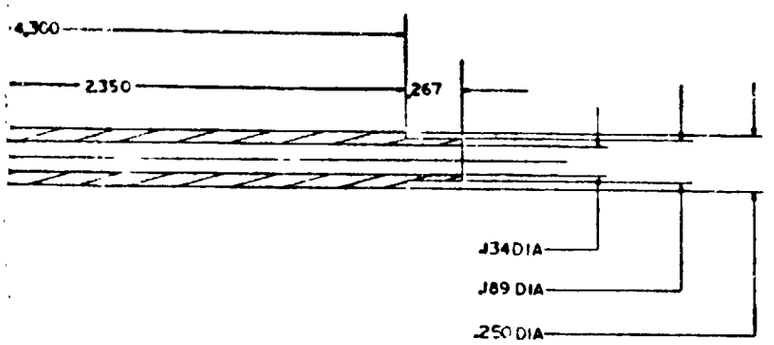

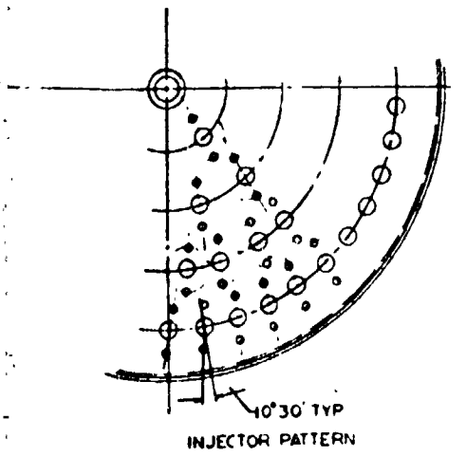

INJECTOR PATTERN

91 ELEMENTS, TRIPLET

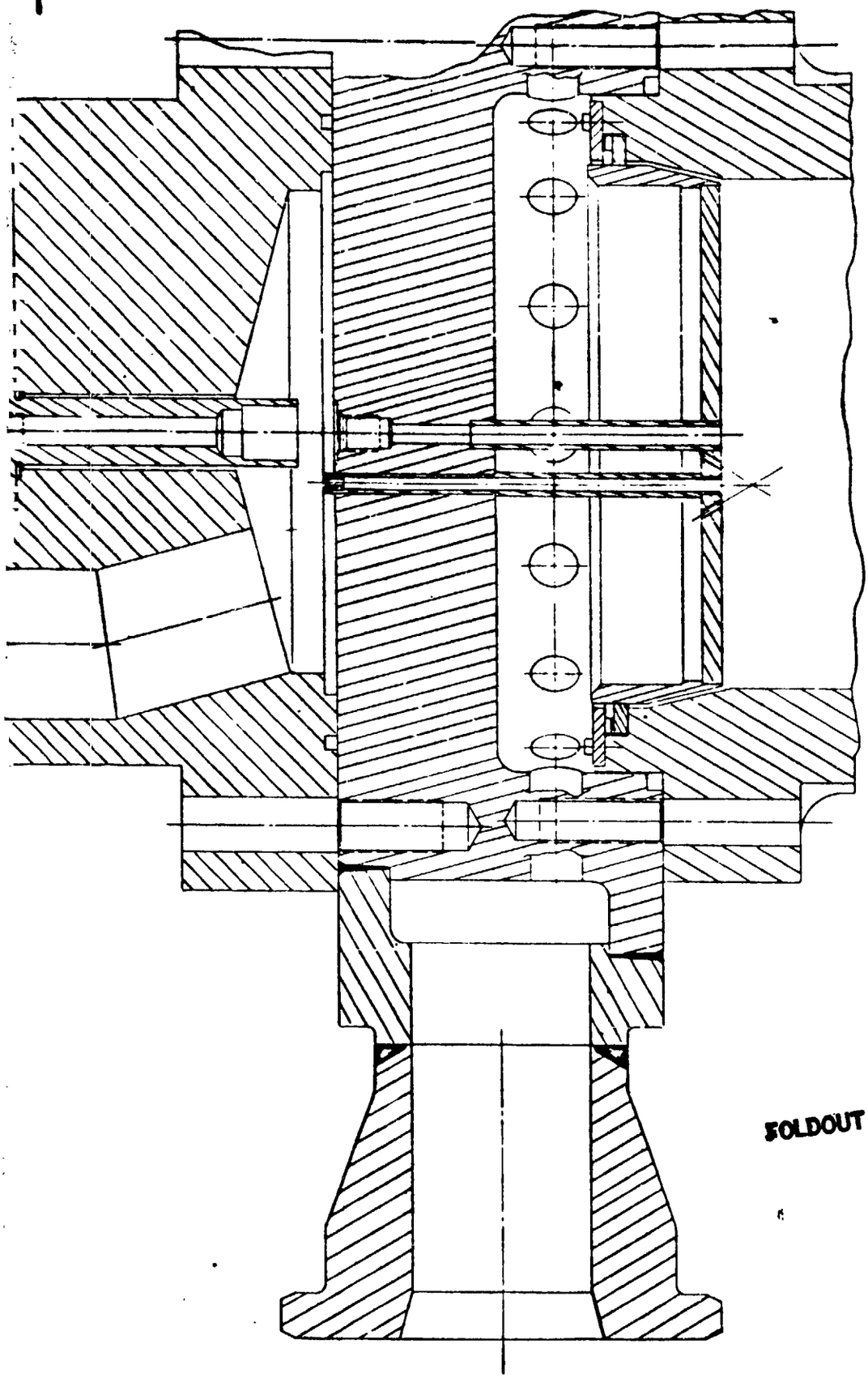

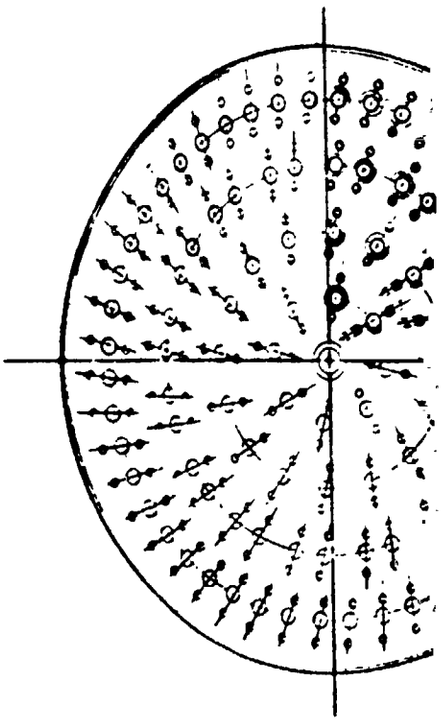

FOLDOUT FRAME 3

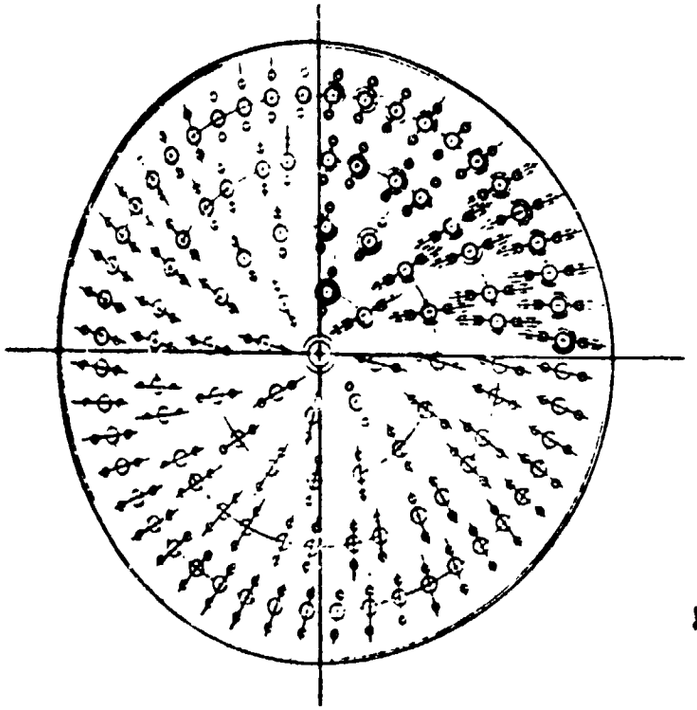

104 ELEMENT, TRIPLET

FOLDOUT FRAME 2

FOLDOUT FRAME 3

Figure 14. LOX Methane Triplet Injector Concept

The injector flow distribution for the 108 element pattern (Fig. 13) is:

Radius, in.	Elements	(lb/sec, in.^{2})
2.34	48	(5.144)
1.75	32	(6.356)
1.16	16	(4.794)
0.57	8	(4.385)
	104	

The design of the fuel inlet, the distribution manifold, the crossover passages, and the flow area between the oxidizer posts is based on maintaining a fuel flow area four times that of the fuel discharge orifices. This will result in a low pressure drop system and should also result in good propellant distribution over the backside of the injector face plate.

The oxidizer dome and the combustion chamber shown in Fig. 14 are existing pieces of hardware required to complete an injector assembly.

One possible configuration of an acoustic cavity that could be designed into the injector body also is depicted in Fig. 14. The design shows a film-cooled outer wall and also utilizes the cooled wall of the combustion chamber. The acoustic cavity inlet area is 15% of the combustion chamber cross-sectional area. This results in a reduction of the injector elements from 104 to 91. The injector flow distribution for the 91-element pattern (Fig. 13) is:

Radius, in.	Elements	Flow, in.^{2}
2.175	42	4.504
1.64	28	7.479
1.105	14	5.551
0.57	7	4.677
	91	

An alternative to incorporating the acoustic cavity into the injector body is to fabricate an acoustic cavity ring to be installed between the injector and the combustion chamber. The preliminary design of such a ring is shown in Fig. 15. The ring has 16 quarter-wave acoustic cavities spaced between the 16-bolt hole pattern. The ring will require cooling due to the high heat flux, and an independent water coolant system is shown. A film coolant passage into the cavity also is shown. The method of fabricating the cooled wall of the ring will require extensive design, heat transfer, and stress analysis and will be very sensitive to the hot-firing duration. The design and fabrication of this acoustic cavity ring should be compared to the design and fabrication of a combustion chamber.

Coaxial Injector. The design study of the coaxial injector was initiated with the study of single coaxial elements, using the element configuration shown in Fig. 16 (40K LOX/methane injector concept) as a reference point. The major design consideration is to minimize the face nut diameter for maximum number of elements, while still maintaining sufficient structural wall between the root of the nuts threads and the internal diameter of the nut so that various internal diameter nuts can be fabricated for the same face plate. This would provide development versatility during the program. Figure 17 shows two possible designs for the same propellant momentum ratio. The thick wall face nut (Fig. 18A) provides the versatility required and also allows the nut to be installed with more reasonable torquing requirements.

The baseline coaxial injector design is depicted in Fig. 18. The oxidizer element would be constructed from a thin-wall tube (321 CRES, nickel plated), which would be brazed into a heavy wall oxidizer post (316L CRES). The post, in turn, would be brazed into the injector body, which would also be fabricated from 316L CRES. The internal diameter of the oxidizer tube would be machined to control the oxidizer discharge area and the external diameter of the same tube would be machined to control the fuel discharge gap. The oxidizer post design does not contain an integral orifice; however, a replaceable orifice can easily be incorporated into the design if required. The element sleeve (321 CRES) would be internally threaded so that it can be threaded to the oxidizer post, and the face nut can, in turn,

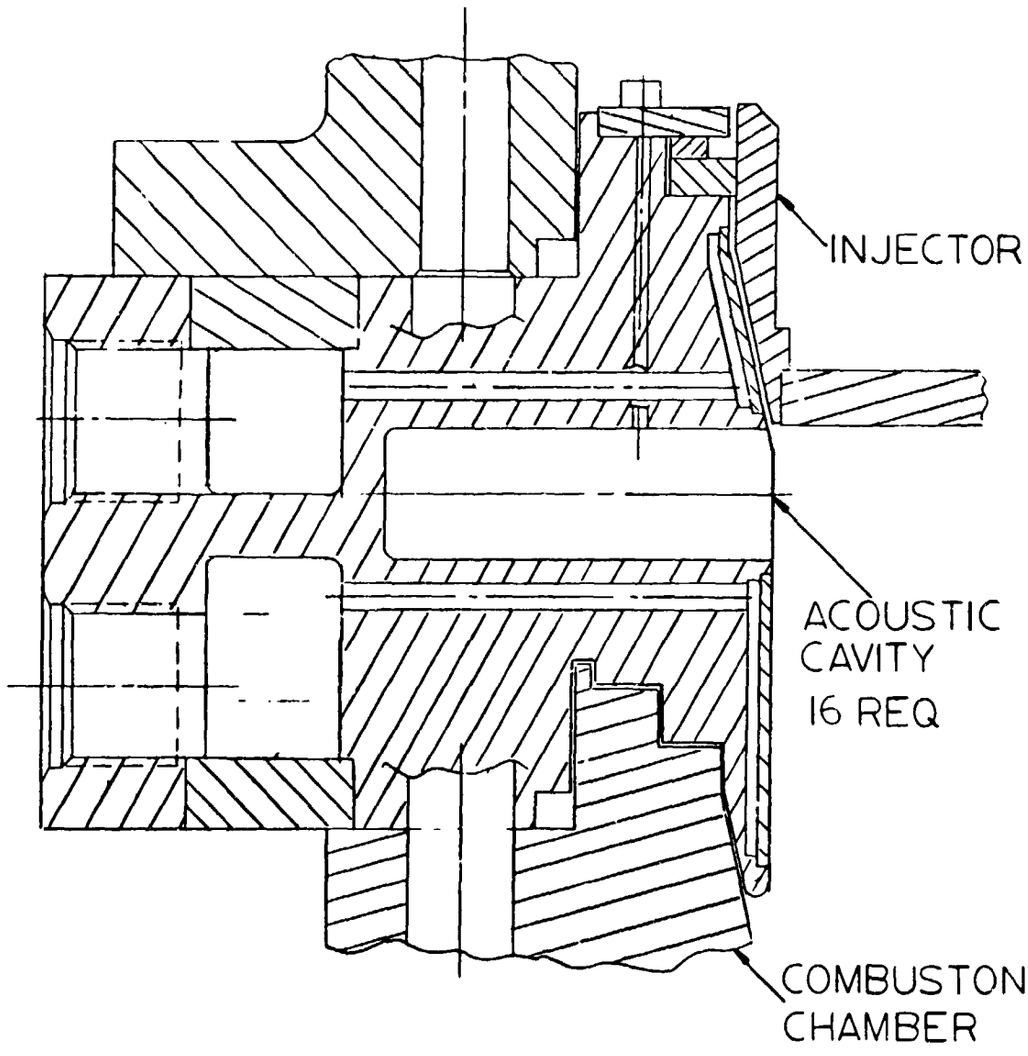

Figure 15. Acoustic Cavity Ring

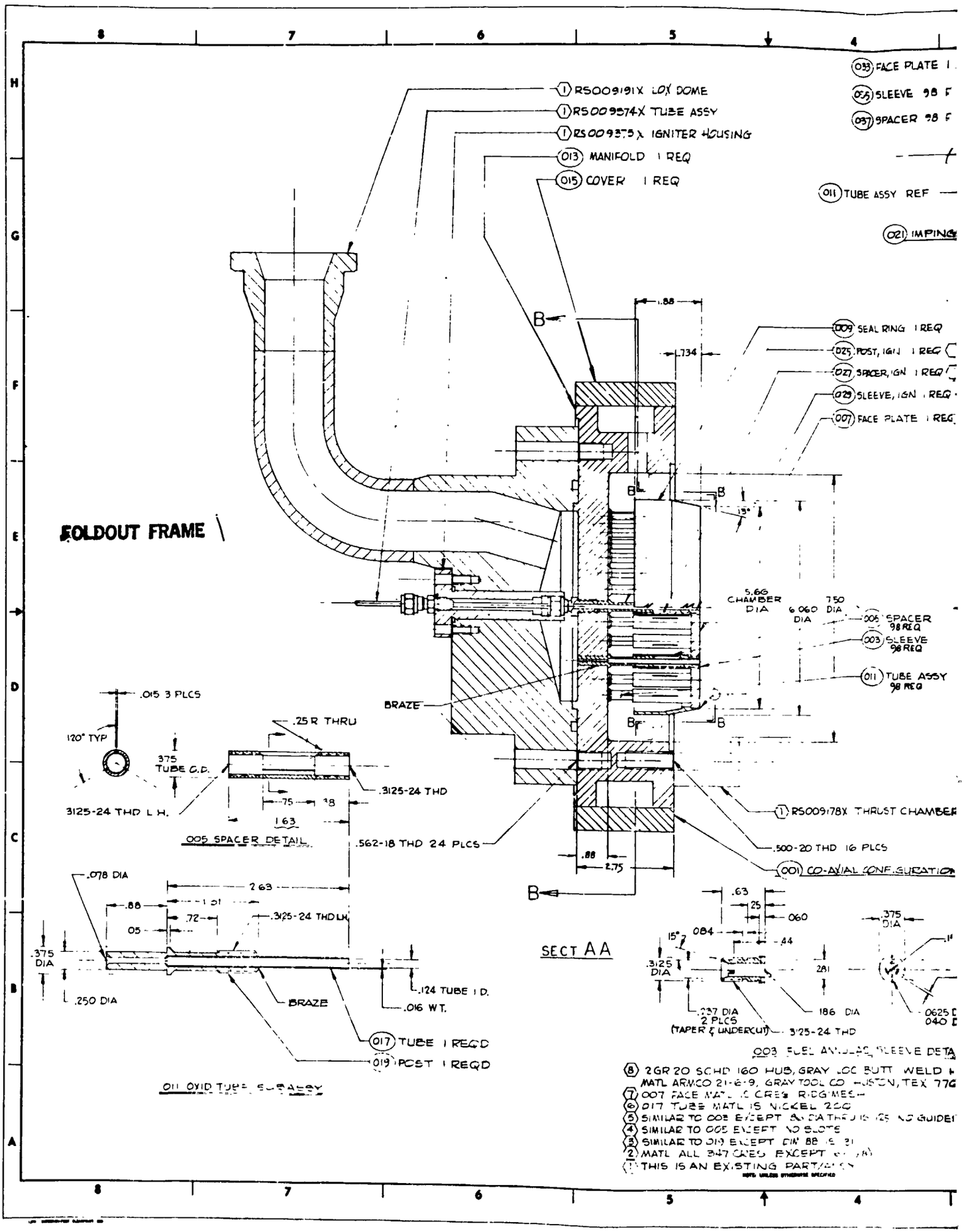
FOLDOUT FRAME
(1) RS009191X LOX DOME
(1) RS009574X TUBE ASSY
(1) RS009375X IGNITER HOUSING
(013) MANIFOLD 1 REQ
(015) COVER 1 REQ
(033) FACE PLATE 1
(035) SLEEVE 98 F
(037) SPACER 98 F
(011) TUBE ASSY REF
(021) IMPING
(009) SEAL RING 1 REQ
(025) POST, IGN 1 REQ
(027) SPACER, IGN 1 REQ
(029) SLEEVE, IGN 1 REQ
(007) FACE PLATE 1 REQ
.88
.734
B
5.66 CHAMBER DIA
6.060 DIA
750 DIA
(005) SPACER 98 REQ
(003) SLEEVE 98 REQ
(011) TUBE ASSY 98 REQ
BRAZE
.015 3 PLCS
120° TYP
.375 TUBE O.D.
.25 R THRU
.3125-24 THD
3125-24 THD L.H.
.75
.98
1.63
005 SPACER DETAIL
.562-18 THD 24 PLCS
(1) RS009178X THRUST CHAMBER
.500-20 THD 16 PLCS
.88
2.75
(001) CO-AXIAL CONFIGURATION
.078 DIA
2.63
1.91
.88
.72
.3125-24 THD LH
05
.375 DIA
.250 DIA
BRAZE
.124 TUBE I.D.
.016 WT.
(017) TUBE 1 REQD
(019) POST 1 REQD
011 OXID TUBE SUBASSY
SECT AA
.63
.25
.060
15°
.084
.44
.3125 DIA
.281
.375 DIA
.237 DIA 2 PLCS (TAPER & UNDERCUT)
.186 DIA
3125-24 THD
003 FUEL ANNULAR SLEEVE DETA
(8) 2GR 20 SCHD 160 HUB, GRAY LOC BUTT WELD
MATL ARMCO 21-6-9, GRAY TOOL CO HUSTON, TEX 77
(7) 007 FACE MATL IS CRES RIDGMESH
(6) 017 TUBE MATL IS NICKEL 200
(5) SIMILAR TO 005 EXCEPT
(4) SIMILAR TO 005 EXCEPT NO SLOTS
(3) SIMILAR TO 019 EXCEPT
(2) MATL ALL 347 CRES EXCEPT
(1) THIS IS AN EXISTING PART

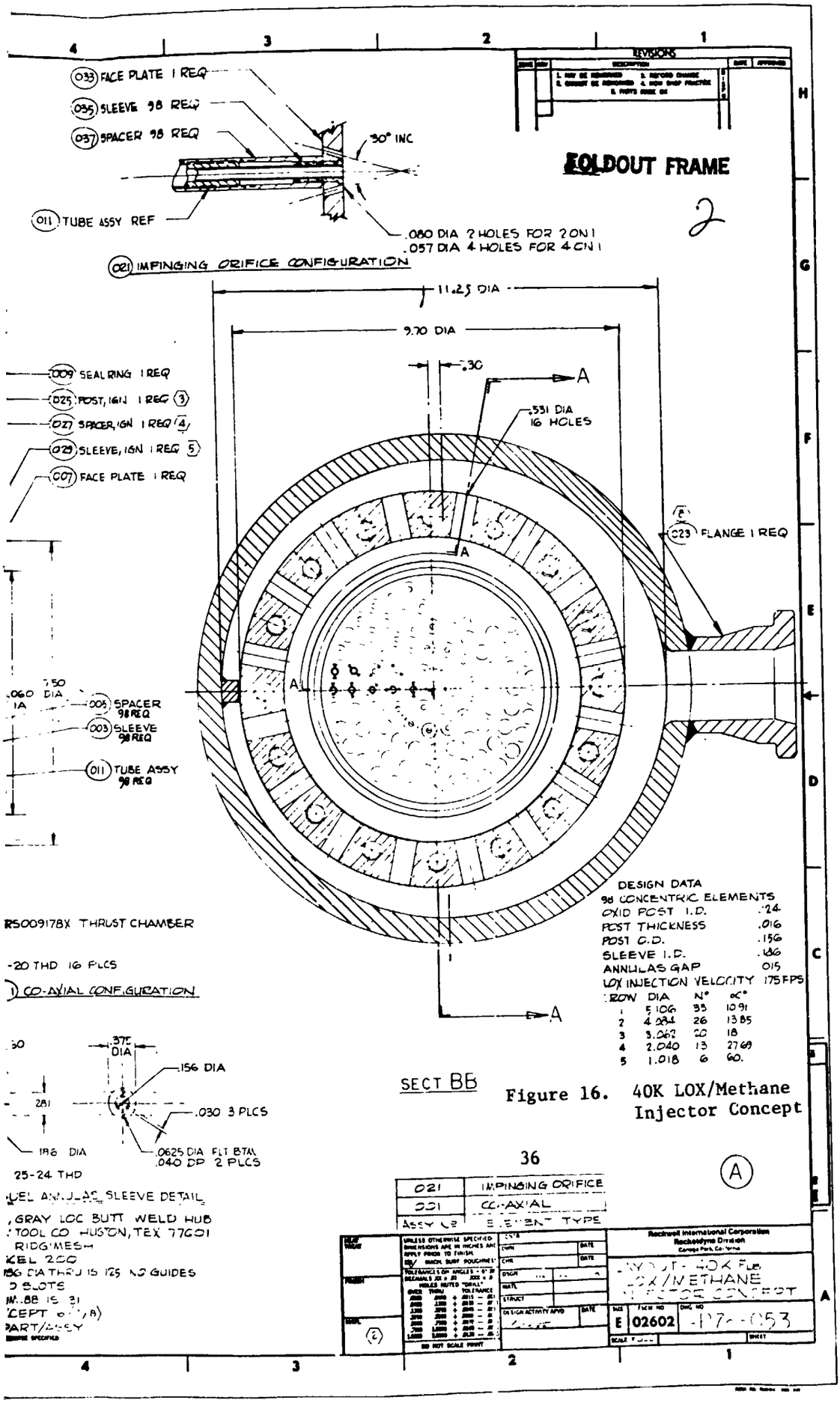

FOLDOUT FRAME 2

Figure 16. 40K LOX/Methane Injector Concept

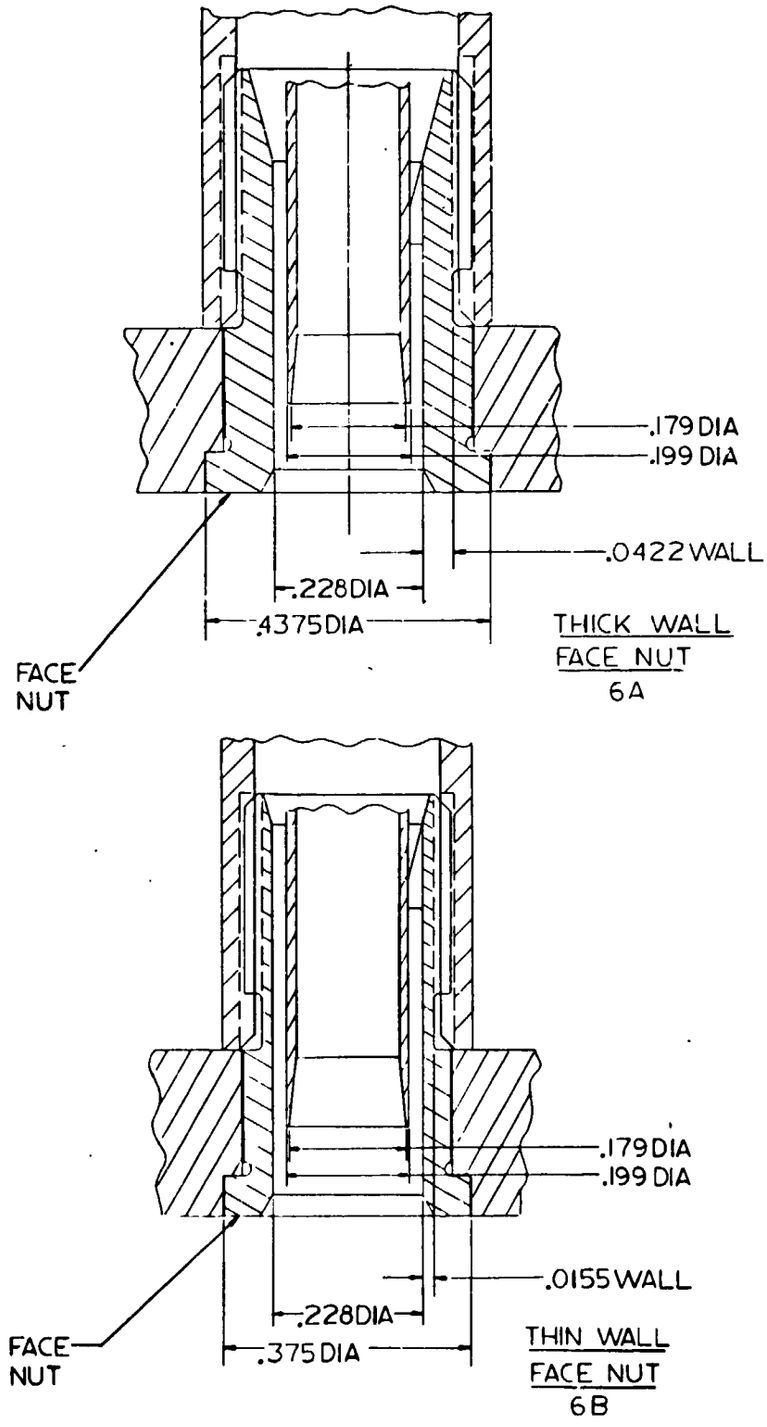

Figure 17. Face Nut Study

FOLDOUT FRAME

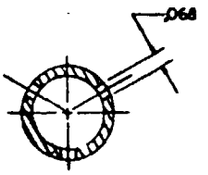

SECTION D-D

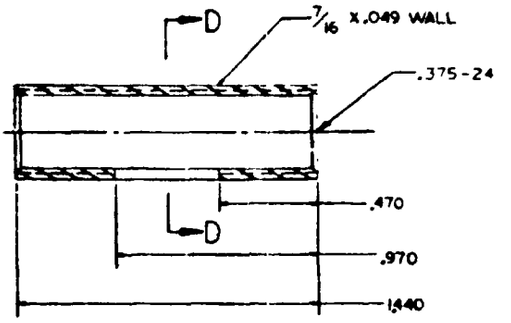

SLEEVE
SCALE 4X

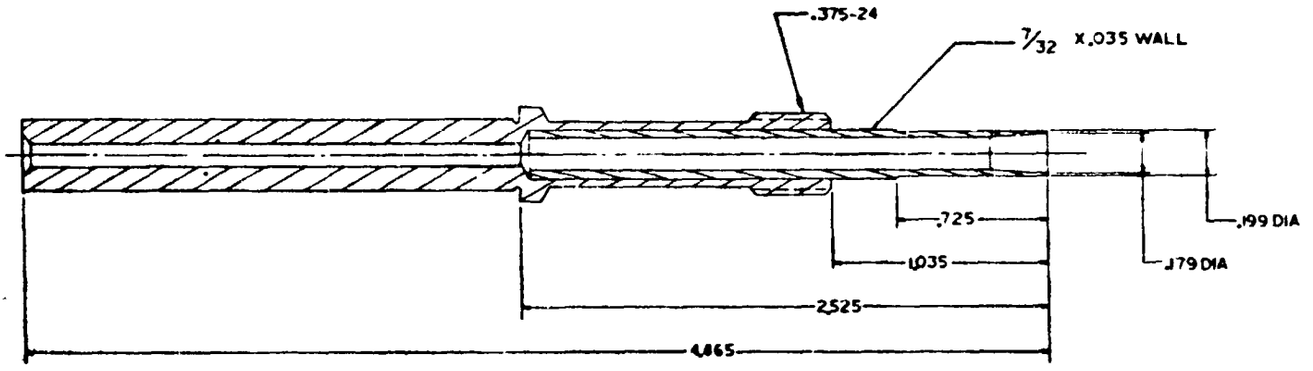

OXIDIZER ELEMENT
SCALE 4X

FACE NUT
SCALE 4X

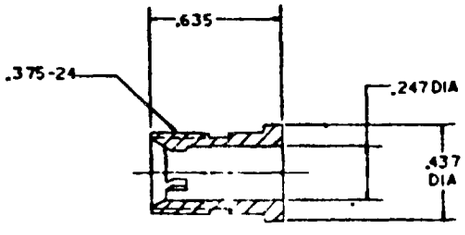

SECTION C-C

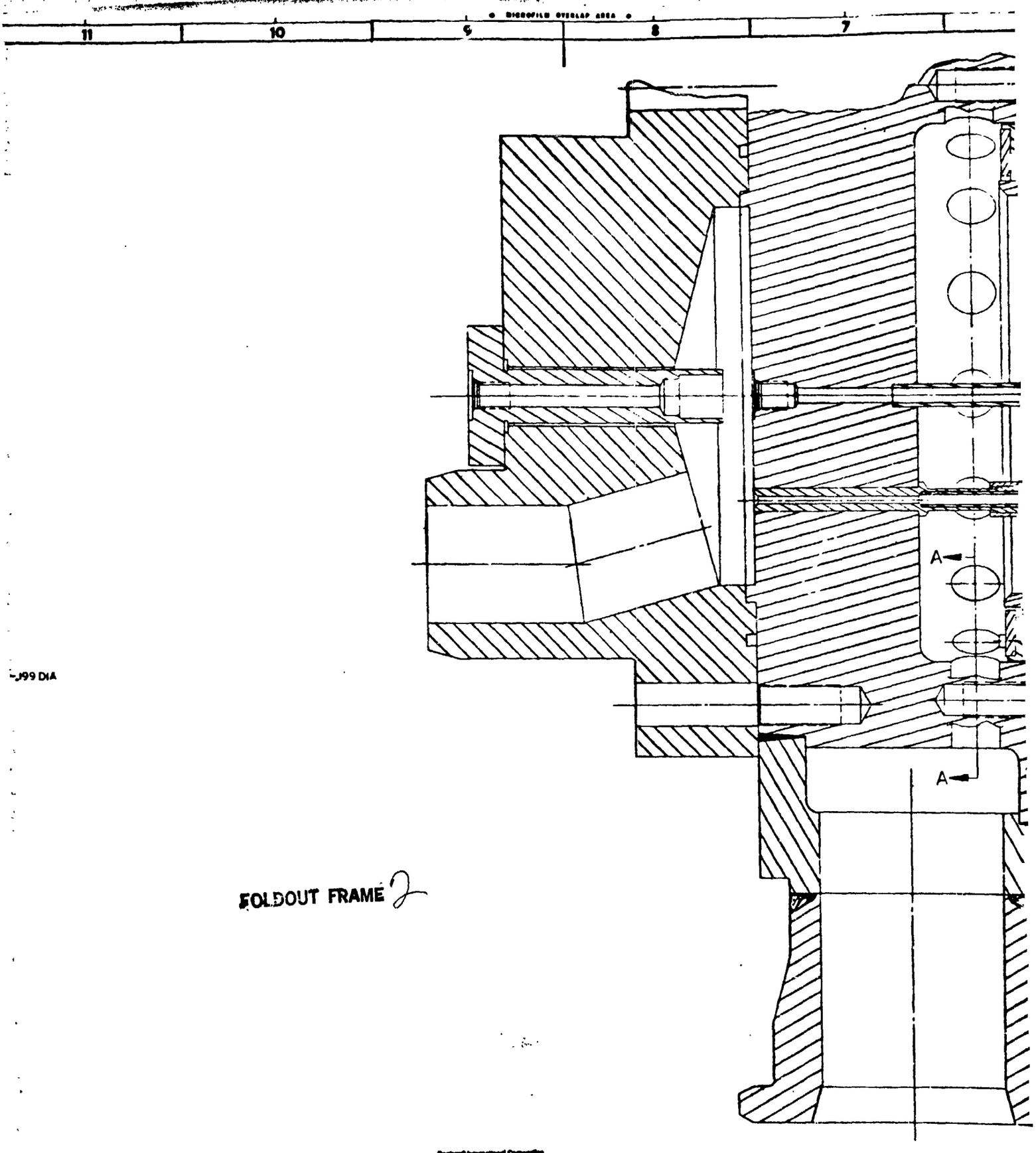

-.199 DIA

FOLDOUT FRAME 2

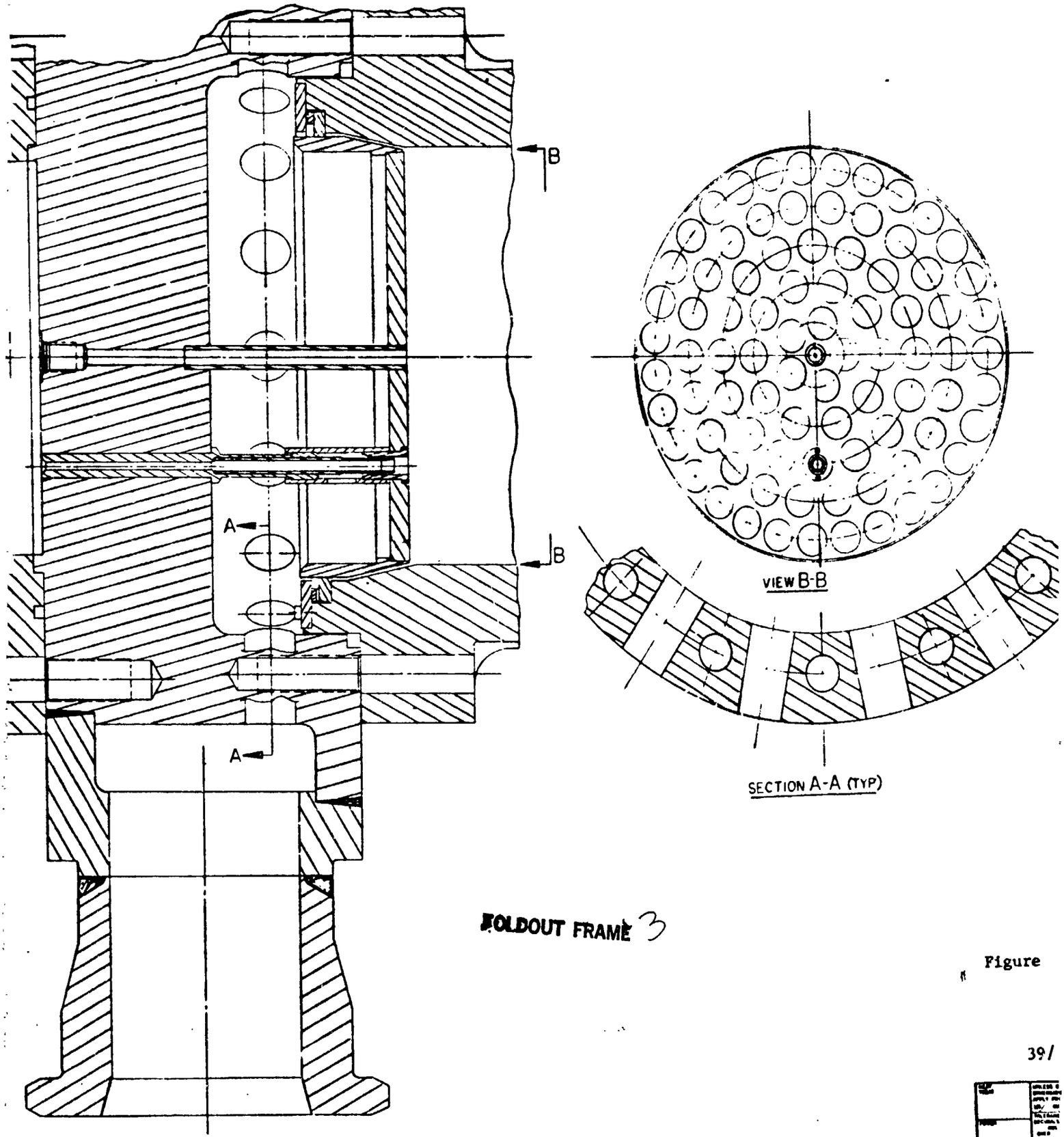

FOLDOUT FRAME 3

Figure

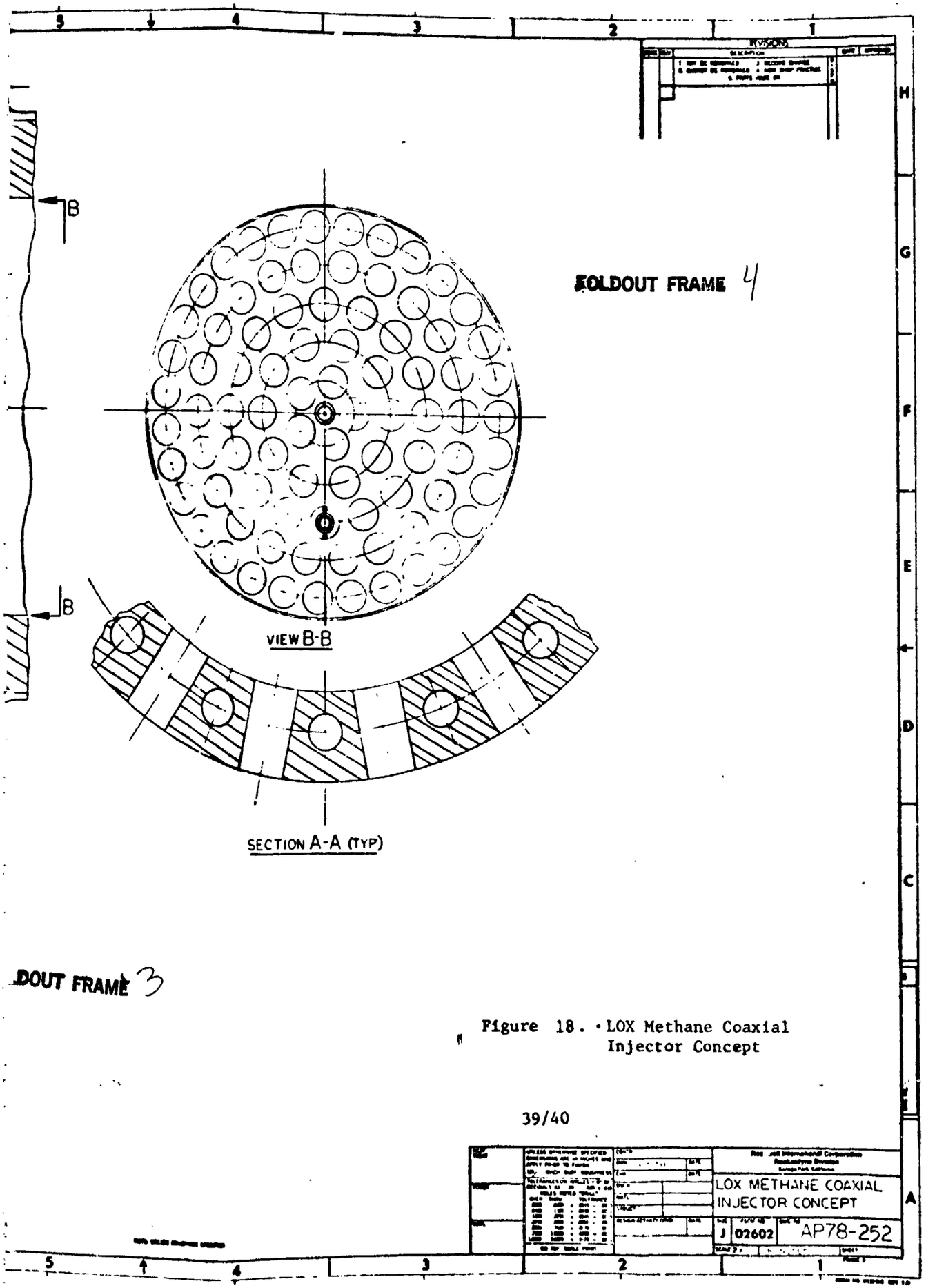

Figure 18. · LOX Methane Coaxial Injector Concept

be threaded into the sleeve. The injector face plate would therefore be restrained between the sleeve and the face nut.

The sleeve also would have three slots machined into the side walls to serve as controlled entrances to the elements annular discharge area. The thick wall face nut controls the outside diameter of the annular fuel discharge gap. Three tabs would be machined into the internal diameter of the face nut to ensure the correct concentricity between the oxidizer flow and the fuel flow. The face nuts (321 CRES) can be fabricated to deliver a fuel velocity from 200 to 400 ft/sec.

The injector face plate would be fabricated from 1/4-inch-thick Rigimesh (321 CRES) which would be electron-beam welded to a 316L CRES support ring. The face plate would first be drilled to the indicated pattern and then installed on the oxidizer posts. Prior to installing the face plate assembly, the sleeves would be threaded to the oxidizer post and adjusted for the desired cup depth, i.e., the distance from the end of the oxidizer post to the discharge end of the face nut, D1, Fig. 19. By adjusting the sleeves position on the oxidizer post, the cup depth can be varied. The design depicted in Fig. 17 is for a 1-diameter (diameter of the oxidizer post) maximum cup depth. By making several modifications to the design, the cup depth can be increased to 2 diameters. Once the face plate assembly has been installed, the face nuts would be threaded into the sleeve to complete the injector assembly. The igniter tube, which is in the center of the face plate, would not be attached to the face plate since its thermal expansion will differ from the oxidizer tubes. An injector pattern based on 84 elements was finally selected based on desired tube thickness, nut thickness, Rigimesh thickness between elements, and fuel distribution.

The injector flow distribution for the 84-element pattern (Fig. 17) is:

Radius, in.	Elements	Flow, lb/sec-in.^{2}
2.504	31	5.314
1.989	22	5.453
1.474	16	5.351
0.959	10	5.141
0.444	5	5.159
	84	

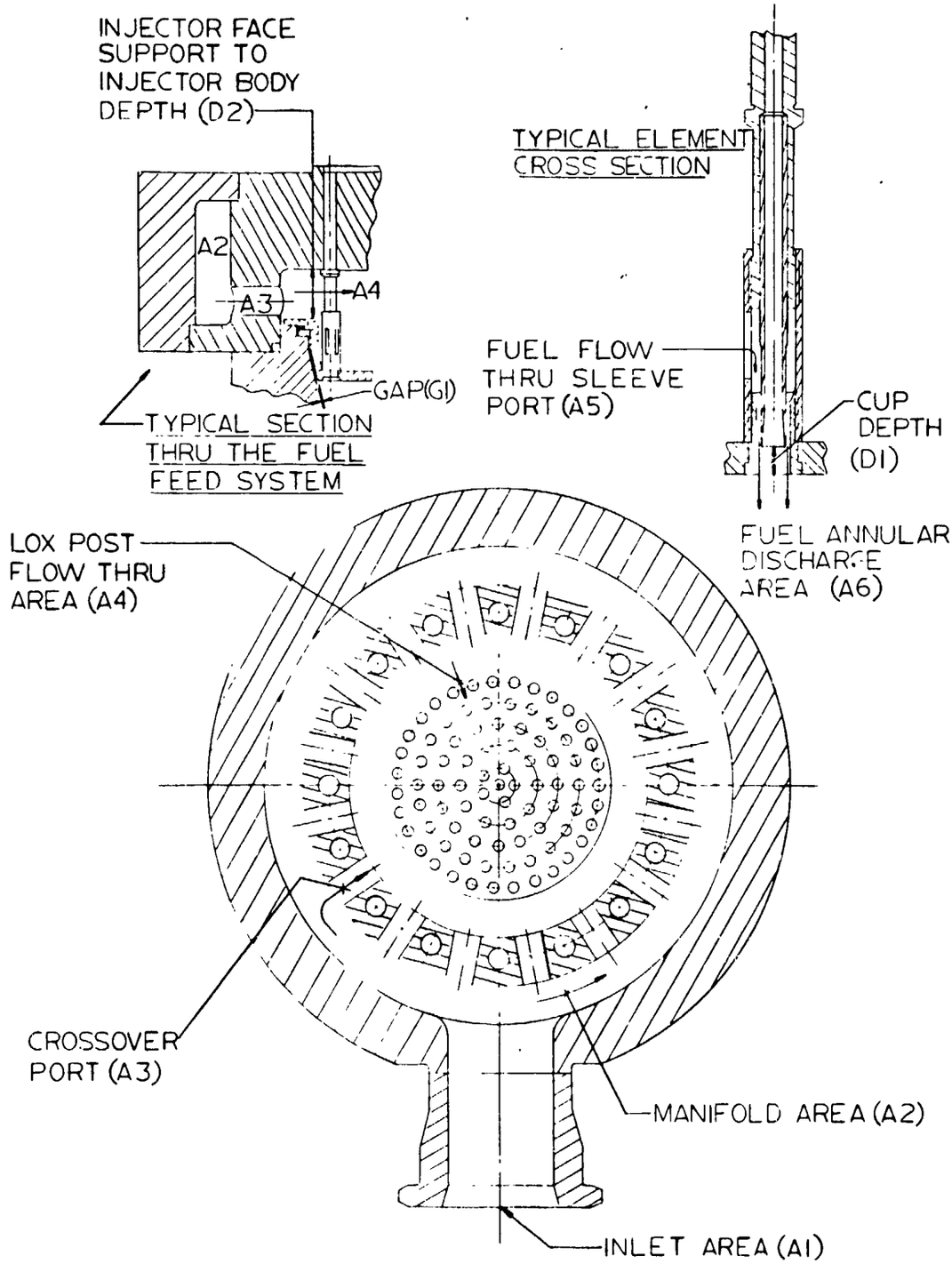

Figure 19. Fuel Feed System

The fuel inlet, the distribution manifold, the crossover passages, the flow area between the oxidizer posts, and the slots in the sleeves are designed to maintain a fuel flow area 4 times the fuel annular discharge area. It must be noted that changing the cup depth has an effect on several of these flow areas. As the cup depth is reduced, for a fixed configuration, the face plate support ring reduces the flow area between this ring and the injector body; also, as the cup depth is reduced from its maximum value, the slot area in the sleeves could be reduced. The same adjustment to the cup depth can also influence the outer diameter of the LOX post. Therefore, maximum cup depth required will establish the internal geometry of the injector body, the length of the oxidizer posts, and the length of the sleeves. The fuel feed system for the baseline design is shown in Fig. 19. Areas A1, A2, A3, A4, and A5 are to be designed for 4 times the sum of area A6 (84 elements). These areas, as previously indicated, are controlled by the maximum A6 area and the maximum cup depth, D1. It should be noted that as the cup depth is reduced from the initial maximum cup depth, the gap, G1, between the injector body and the face plate ring will increase. This gap area could provide a thermal problem that will have to be evaluated.

The baseline design shows a 5/16-inch-diameter igniter tube. By rotating the innermost 5 elements in the pattern so that they are symmetrical with the 10 elements in the next row, the 5 elements can be moved outboard. This allows the use of a 3/8-inch-diameter igniter tube.

Methods of incorporating an acoustic cavity into the coaxial injector also were investigated and the results are shown in Fig. 20. In the Fig. 20A design, the acoustic cavity (quarter wave) is incorporated into the injector body with the gap established for 5% of the injector face area. The length of the acoustic cavity is established by the tunning frequency. Using the baseline injector pattern configuration was impossible with this design; however, the face plate axial location was recessed slightly into the conical section of the combustion chamber to obtain as many elements (78) in the injector pattern as possible. The injector flow distribution for the 78 element pattern is:

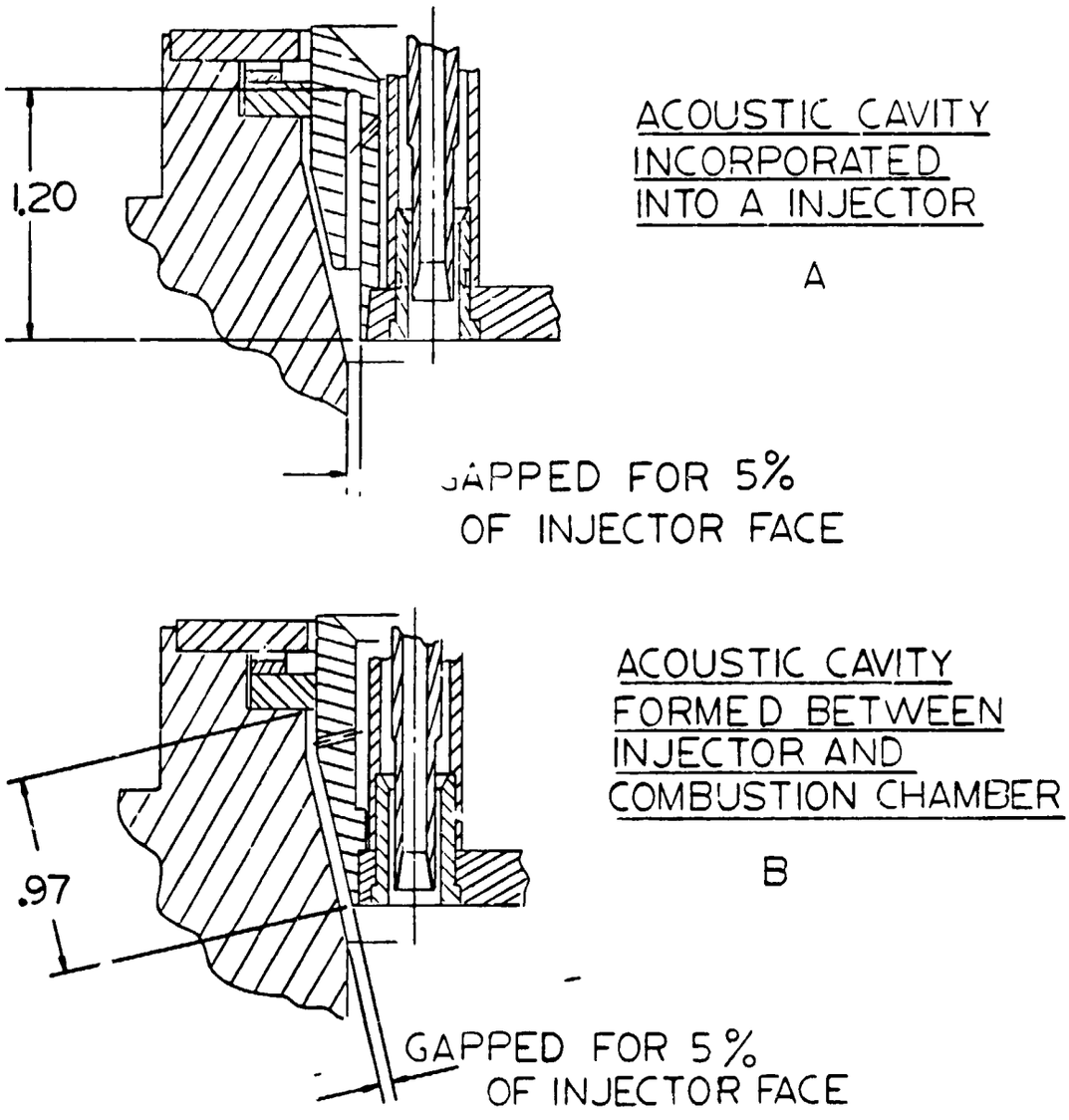

Figure 20. Acoustic Cavity Study

Radius, in.	Elements	Flow, lb/sec-in.^{2}
2.375	29	4.499
1.86	23	6.565
1.345	16	6.316
0.83	10	5.411
	78	

In Fig. 20B design, the acoustic cavity is formed by the gap between the injector and the combustion chamber. With this concept, the baseline injector pattern can be maintained; however, the tuning frequency is not that specified (cavity depth is not sufficient). Note that the tuning frequency as well as the percentage gap area-to-face plate area will vary with the element cup depth adjustment. Also, the requirements for cooling the uncooled portion of the combustion chamber may become excessive (this will be dependent on the seal leakage).

A method of converting the coaxial element configuration into a triplet element configuration also was contemplated and the results are shown in Fig. 21. Figure 21A shows a design where the fuel orifice would be drilled only through the face plate. This required a reduction in the face plate nut diameter and a reduction from the normal impingement angle of 60 to 40 degrees. A further reduction has to be made in the sleeve diameter adjacent to the face plate (the 0.390-inch diameter) since adjacent element fuel holes had a tendency to intersect the sleeves when the face pattern was developed. Even with these modifications to the face nut and sleeve, the cant angle of the triplet varied from radial between 8 and 40 degrees randomly (Fig. 22).

Figure 21B shows a design where the fuel orifices are drilled through the face nut. The problems with this design are associated with fabricating and cleaning a final assembly since the fuel orifices have to be formed after the face nuts are installed. The cant angle variation has not been established but it is assumed to be better than that of the Fig. 21A design.

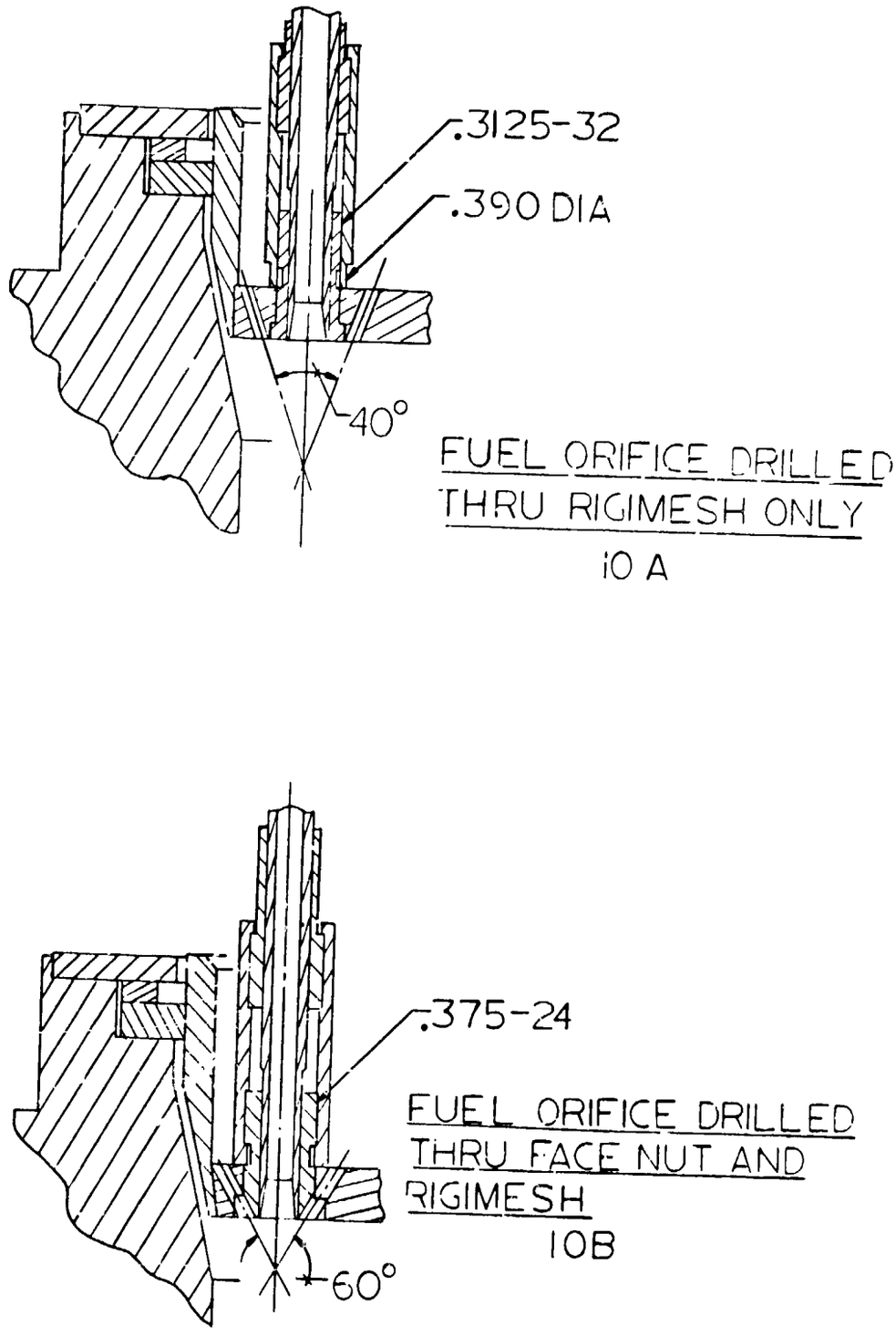

Figure 21. Coaxial Injector Element Conversion to a Triplet

ROW	DIA	ELEMENTS
1	5.008	31
2	3.978	22
3	2.948	16
4	1.918	10
5	.888	5

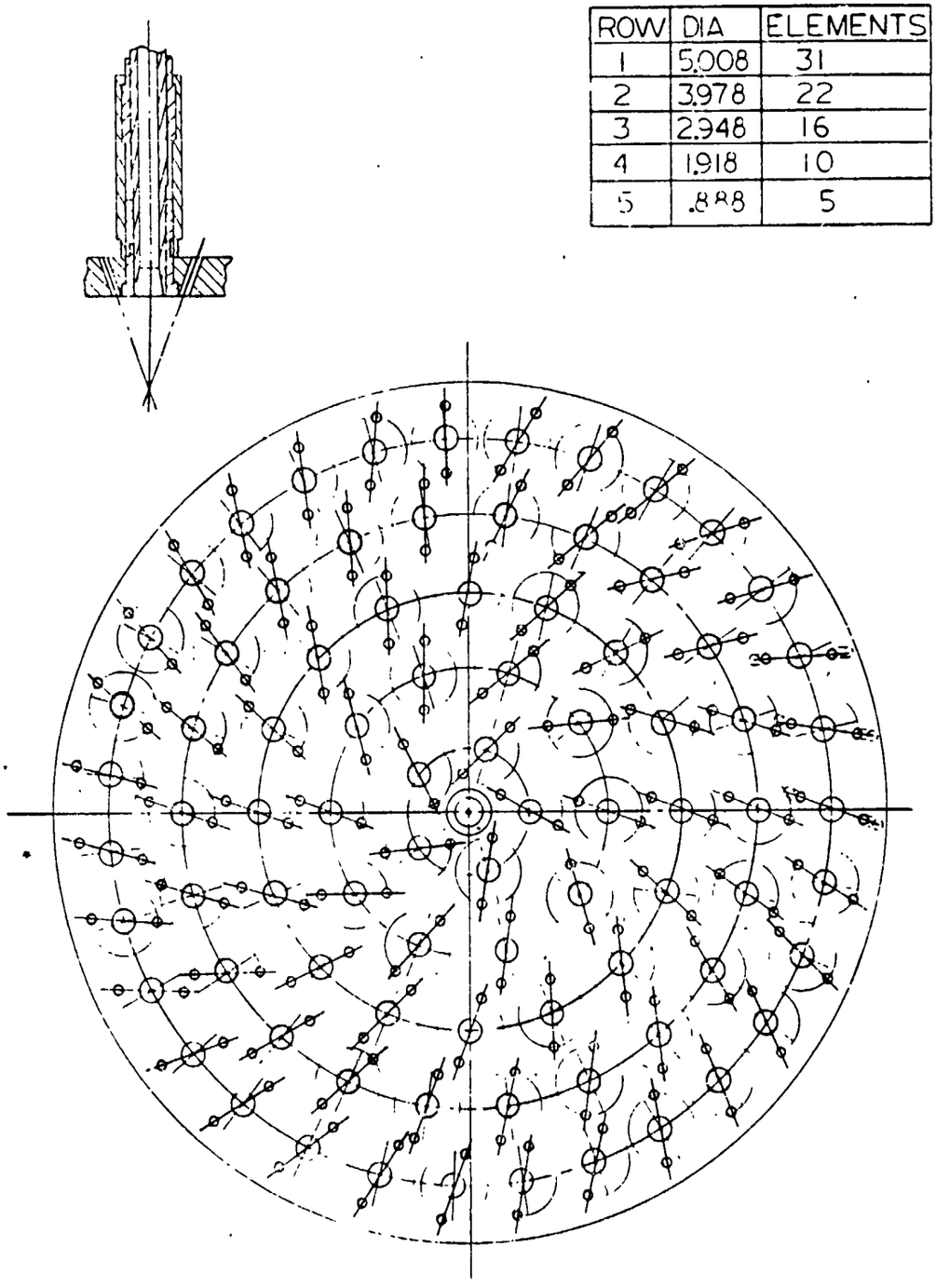

Figure 22. Injector Face Pattern Coaxial Element Conversion to Triplet Element

To obtain a uniform cant angle conversion of the coaxial injector to a triplet injector, the number of elements in each row of the coaxial injector would have to meet the criteria used in the design of the triplet injector. The two outer rows have a 3 to 2 ratio, and after the two outer rows are established, each of the inner rows is, in number of elements, one-half the number of elements in the previous row. To be specific with the present baseline design, the outer row has 31 elements followed by 22, 16, 10, and 5 (for a total of 84 elements). This would be reduced by the triplet criteria to 30, 20, 10, and 5 (for a total of 65 elements) or a 23% loss of coaxial elements.

Injector Face Heat Transfer/Cooling Characteristics

The injector face heating characteristics and cooling requirements were investigated for the coaxial and triplet injector designs for operating chamber pressures from 1800 to 3000 psia. In both designs, the injector face is transpiration cooled through a Rigimesh face plate. The primary objective in this analysis was to establish relative heat loads, coolant flowrates, and injector face operating temperatures for the two injector concepts as a function of operating chamber pressure.

Because of difficulties in measuring injector face heat transfer coefficient, a common means of predicting the injector face heat transfer coefficient was to assume the same value as that determined for the combustion chamber wall near the injector. The injector and heat transfer coefficient scaled from the SSME 40K subscale LOX/H_2 chamber test program applies to the coaxial injector. Flowrate and property corrections are based on standard Nusselt number correlations. The face heat flux was calculated using the gas temperature, face temperature, and heat transfer coefficient. It was assumed that the Rigimesh face and the face coolant discharge are at the same temperature.

Triplet element injectors historically have had higher face heat fluxes than coaxial element injectors. A review of previous Rocketdyne test programs (Ref. 2 and 3), where both triplet and coaxial injectors were tested and results compared, showed that the injector end heat flux of the triplet injector is typically twice that of the coaxial injector. This ratio was therefore assumed for the relative comparison.

The face heat flux as a function of chamber pressure for the two injector configurations is shown in Fig. 23. These results are for a face temperature of 400 F. The estimated throat heat flux also is shown for comparative purposes. The required face coolant flowrate as a function of chamber pressure and face temperature is shown in Fig. 24a for the two injectors. In Fig. 24b, the required flowrate as a percentage of the fuel flowrate is shown. At a given chamber pressure and face temperature, the triplet element injector requires three times as much coolant flow because it has twice the heat flux of and a 50% greater Rigimesh face area than the coaxial element injector.

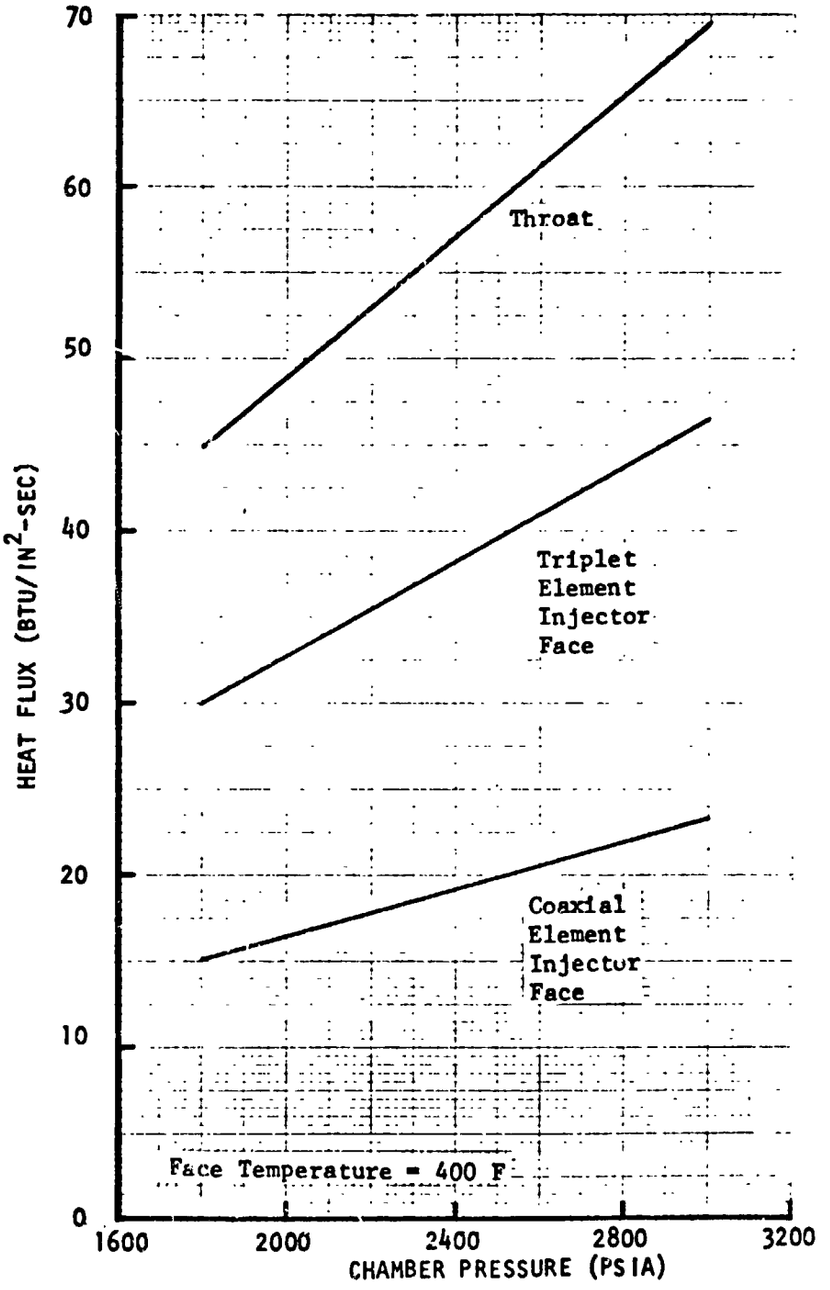

Figure 23. Comparison of Face Heat luxes

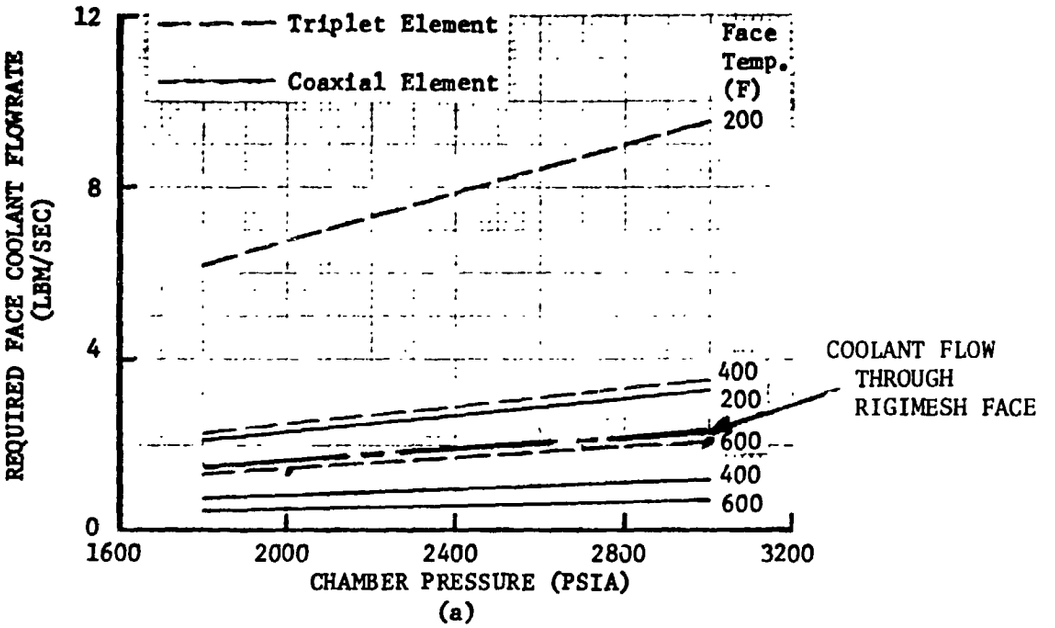

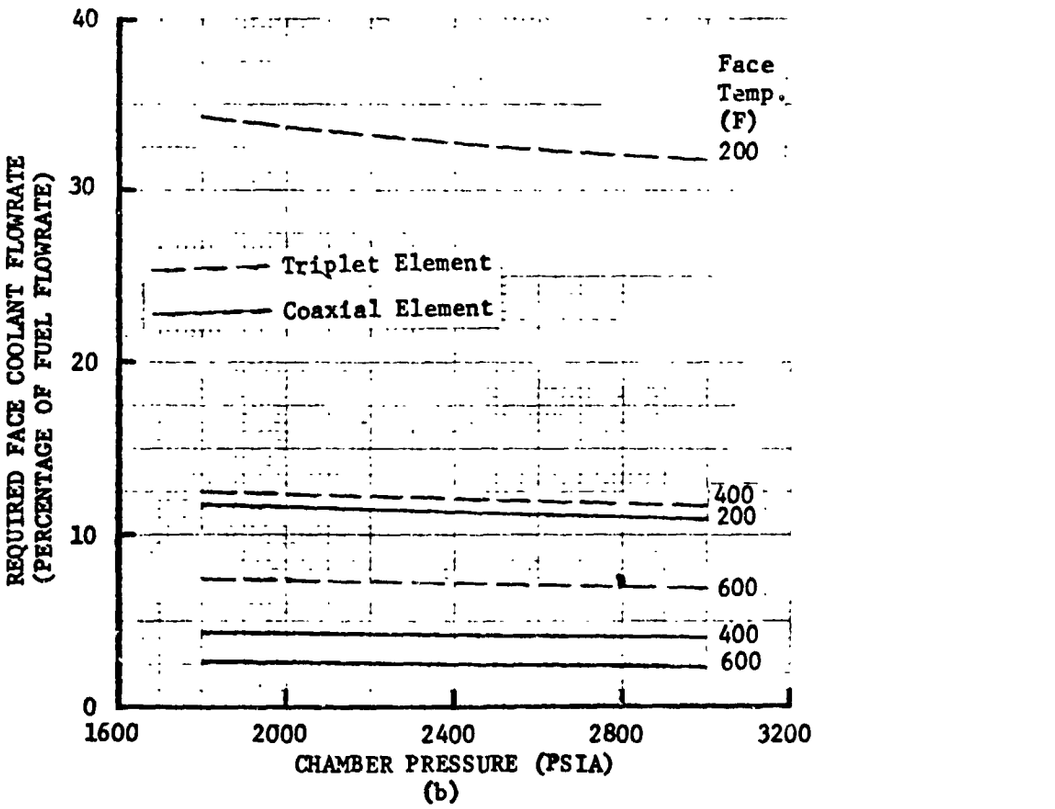

Figure 24. Face Coolant Flowrate Requirements

These results show that the coaxial injector will operate with a face temperature of approximately 300 F over the entire operating range. The triplet injector would operate near 600 F. It would probably be desirable to increase the porosity of the Rigimesh material for the triplet injector.

Injector/Chamber Compatibility

Combustion chamber wall temperature profiles also were determined for the two injector types used in conjunction with the existing regeneratively cooled chambers. The hot-gas chamber wall heat transfer coefficients were established based on the same information used in developing the relative injector face heating characteristics. It was found that with the coaxial injector, the combustion chamber can be regeneratively cooled in an uppass circuit at 3000 psia, but the wall temperature would be 1030 F. At 3000 psia with the triplet injector, the combustion chamber can be cooled in a downpass configuration, but the wall temperature will be 1150 F. The uppass circuit with the triplet injector results in even higher gas-side wall temperatures in the combustion zone. Therefore, for the same wall temperature, the coaxial injector can operate at a higher chamber pressure.

Ignition System

A liquid oxygen/methane injector requires a reliable, relatively high-energy ignition system for positive main propellant ignition to ensure that large amounts of mixed propellants are not accumulated within the thrust chamber prior to ignition. Previous experience indicates that hypergol-type igniters provide a high degree of reliability and simplicity. Two hypergolic compounds were considered relative to ignition requirements of the liquid oxygen/methane injector configuration: chlorine trifluoride (ClF_3) and triethylaluminum (TEA).

The following items were addressed leading to the design of an optimum hypergolic ignition system:

- Selection of the hypergol compound
- Design of the hypergol injection system
- Selection of ignition phase propellant and hypergol sequencing

The goal of this study was to provide a reliable system that minimizes complexity relative to ignition phase and test stand operation.

The candidate hypergol materials are chlorine trifluoride (ClF_3), triethylaluminum (TEA). Triethylaluminum is a fuel that is hypergolic with liquid oxygen, whereas ClF_3 is a highly reactive oxidizer which is hypergolic with methane. The major item relative to the selection of the hypergol to be used for this injector was the ignition phase propellant, i.e., fuel or oxidizer, test stand hypergol handling hardware compatibility, and cleaning and inerting requirements. The characteristics of the candidate hypergol fluids are presented in Table 3.

TABLE 3. HYPERGOL COMPOUND CHARACTERISTICS

Hypergol	Characteristics	Advantages	Disadvantages
Triethylaluminum (TEA)	• Fuel reactive with O_2 • Boiling point +381 F • Freezing point -62.5 F • Low vapor pressure	• Extensive ignition background • Compatible with most metals • Normal hardware cleaning and drying procedures adequate • Less toxic than ClF_3	• Products of combustion • Produces contamination • Freezes at high temperature
Chlorine Trifluoride (ClF_3)	• Oxidizer reactive with fuel • Boiling point 53 F • Freezing point -105 F	• Extensive ignition background • Low Freezing poing	• Highly reactive; hardware must be clean and dry • Requires care in selection of materials • Highly toxic

Triethylaluminum produces residue in the form of aluminum oxide, which can be plated on the thrust chamber walls causing localized disturbance of the chamber wall boundary layer and ultimately producing misleading thrust chamber heat transfer data. Triethylaluminum also tends to form residue within the igniter element. Triethylaluminum being hypergolic with oxygen in the atmosphere presents problems relative to handling on the test stand. Engine systems using triethylaluminum or triethylboron have employed cylindrical cartridges equipped with burst diaphragms as shown in Fig. 25. These cartridges are loaded in a controlled atmosphere and, as such, represent an expense. The techniques required to load a cartridge with TEA equipped with inlet and outlet valves, as shown in Fig. 26 are difficult in a test stand environment. The residue problem and test stand handling problem relative to TEA makes this hypergol an unattractive option.

BURST DIAPHRAGMS

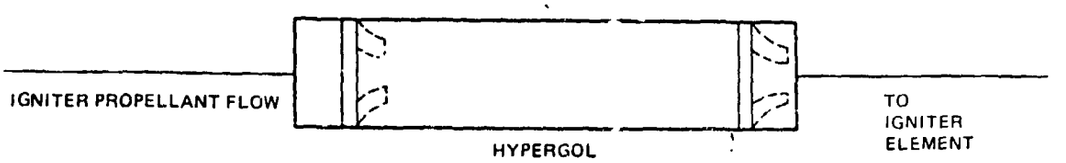

Figure 25. Typical Hypergol Burst Diaphragm Cartridge

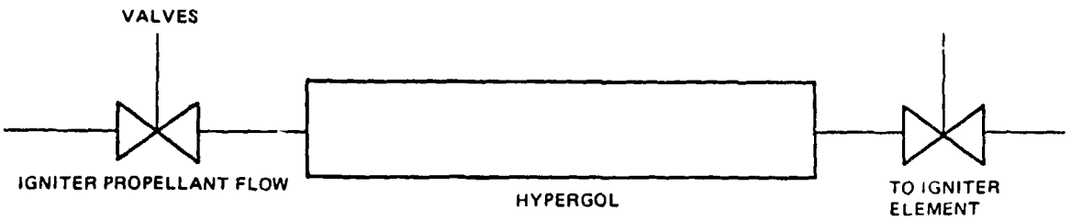

Figure 26. Typical Hypergol Cartridge With Valves

Chlorinetrifluoride does not produce a residue to mask thrust chamber heat transfer results and can be easily loaded in a test stand cartridge equipped with valves. This system was successfully employed on the 40K SSME test series. Use of ClF_3 requires a clean, dry hypergol system. This can be achieved by providing LOX-clean hardware and continuous-duty drying purges of the system on the test stand when not in use.

Based on these considerations, ClF_3 appears to be a more attractive hypergol compound for use for small-diameter, research-type injectors. The major concern relative to the selection then becomes the ignition phase propellant lead. Triethylaluminum being hypergolic with LOX requires a LOX lead, whereas ClF_3 requires a fuel lead to achieve ignition. For a research-type program, the ability to select the ignition phase propellant lead may be desirable. However, a fuel lead would probably be required with a regeneratively cooled chamber. The selection of the hypergol can be influenced by the propellant lead required or either an oxidizer-rich or fuel-rich lead can be accomplished with either hypergol at the

cost of increased complexity in the igniter element and the igniter element propellant feed system (i.e., the igniter element would function as a pilot element which, in turn, lights the main injector).

Two types of hypergol ignition systems have been successfully used on rocket engines: (1) injection of hypergol through all of the injection elements and (2) single-element hypergol injection.

Full-face hypergol injection provides uniform injection; however, this type of system is not warranted with small-diameter injector such as the 5.66-inch-diameter LOX methane injector. The full-face injection requires significantly more hypergol than the single element.

Two types of single element hypergolic igniters (Fig. 27) have been successfully used:

1. Single element, which simply sprays the hypergol into the combustion chamber igniting the initial propellant lead
2. Coaxial element, which injects the hypergol slug through the center of the igniter element, just in front of the oxidizer flow, and fuel through the outer concentric portion of the element. This type of ignition element was successfully used during the SSME 40K thrust chamber program using ClF_3.

Table 4 presents the advantages and disadvantages of the four types of hypergol injection systems. The full-face and single-element systems can restrict the propellant lead to either fuel or oxidizer depending on the type of hypergol being used. The coaxial element continues to operate as a conventional coaxial element during mainstage operation.

The recommended LOX/methane igniter uses chlorinetrifluoride hypergol injected through a single coaxial injection element. Chlorinetrifluoride was selected

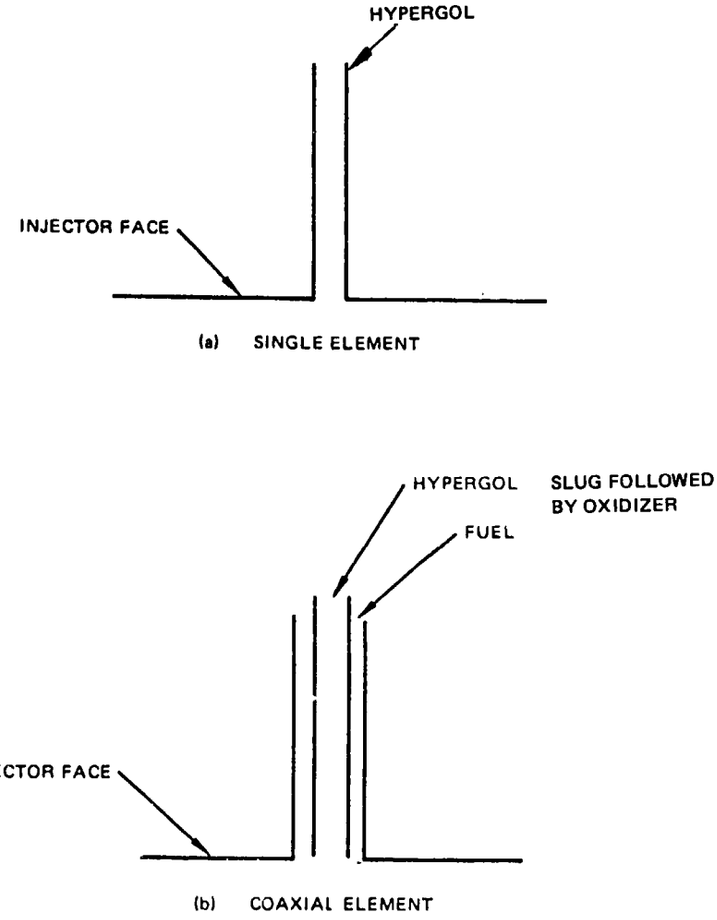

Figure 27. Single-Element Hypergolic Igniters

TABLE 4. HYPERGOLIC INJECTION SYSTEM COMPARISON

Hypergol Injection Type	Advantage	Disadvantage
Full-Face Injection	Uniform hypergol injection through all injector elements	Restricts propellant lead
Single Element	Fabrication simplicity	1. Restricts propellant lead 2. Nonfunctional during mainstage operation; may cause cooling problems
Coaxial Element	Operates as a standard coaxial injector element following hypergol injection and ignition	Restricts propellant lead

based on the ease of handling on the test facility and the successful performance of this hypergol using a single coaxial element on similar small research and development engines.

The LOX flow to the igniter element will be independently fed. Igniter fuel will come from the main element manifold behind the face. A ClF_3 cartridge will be located in the igniter LOX line allowing the igniter LOX flow to push a "slug" of ClF_3 through the center portion of the coaxial element.

Task I Conclusions

1. As a result of analyzing the proposed triplet and coaxial elements considered for the LOX/methane injector design, the coaxial element was recommended for its stable combustion characteristics as well as its potential for high performance:

   a. Triplet mixing efficiency can be in excess of 99%.
   b. Triplet vaporization efficiency should be 100%.
   c. Coaxial mixing efficiency to exceed 97.7%.

d. Coaxial vaporization efficiency should approach 100% with a recessed post (recess should be greater than post ID).

e. High burn rate of impinging element injectors are more likely to experience combustion instability from past experience.

f. Distributed reaction of coaxial element from experience has been relatively stable.

g. Priem stability analysis indicates coaxial element should be more stable than the triplet and slightly more stable than the "rated stable" J-2 injector.

2. A preliminary design of both the triplet and coaxial element injectors indicated that both concepts were feasible and of approximately equal complexity from a fabrication standpoint.

3. Heat transfer analysis indicated that the coaxial element injector would operate with an average face temperature of 300 F and the triplet injector would operate near 600 F.

4. The coaxial injector will permit higher chamber pressure operation than a triplet injector in a regeneratively coded chamber with equal wall temperatures.

5. The selected igniter configuration uses chlorinetrifluoride hypergol injected through a single coaxial injection element.

TASK II - DETAIL DESIGN AND FABRICATION

Ignition System

The Task II effort was initiated with a detailed design analysis of the selected ignitor configuration.

Hypergolic ignition of the 40K LOX/methane injector will be accomplished using chlorine trifluoride (ClF_3). Figure 28 illustrates the ClF_3 injection system, employing a centrally located coaxial igniter element. The ClF_3 will be injected from a cartridge mounted in the feed line by oxidizer delivered from upstream of the main oxidizer flow control venturi. A cavitating venturi downstream of the ClF_3 cartridge will be used for flow control of both the ClF_3 during the ignition phase and the subsequent LOX flow following complete expulsion of the ClF_3 cartridge contents.

The quantity of ClF_3 and size of the flow control venturi were based on delivering a sufficient quantity of ClF_3 over a 1-second interval during full fuel flow to achieve a measurable rise in chamber pressure to be used as an ignition detection signal. The ignition detection signal will be used as a constraint to opening the main oxidizer valve. Figure 29 presents the calculated chamber pressure vs ClF_3 flow based on full fuel flow at the 1800- and 3000-psia chamber pressures.

A ClF_3 flowrate of 2 lb/sec was selected, which will yield a chamber pressure increase of approximately 42 psi when ignited with the methane. Experience with the 40K SSME hardware indicated that a 40-psi chamber pressure increase was sufficient to provide a reliable ignition detect signal. The cartridge will be sized to hold 2 pounds of ClF_3, sufficient for 1 second of flow following actuation of the igniter valve, ensuring that ClF_3 is flowing during the entire ignition and transition to mainstage.

The calculated chamber and igniter variables at the 1800- and 3000-psia chamber pressure conditions are presented in Table 5 . The igniter flowrates have been selected based on assumed oxidizer inlet pressures employed during the SSME 40K program.

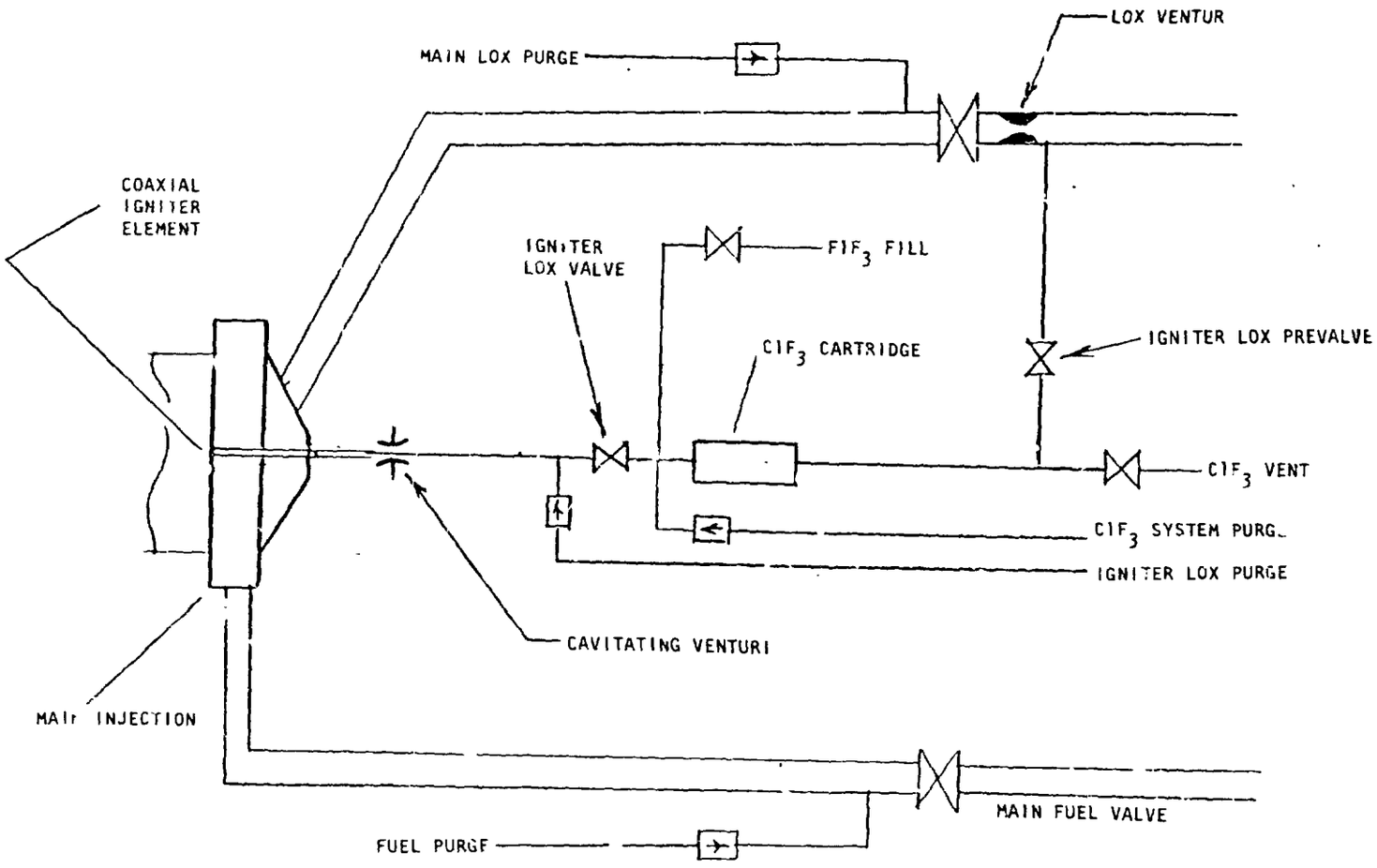

Figure 28. LOX/Methane Injector Hypergol Ignition System

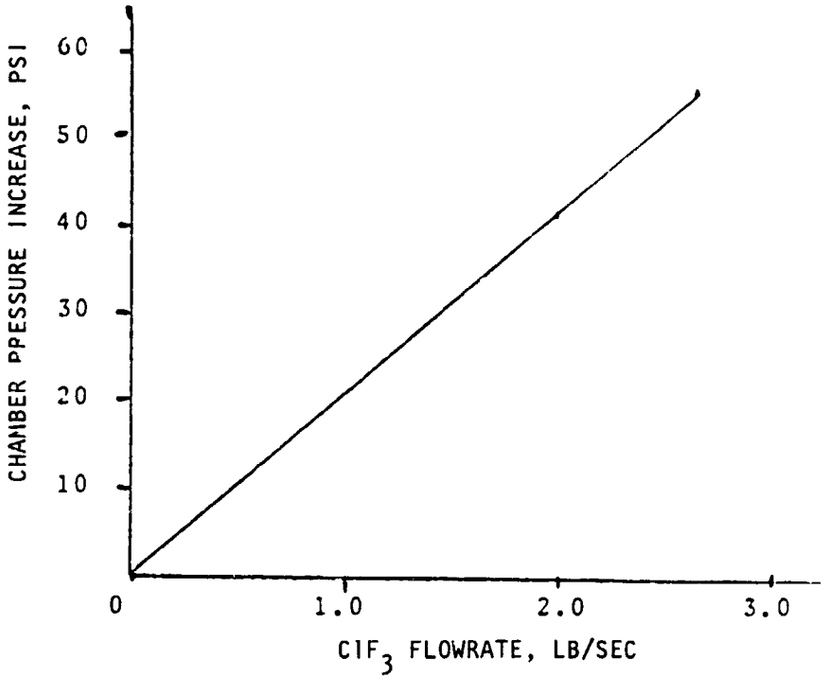

Figure 29. Chamber Pressure Increase vs ClF_3 Flow

TABLE 5. IGNITER ELEMENT OPERATING CHARACTERISTICS

	P_c	
	3000	1800
Ignition Phase		
Igniter Element ClF_3 Flowrate, lb/sec	2	2
Igniter Element CH_4 Flowrate, lb/sec	0.2047	0.1184
Igniter Element MR (ClF_3/CH_4)	9.77	16.89
Igniter Element Flame Temperature, F	5240	4000+
Main Chamber Fuel Flowrate, ib/sec	31	18
Main Chamber P_c (fuel flow only), psia	191	111
Main Chamber Fuel Manifold Pressure, psia	1732	1005
Assumed Oxidizer Igniter System Inlet Pressure, psia	4700	3000
Mainstage Operation		
Igniter LOX Flow, lb/sec	1.357*	1.34*
Igniter Fuel Flow, lb/sec	0.2834	0.1688
Igniter MR (LOX/CH_4)	4.788	7.938

*LOX flowrate during mainstage based on ρ = 55 lb/ft^3

The ignition system flowrates and mixture ratio are based on the minimum quantity of ClF_3 required to achieve a reliable indication of ignition (chamber pressure increase). Upon completion of ClF_3 expulsion, the initial LOX flow will be low due to two-phase flow in the warm igniter oxidizer line. As the run duration progresses, the LOX quality will improve and the igniter LOX flowrate will increase reaching a maximum value after approximately 15 seconds based on SSME 40K thrust chamber data. An estimate of the maximum values is given in Table 5.

The significant dimensions associated with the igniter element are shown in Fig. 30. Ignition and cutoff valve sequencing is shown in Fig. 31.

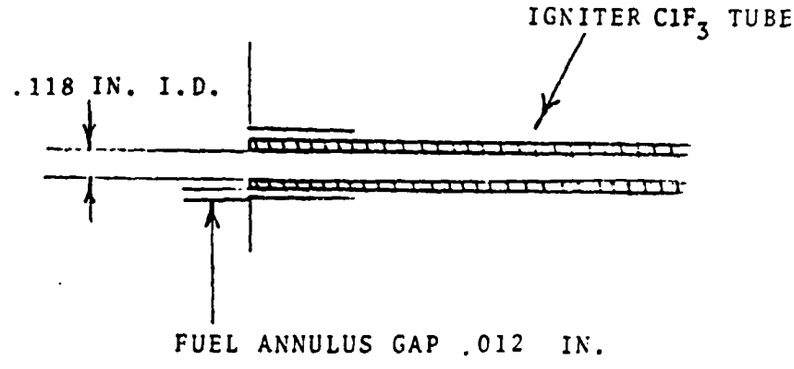

Figure 30. LOX/Methane Injector [illegible] Element

Design Description

The 82-element coaxial injector assembly illustrated in Fig. 32 consists of the faceplate assembly, oxidizer post assembly, igniter assembly, and injector body assembly with the fuel manifold. Additional components for the hot-firing configuration (Fig. 33) are the LOX dome assembly, the thrust chamber assembly, and the thrust mount. All of these additional components are mechanically connected to the injector assembly. The injector design parameters are shown in Table 6.

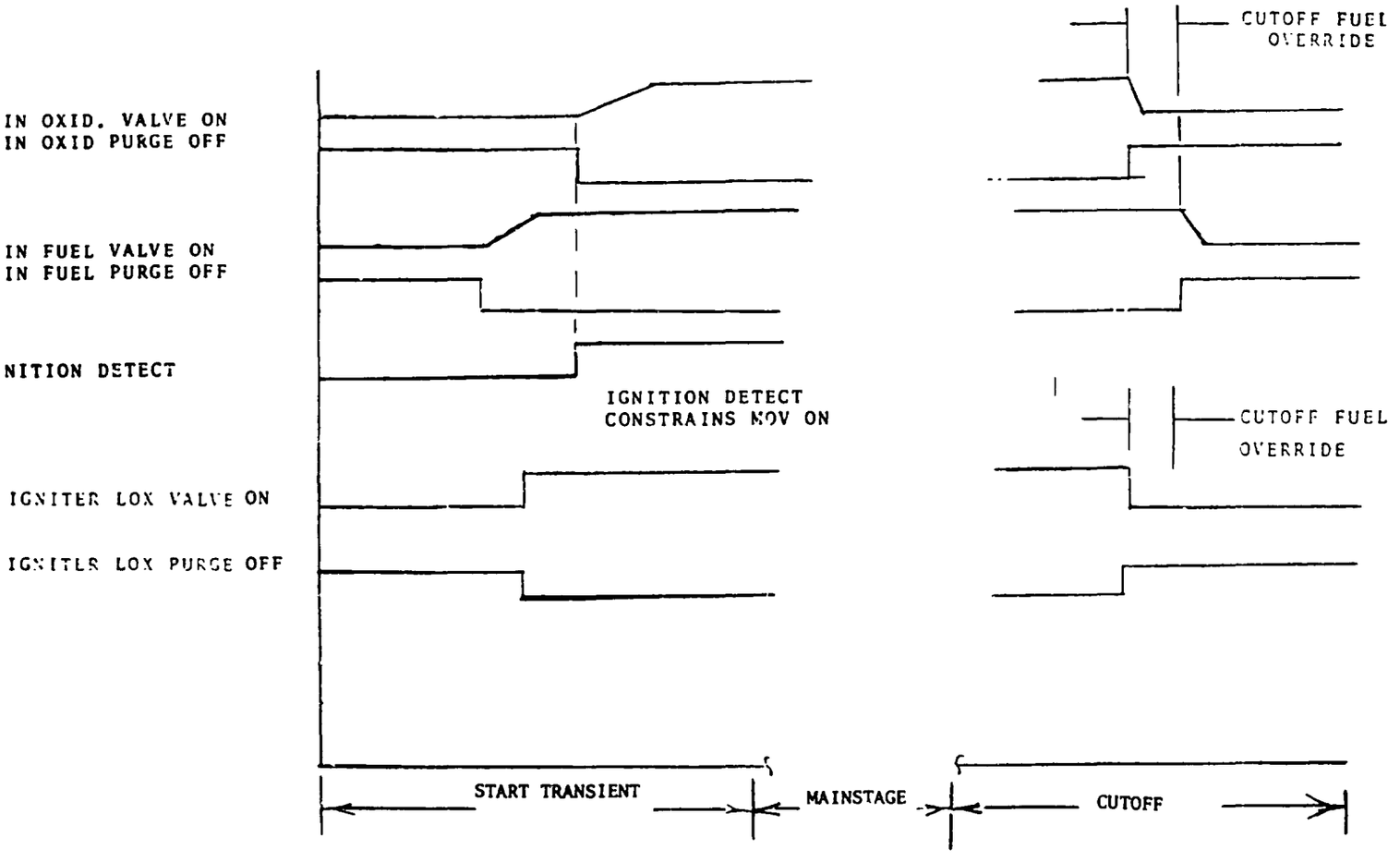

Figure 31. LOX/Methane Ignition and Cutoff Transient

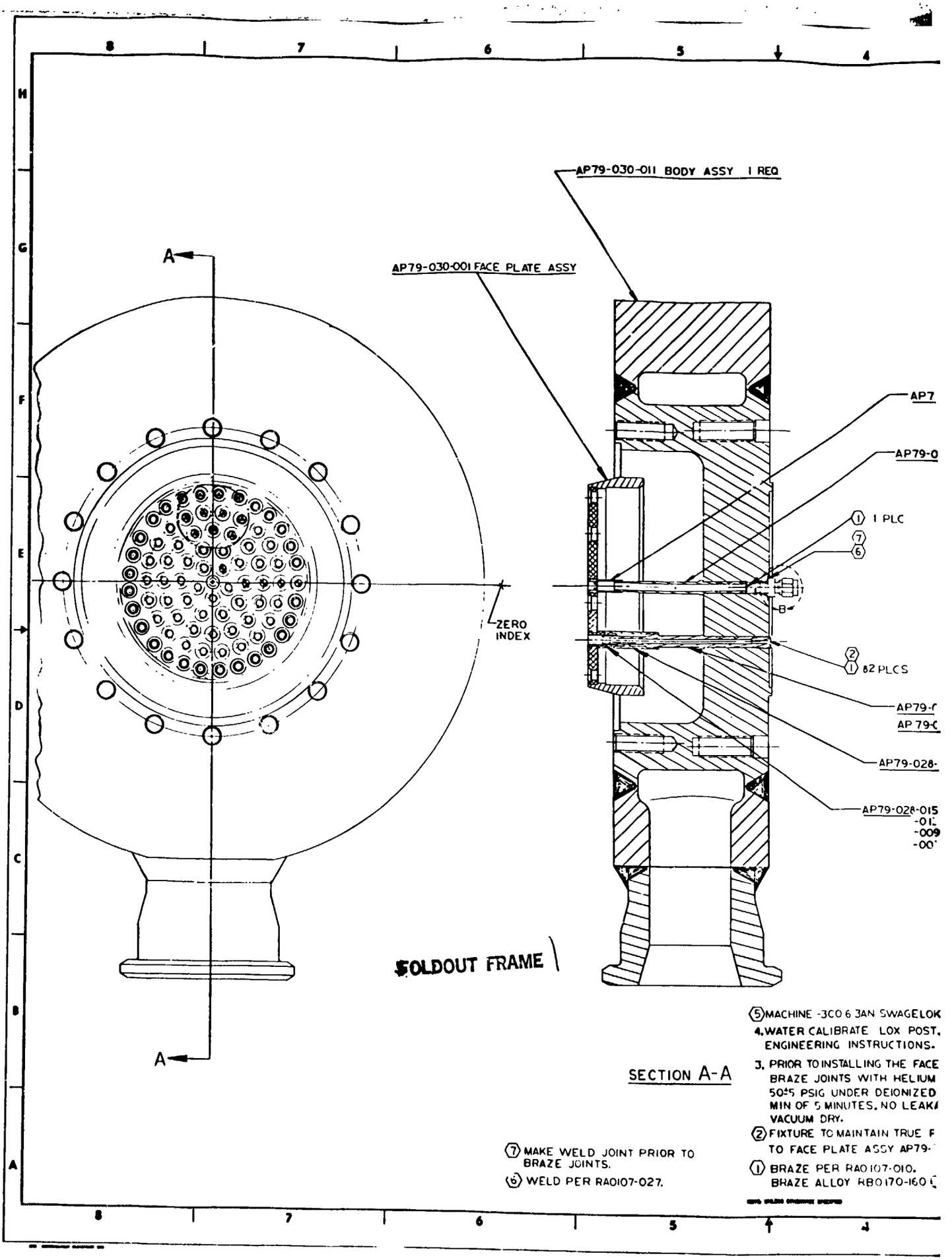
AP79-030-011 BODY ASSY 1 REQ
AP79-030-001 FACE PLATE ASSY
A
A
ZERO INDEX
AP7
AP79-0
1 PLC
7
6
B
2
1 82 PLCS
AP79-(
AP 79-(
AP79-028-
AP79-028-015
-01
-009
-00
FOLDOUT FRAME
SECTION A-A
5 MACHINE -3C0 6 3AN SWAGELOK
4. WATER CALIBRATE LOX POST. ENGINEERING INSTRUCTIONS.
3. PRIOR TO INSTALLING THE FACE BRAZE JOINTS WITH HELIUM 50±5 PSIG UNDER DEIONIZED MIN OF 5 MINUTES. NO LEAK/ VACUUM DRY.
2 FIXTURE TO MAINTAIN TRUE F TO FACE PLATE ASSY AP79-
1 BRAZE PER RA0107-010. BRAZE ALLOY RB0170-160
7 MAKE WELD JOINT PRIOR TO BRAZE JOINTS.
6 WELD PER RA0107-027.

FOLDOUT FRAME 2

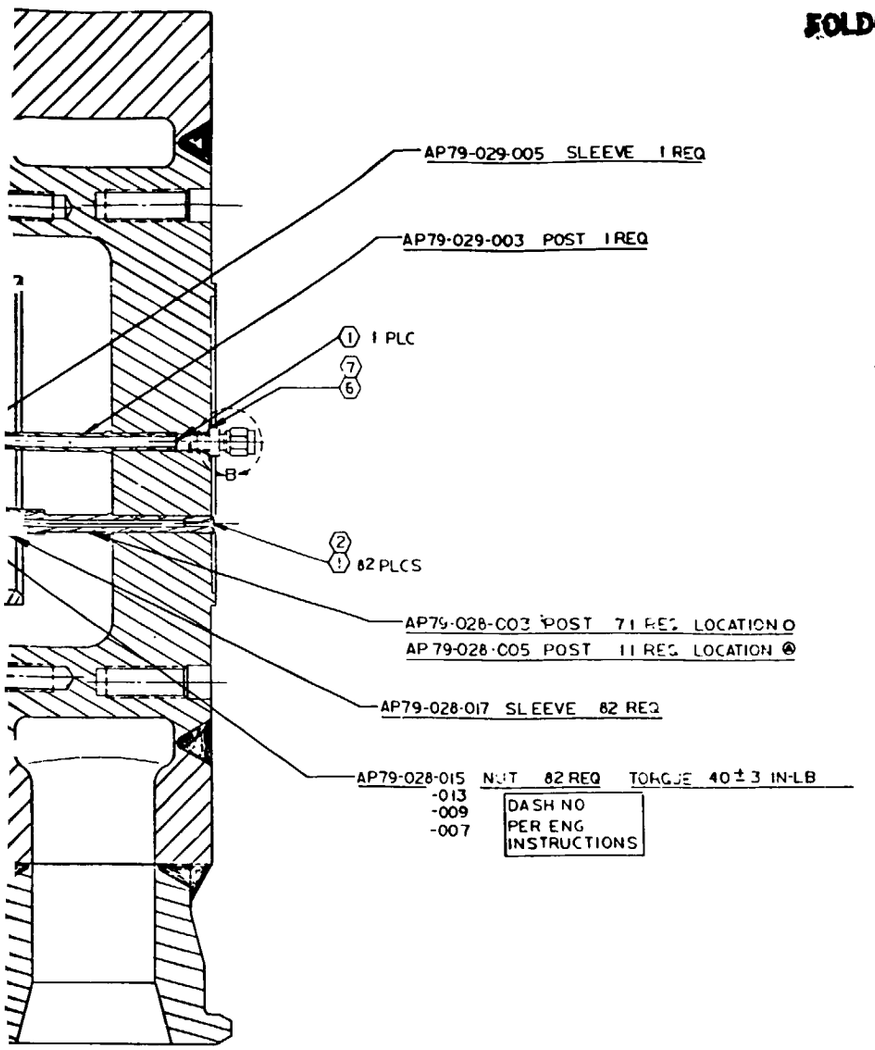

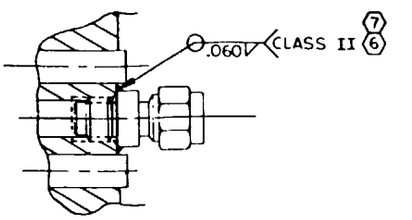

VIEW B
SCALE 2/1

Figure 32. 40K Injector Assembly

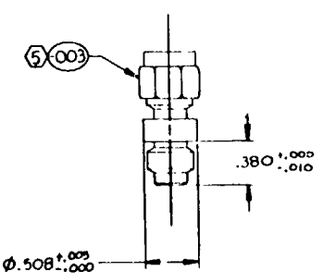

SCALE 2/1

⑤ MACHINE -3CO-6-3AN SWAGELOK PER DIMENSIONS SHOWN.

4. WATER CALIBRATE LOX POSTS PER ENGINEERING INSTRUCTIONS.

3. PRIOR TO INSTALLING THE FACE PLATE, LEAK TEST BRAZE JOINTS WITH HELIUM (MIL-P-27407) AT 50±5 PSIG UNDER DEIONIZED WATER FOR A MIN OF 5 MINUTES. NO LEAKAGE ALLOWED. VACUUM DRY.

② FIXTURE TO MAINTAIN TRUE POSITION RELATIVE TO FACE PLATE ASSY AP79-030-001 HOLES.

① BRAZE PER RA0107-010. BRAZE ALLOY RB0170-160 (PALNIRO NO. 7).

-011 BODY ASSY 1 REQ

ECTION A-A

PRIOR TO

-027.

NO	MATERIAL	SIZE	SPECIFICATIONS	QTY	ZONE
-003	316 SS	NOTED			

-001

Rocketdyne Division, Rockwell International Corporation, Canoga Park, California

40K INJECTOR ASSY

SIZE E | FSCM NO. 02602 | PART NO. AP79-031

SCALE FULL | SHEET

64

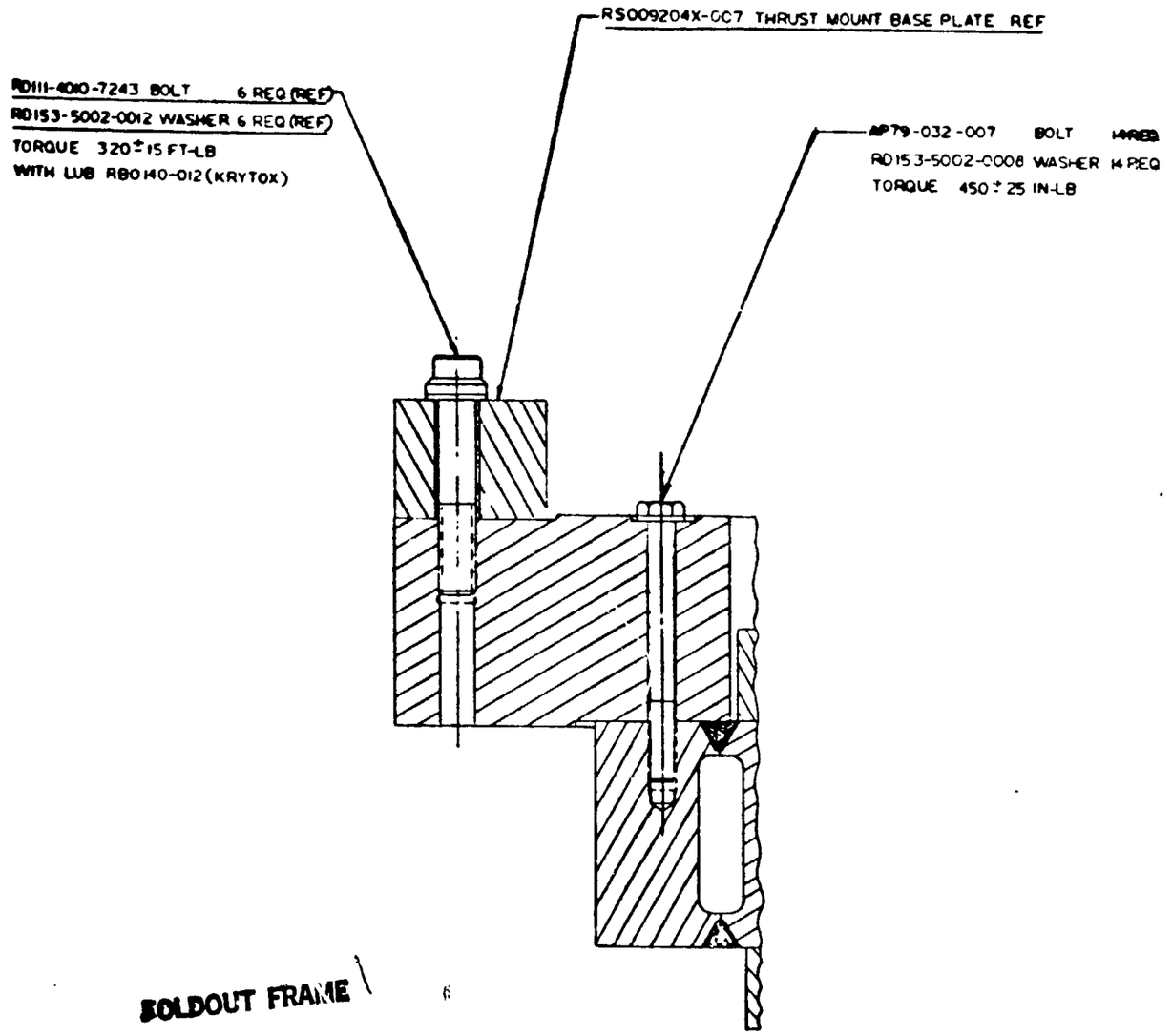

BOLDOUT FRAME

SECTION B-B

FOLDOUT FRAME 2

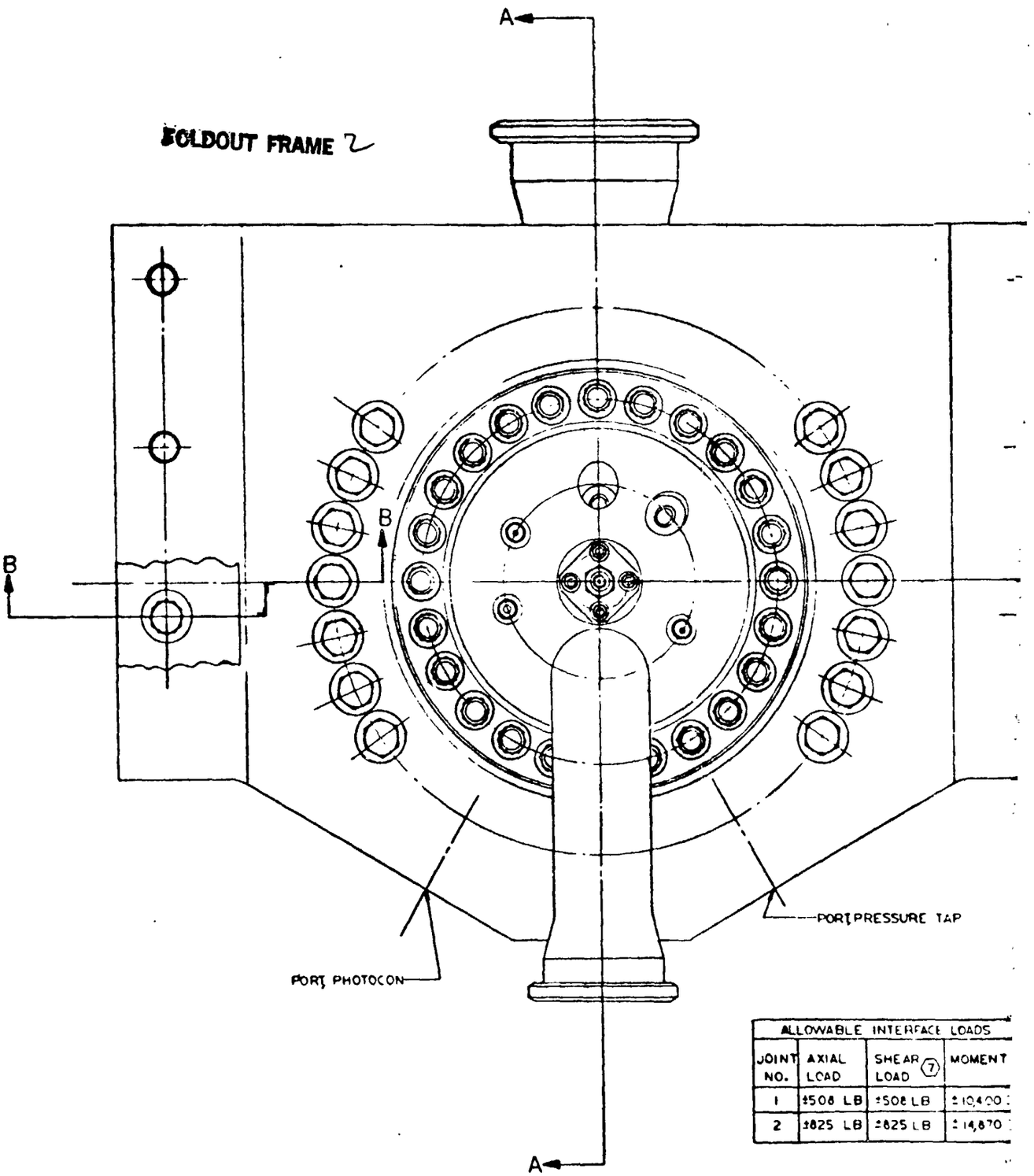

ALLOWABLE INTERFACE LOADS			
JOINT NO.	AXIAL LOAD	SHEAR LOAD (7)	MOMENT
1	±508 LB	±508 LB	± 10,400
2	±825 LB	±825 LB	± 14,870

94237	SEAL	1 REQ	
46503	2 PIECE CLAMP	1 REQ	(REF)
70414	STUD WITH NUTS	4 REQ	

FOLDOUT FRAME 3

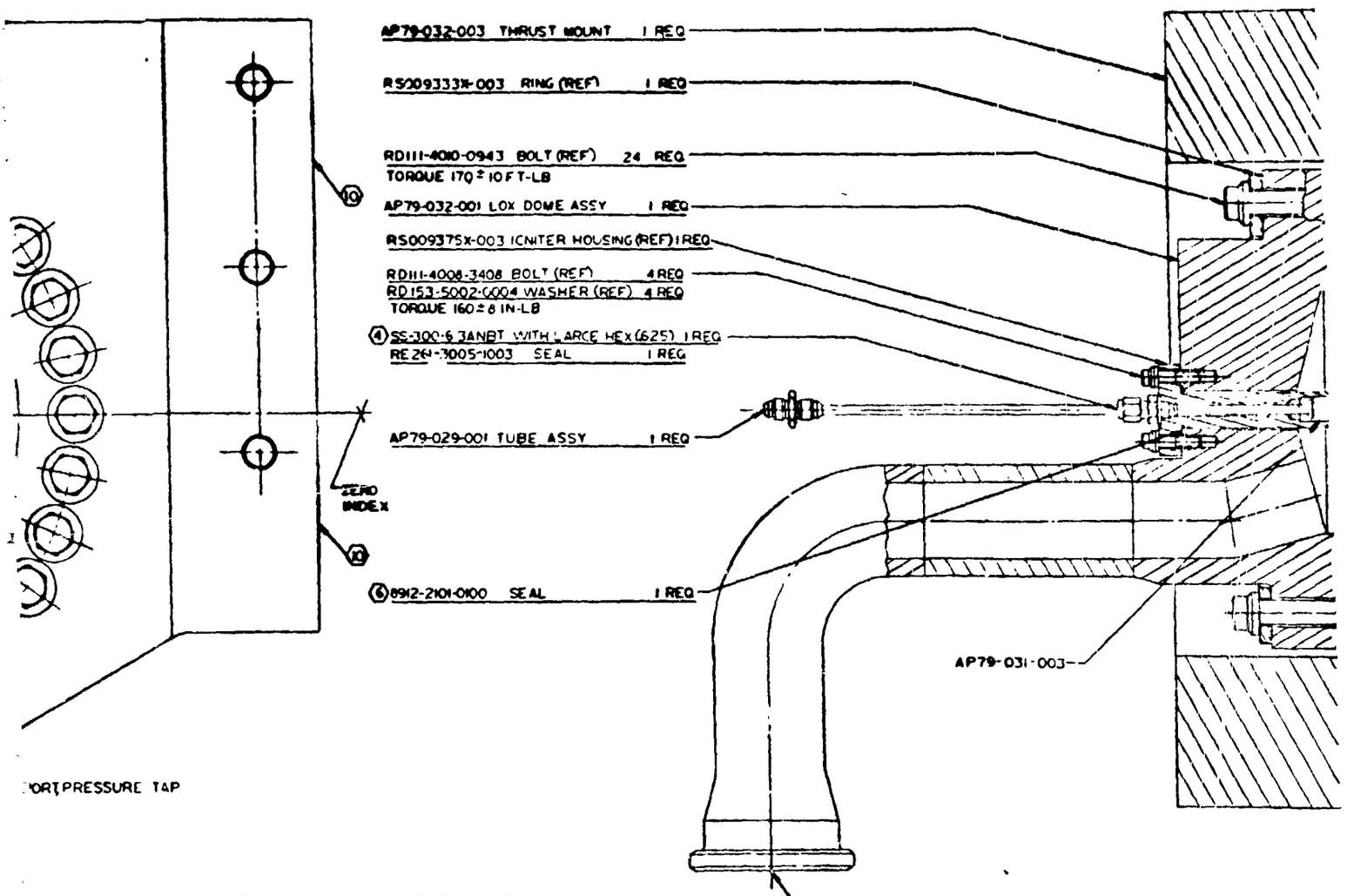

VABLE INTERFACE LOADS			
IAL AD	SHEAR LOAD (7)	MOMENT (7)	FITTING REF (9)
LB	±508 LB	±10,400 IN-LB	2GR 20 SCH 160 ARMCO 21-6-9
LB	±825 LB	±14,870 IN-LB	3GR 25 SCH XX SA-182-F316

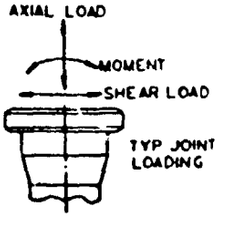

SECTION A-A

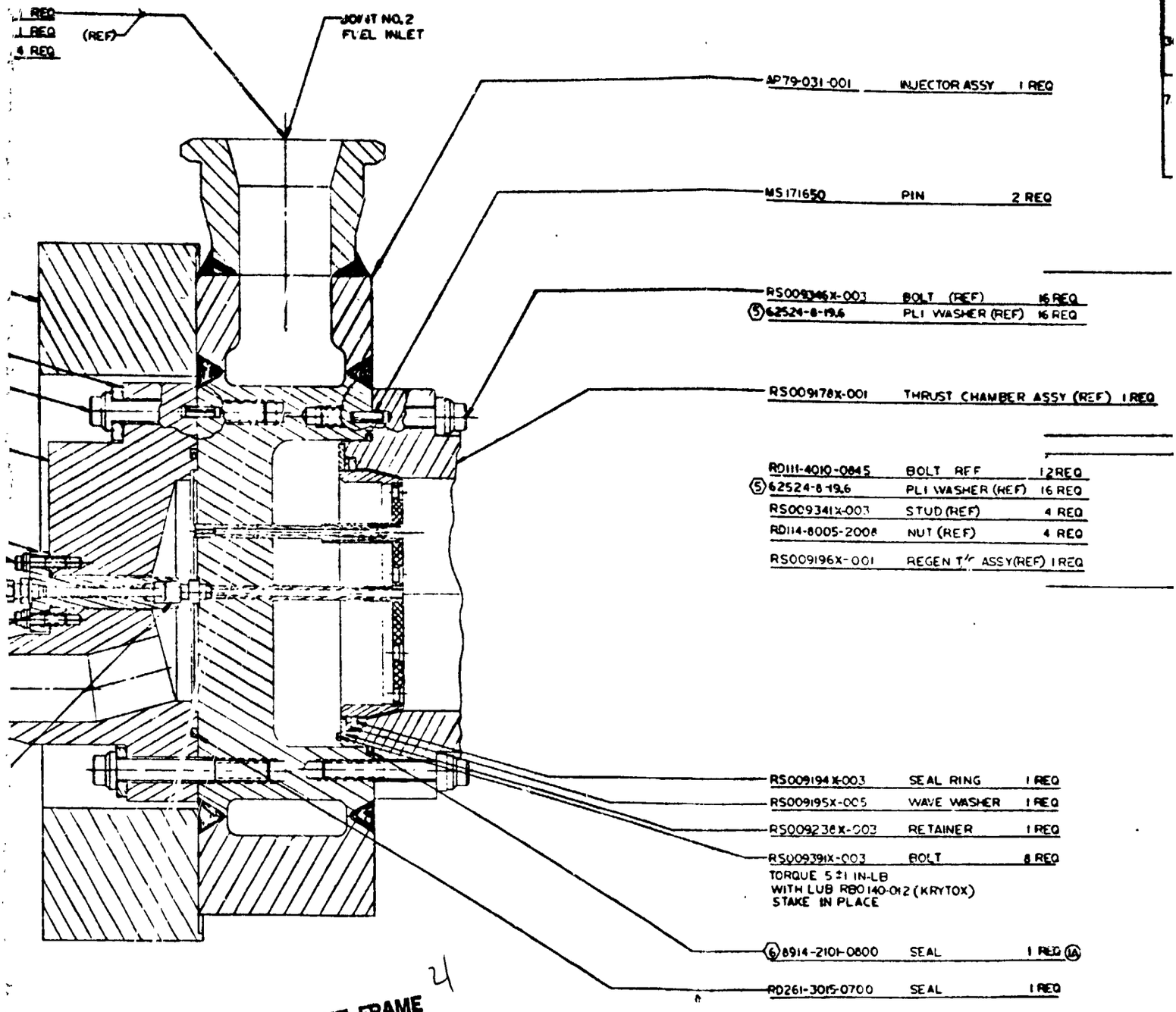

FOLDOUT FRAME 4

(K) AMERICAN SAFTY HOIST RING ADB 2 J002
TORQUE 25 FT-LB.

⑨ GRAY TOOL COMPANY. NORWALK, CAL. (921-7761)
8. CLEAN AND HANDLE PER RA0110-004.
⑦ LIMIT LOAD, SHEAR LOAD AND MOMENT MAY BE ROTATED IN THE PLANE OF THE FLANGE INTERFACE.
⑥ PARKER SEAL CO., CULVER CITY, CALIF.
⑤ PRECISION FASTENER DIV. STANDARD PRESS STEEL CO, JENKINTOWN, PENN.
④ CRAWFORD FITTING CO, SOLON, OHIO.
3. CAP AND PLUG STANDARD PORTS PER RA0116-054.
2. BUBBLE LEAK CHECK SEALS WITH HELIUM AT 100 ± 10 PSIG. NO LEAKAGE ALLOWED.
1. INSTALL THREADED FASTENERS PER RA0101-002.

Figur

-011
-001

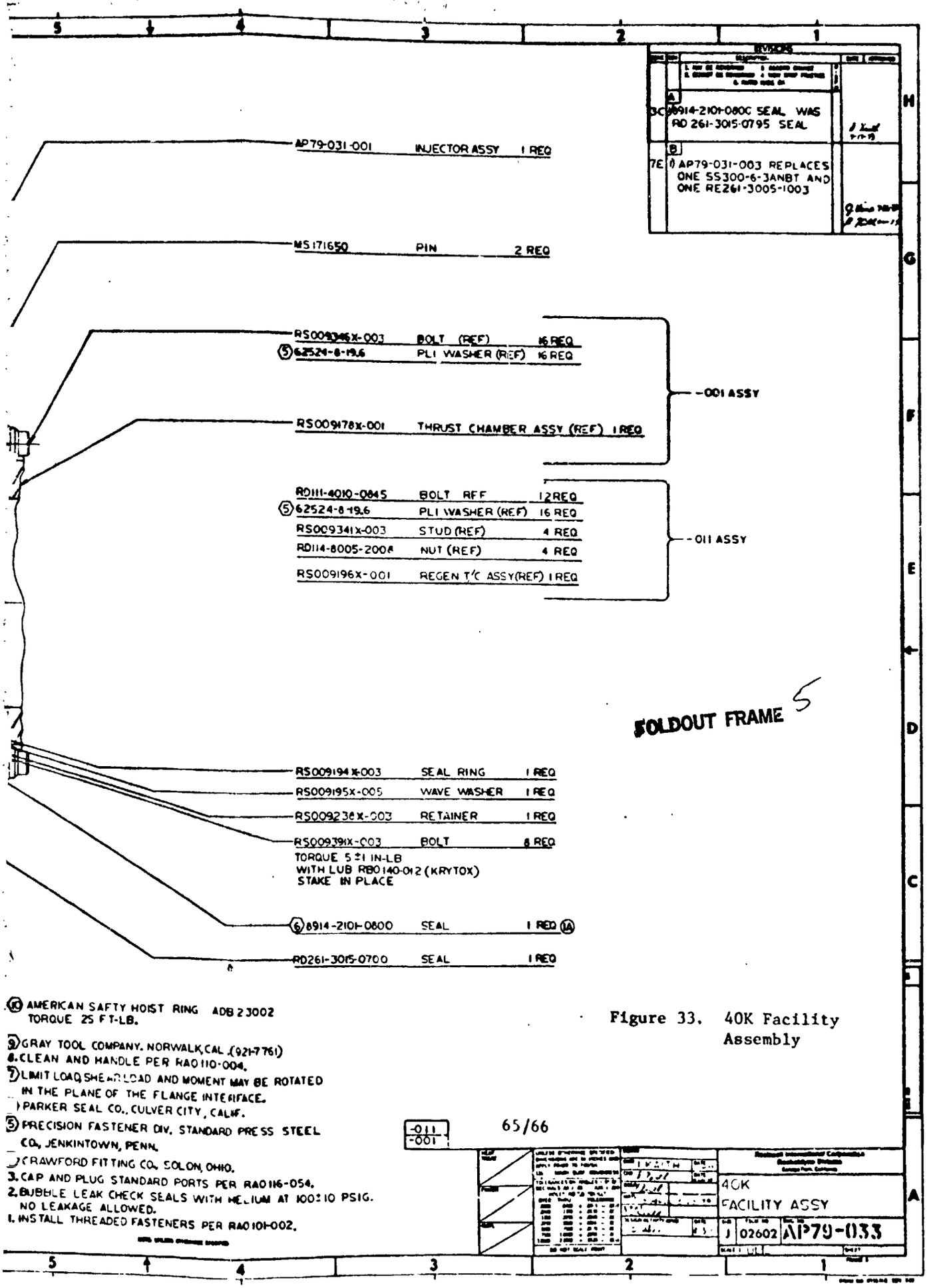

Figure 33. 40K Facility Assembly

TABLE 6. 40K LOX-METHANE INJECTOR DESIGN PARAMETERS

P_c, psia	3000
Mixture Ratio	3.5
c*, ft/sec	5947
Chamber Throat, $in.^2$	8.60
$\dot{W}$ Oxidizer, lb/sec	108.7
$\dot{W}$ Fuel, lb/sec	31.0
Density Oxidizer, lb/ft^3	71
Density Fuel, lb/ft^3	11.48

The pressures and temperatures used for stress analysis are:

	Nominal	Maximum
Injector End Pressure (P_c), psia	3000	3150
Injector LOX Dome Pressure, psia	4000	4400
Injector Fuel Manifold Pressure, psia	3400	3550
Face Pressure ΔP During Fuel Lead, psia	1550	1650
Igniter Tube Pressure (ClF_3), psia	3100	3250
Fuel Inlet Temperature, F	60	100
Oxidizer Inlet Temperature, F	-290	-270
Injector Face Temperature, F	300	400

Faceplate Assembly. The faceplate assembly consists of the faceplate and attaching ring. The ring is machined from A286 CRES plate and ground on the OD to the tight tolerances required by the piston ring seal used in the final assembly. The faceplate is 347 CRES porous plate (Rigimesh) joined to the ring by an EB weld. The porous plate allows the exposed face surface to be cooled by the fuel. The faceplate assembly is attached to the injector body through the oxidizer post assemblies. The holes in the faceplate are machined to mate with the face nuts except for the center port, which is [illegible]ed to receive the igniter sleeve.

Oxidizer Post Assembly. The oxidizer post assembly consists of the oxidizer post, the oxidizer post sleeve, and the face nut. The oxidizer post is machined from 316L CRES bar. This material was selected because of its brazing properties. The inlet to the post is an orifice designed to control the oxidizer flowrate. Seventy-one of the posts have an orifice diameter of 0.086 inch. Eleven of the posts have an inlet diameter of 0.085 inch. These 11 posts are in the direct flow path of the oxidizer inlet manifold, and the reduced orifice diameter is designed to improve the oxidizer distribution at the injector face. The discharge diameter of the oxidizer post is 0.182 inch. The post also has a left-hand thread area on which the oxidizer post sleeve is threaded during assembly of the injector.

The oxidizer post sleeve is machined from 321 CRES bar. The sleeve has three orifice slots which emit the fuel into the annular area formed by the oxidizer post and the face nut. It also has three tangs which center the sleeve on the post. One end of the sleeve has internal left-hand threads which thread to the post, and the other end of the sleeve has internal right-hand threads into which the face nut is threaded. The threads are dry-film lubricated to allow easy assembly and disassembly of the parts.

The face nuts are machined from a 286 CRES bar. This material was selected because better tensile properties were required for the face nuts than for the oxidizer posts and the oxidizer post sleeves. Several different face nuts were designed to deliver the fuel over a range of velocities to develop injector-element performance characteristics over a range of momentum ratios.

It should be noted that the oxidizer post sleeve has a "turnbuckle" effect which is used to adjust the injector-element cup depth, i.e., the distance between the end of the oxidizer post and the hot side of the faceplate. Once the oxidizer posts are brazed into the injector body (along with the igniter post), the sleeves are threaded on the oxidizer posts to a predetermined height based on the desired cup depth. The faceplate is then positioned on the sleeves and attached to the sleeves with the fact nuts. A variety of tooling is used to accomplish this assembly and, once the faceplate nuts are tightened, they are staked in

in place (the staking being done is the Rigimesh). The load path for the pressure drop across the faceplate is through the face nuts which support the Rigimesh into the oxidizer post sleeve which, in turn, passes the load into the oxidizer post which, in turn, passes the load into the oxidizer post braze joint.

The initial setting for the oxidizer post assembly is for a fuel velocity of 500 ft/sec and a cup depth of 1/2 D (D being the OD of the LOX post, 0 202). This will result in a high momentum ratio and a nonburning cup condition.

Igniter Assembly. The igniter assembly consists of the igniter post, the igniter sleeve and the igniter tube (see Fig. 34). The igniter post is machined from 316L CRES bar, a material selected because of its brazing properties. The igniter post is brazed into the injector body along with the oxidizer posts. The igniter post forms a tunnel for the igniter tube.

The igniter sleeve threads into the faceplate, and no mechanical attachment exists between it and the igniter post or the igniter tube. This floating condition eliminates any thermal stress that would be induced by differential temperatures between the igniter tube and the oxidizer posts. The igniter sleeve forms an annular area around the igniter post, thus controlling the fuel flow required during ignition. The igniter sleeve is machined from nickel 200.

The igniter tube assembly consists of a 321 CRES tube (3/16-inch OD) to which a threaded union has been brazed at one end and nickel tube welded at the other. The nickel tube end is used because of better heat transfer characteristics compared to 321 CRES. The tube introduces the hypergolic liquid into the thrust chamber during the ignition phase, and LOX during the remainder of the injector operation. As previously stated, the igniter sleeve controls the flow of the fuel; therefore, during steady-state operation, the igniter element acts the same as the other injector elements except that its flowrate is approximately half of the other elements.

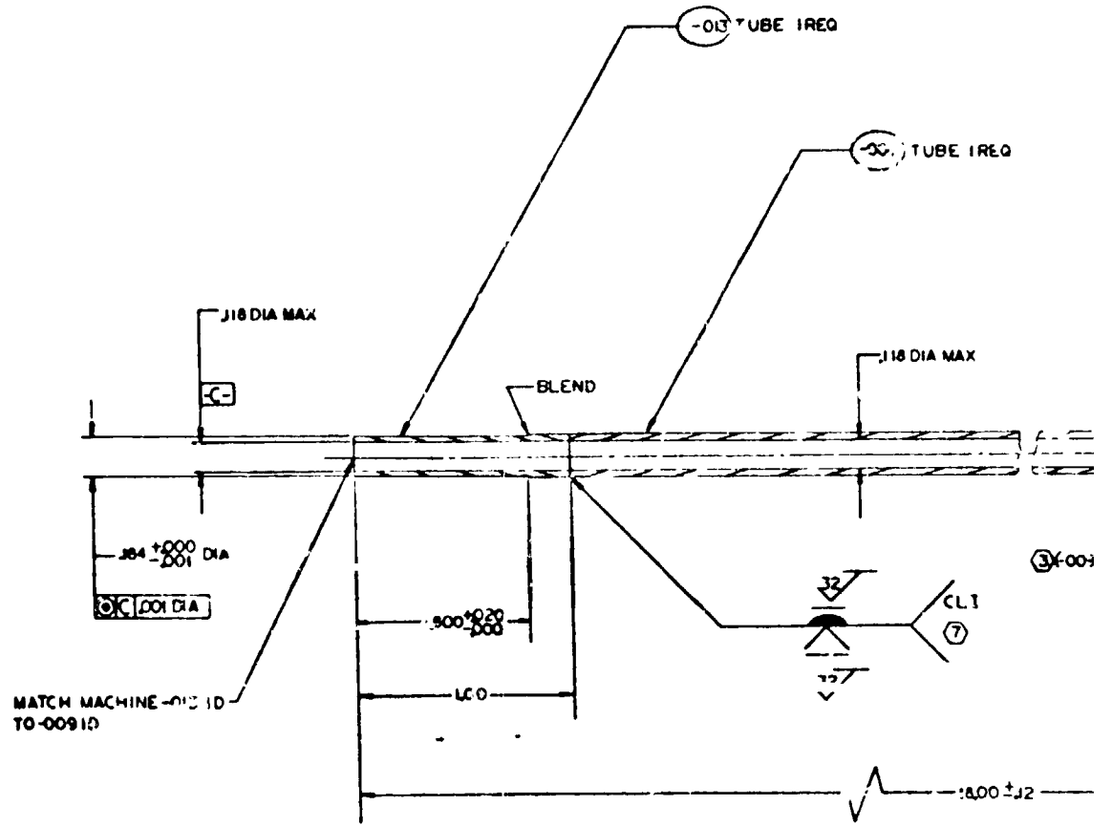

-001 TUBE ASSY (6)(5)

SCALE 4X

FOLDOUT FRAME 1

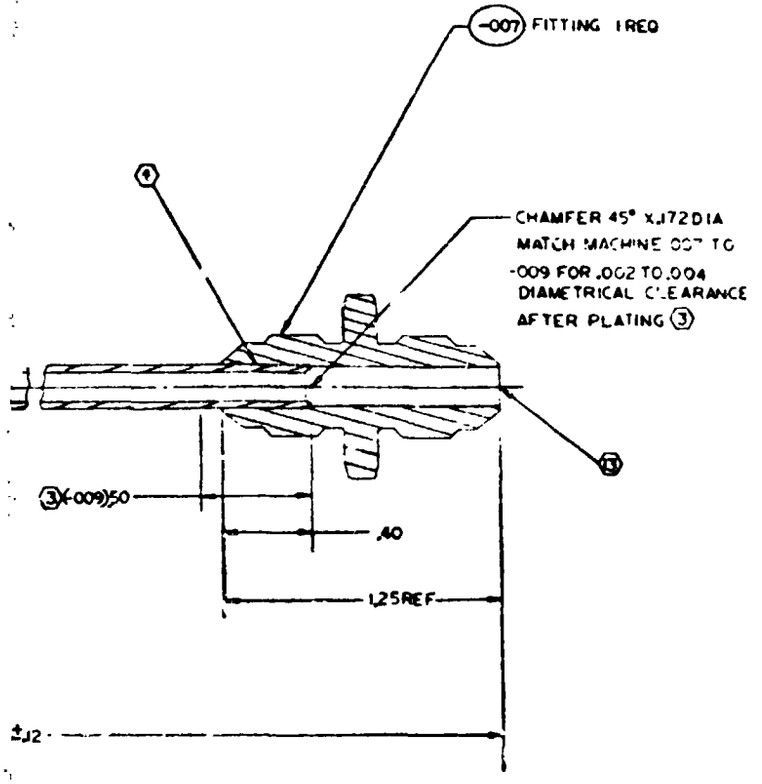

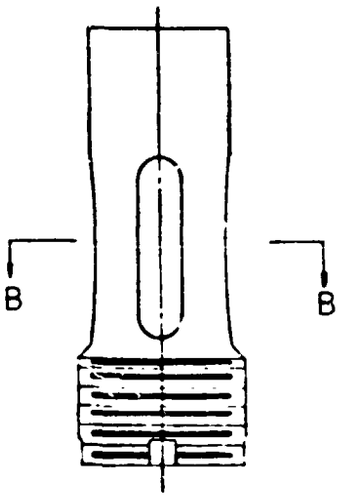

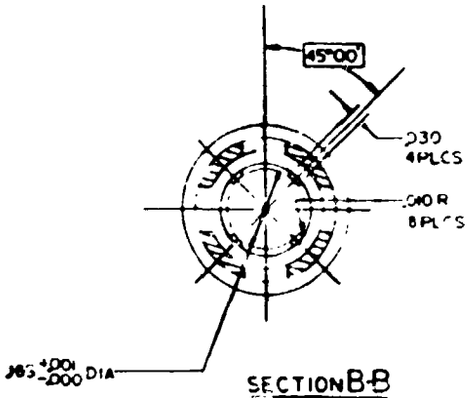

SECTION B-B

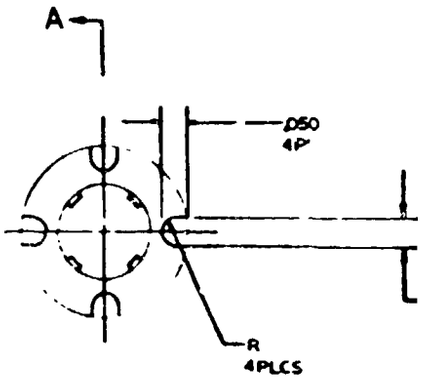

FOLDOUT FRAME 2

B

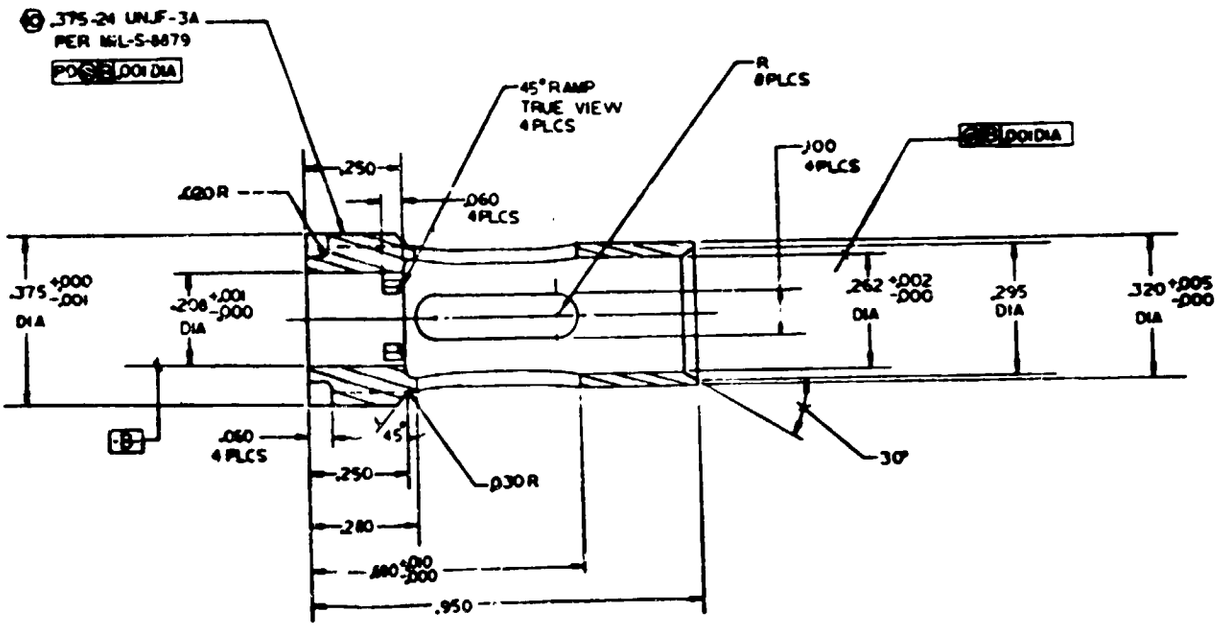

SECTION A-A

.050
4PLCS

.080
4PLCS

R
4PLCS

-005 SLEEVE
SCALE 8X

SOLDOUT FRAME 3

SOLDOUT FRAME 4

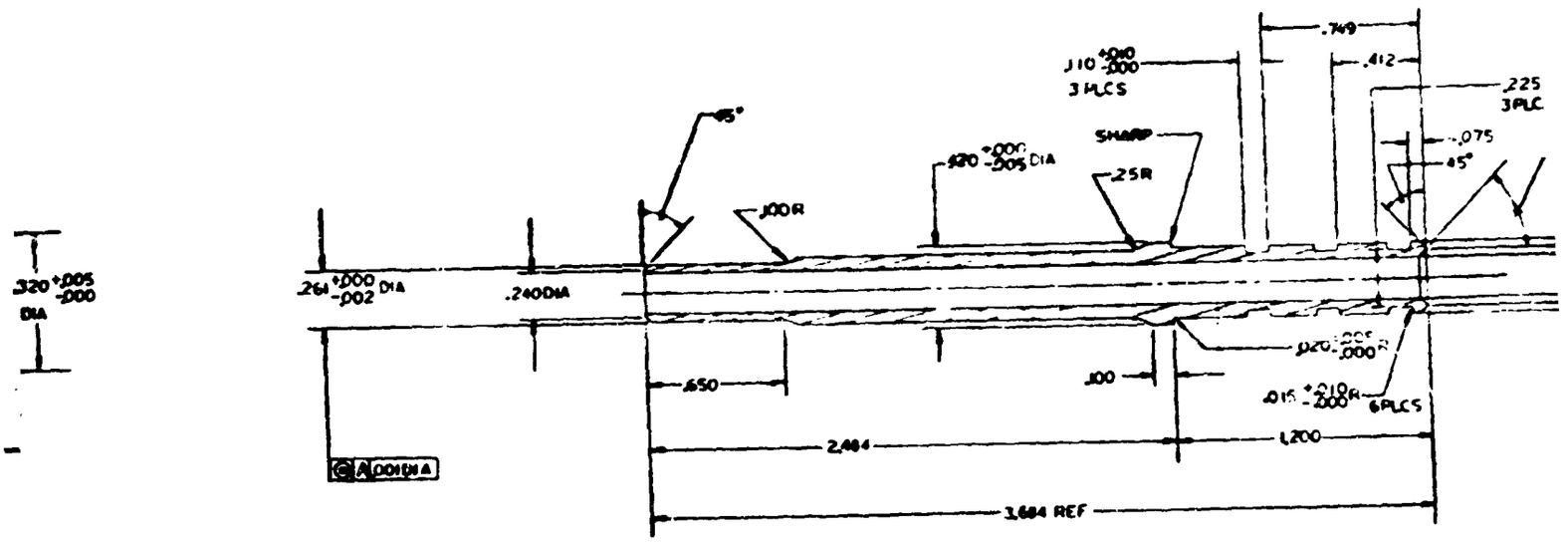

-003 POST
SCALE 4X

(13) PROOF PRESSURE TEST ASSY IN A HAZARD
(MIL-P 27407) AT 1950±40 PSIG. MAINTAIN PROOF
TO ZERO, REPEAT FOR A TOTAL OF 5 TIMES.
CALCULATED BURST PRESSURE AT

(12) MIN TENSILE STRENGTH 55,000 PSI MIN YIEL
(11) PENETRANT INSPECT PER RA0115-116 TYPE
(10) APPLY DRY FILM LUBRICATION TO THREADS
(9) IDENTIFY PER RA0104-008, TAG ONLY.
(8) CLEAN AND HANDLE FOR OXYGEN SERVICE
(7) WELD PER RA0107-027.
(6) LEAK TEST WITH HELIUM (MIL-P-27407 REF)
FOR 5 MINUTES. NO LEAKAGE ALLOWED.
(5) NICKEL EMBRITTLEMENT CONTROL PER RA

(4) BRAZE PER RA0107-010 AT 1950±10°F WITH
(3) NICKEL FLASH TUBE OD PRIOR TO BRAZING.
2. CLEAN DETAILS PER RA0110 016 BEFORE (3).
1. MACHINE PER RA0103-016.

FOLDOUT FRAME 5

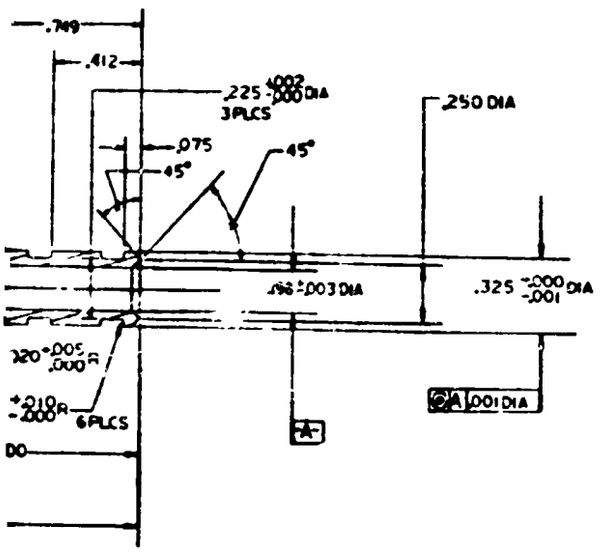

Figure 34. 40K Igniter Assembly

RE TEST ASSY IN A HAZARD TEST CELL AT 70°±20°F WITH HELIUM
1950±40 PSIG. MAINTAIN PROOF PRESSURE FOR 2 MINUTES. REDUCE
AT FOR A TOTAL OF 5 TIMES. NO LEAKAGE ALLOWED.
ATED BURST PRESSURE AT 70°F = 14,575 PSI.

STRENGTH 55,000 PSI, MIN YIELD STRENGTH 15,000 PSI, 40% ELONGATION IN 4D.
INSPECT PER RA0115-116 TYPE 1b.
M LUBRICATION TO THREADS PER RA0112-003, TYPE I.
RA0104-008, TAG ONLY.
ANDLE FOR OXYGEN SERVICE PER RA0110-004.
A0107-027.
H HELIUM (MIL-P-27407 REF) AT 70°±20°F AND 100 ±10 PSIG
NO LEAKAGE ALLOWED.
TTLEMENT CONTROL PER RA0102-004.

A0107-010 AT 1950±10°F WITH RBO 170-160 (PALNIRO 7)
TUBE OD PRIOR TO BRAZING .0002 TO .0004 PER AA1109-005.
PER RA0110 016 BEFORE (3) AND (10).
RA0103-016.

71/72

DASH NO	MATL	SIZE	SPECIFICATION
-001			
-013	NICKEL	3/16 OD X .035 WALL	ASTM B161
-009	321 TUBE	3/16 OD X .035 WALL	MIL-T-8808 TYPE I
-007	304	MAKE FROM MS24392 J4	RP825-3001
-005	NICKEL 200	NOTED	ASTM B160 NICKEL (12)
-003	316L BAR	NOTED	QQ-S-763 CLASS 316L COND A

NOTED

NOTED

40K
IGNITER ASSY

J 02602 AP79-029

The design of the igniter assembly was controlled by the utilization of existing 40K hardware, i.e., the LOX dome. The igniter tube is attached to the injector body and to the LOX dome with Swageloks. One modification was made to the design in that the Swagelok in the injector body is welded in place, thus eliminating a possible leak path.

Injector Body Assembly. The injector body is machined from 304L CRES plate and utilizes a 316 CRES grayloc inlet flange. 304L CRES was selected for the body because of its welding and brazing properties. The fuel manifold is welded to the main portion of the body and forms a constant cross-sectional area passage. This passage feeds 16 fuel ports which are drilled between the thrust chamber bolt holes. Once the fuel passes through these ports, it flows around the LOX tubes and into the LOX sleeve orifices, etc. Some of the fuel passes through the porous face to keep the face cool. It should be noted that the entire fuel flow field is designed for low fuel velocities, which results in most of the system pressure drop being taken in the injector element.

Hot-Firing Configuration. The LOX dome rework configuration is illustrated in Fig. 35. The final welding of the LOX inlet will be accomplished during field installation since the assembly is being mounted into an existing configuration. To this end, all of the existing interfaces have been maintained with the exception of the fuel inlet, which had to be increased in size.

The thrust mount is illustrated in Fig. 35. It is fabricated from T1-U.S. steel plate. It is designed to facilitate the installation and removal of any of the hot-firing components.

The hot-firing configuration itself is depicted in Fig. 33. Metal, static seals are used at all joints. Between the faceplate assembly and the combustion chamber, a piston ring seal (contraction seal) is used. The use of the piston ring seal allows the injector element cup depth to be altered between firings, if so desired.

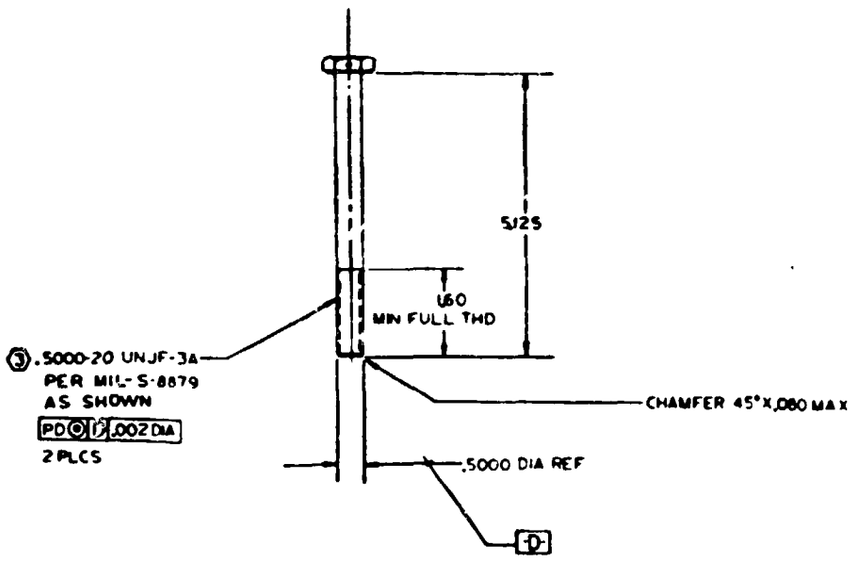

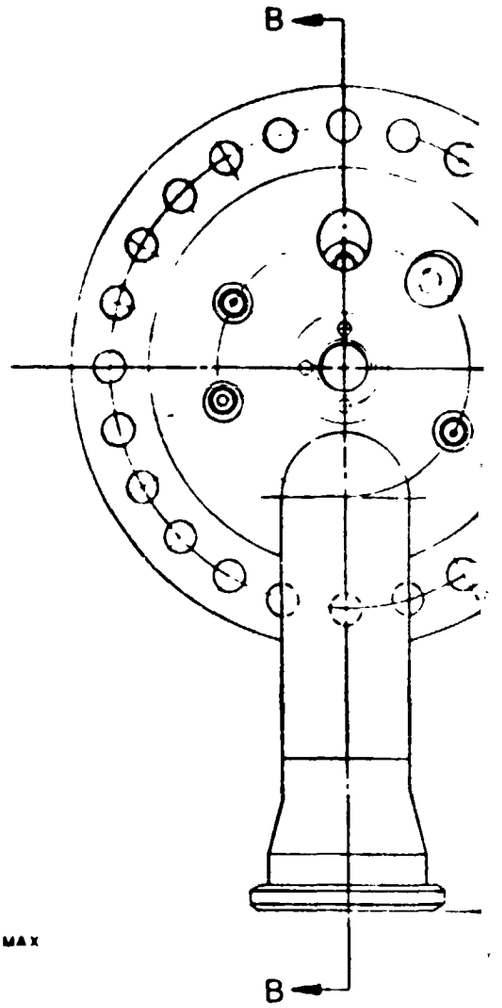

FOLDOUT FRAME

-007 BOLT

SOLDOUT FRAME 2

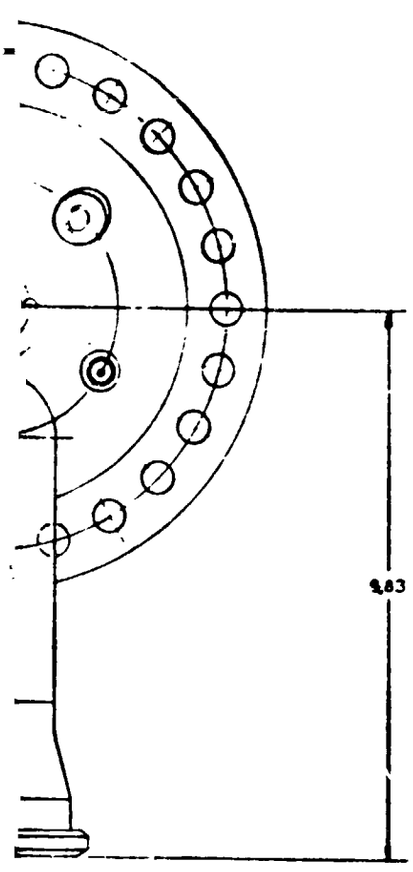

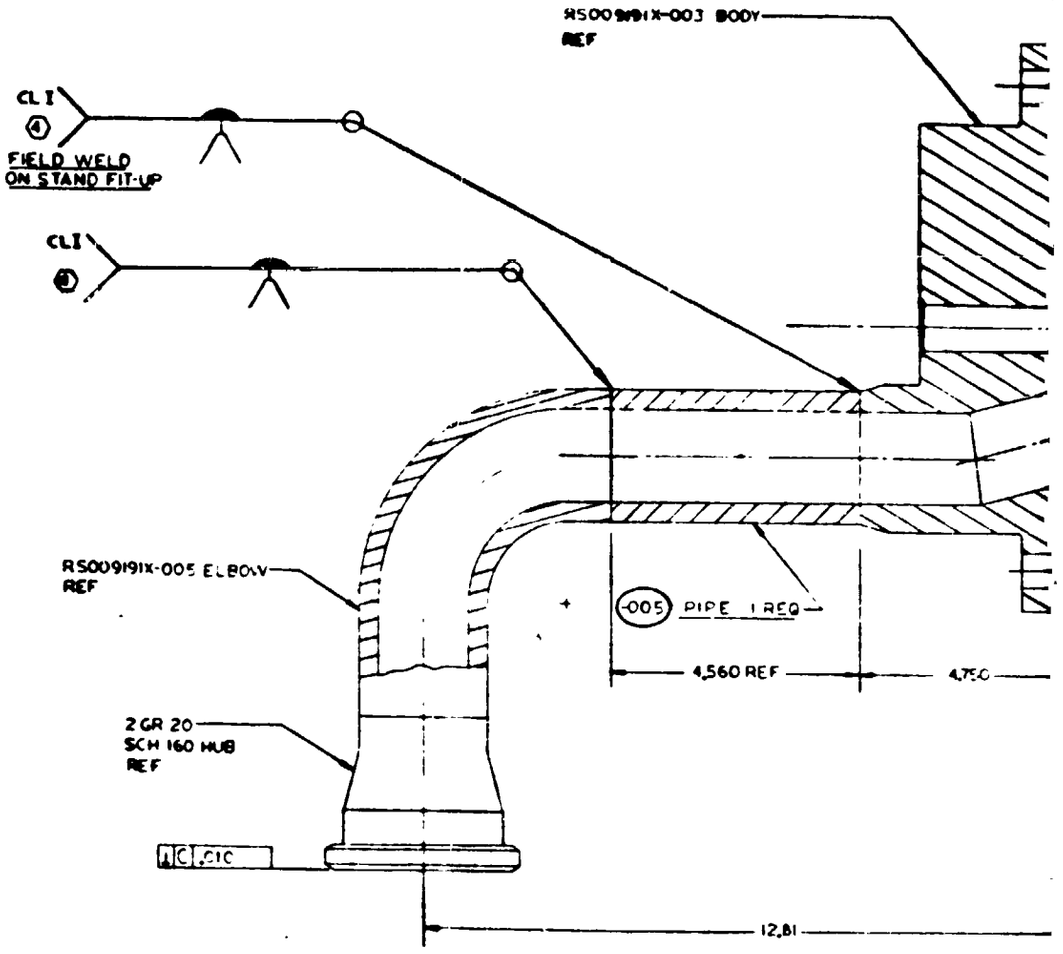

SECTION B-B

-001 LOX DOME ASSY 2 5 6

15 14 13 12 11 10

INSTALL AMERICAN SAFTY HOIST RING (11)
ADB 23002
TORQUE 25 FT-LB
2 PLCS

FOLDOUT FRAME 3

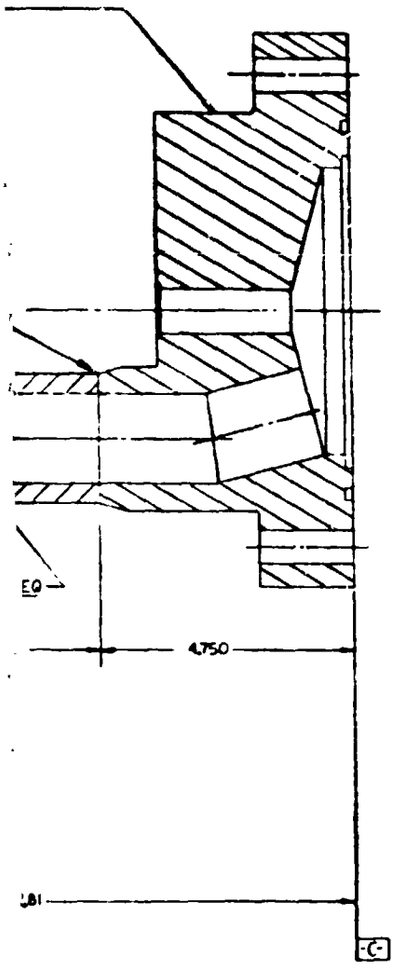

13.000 DIA

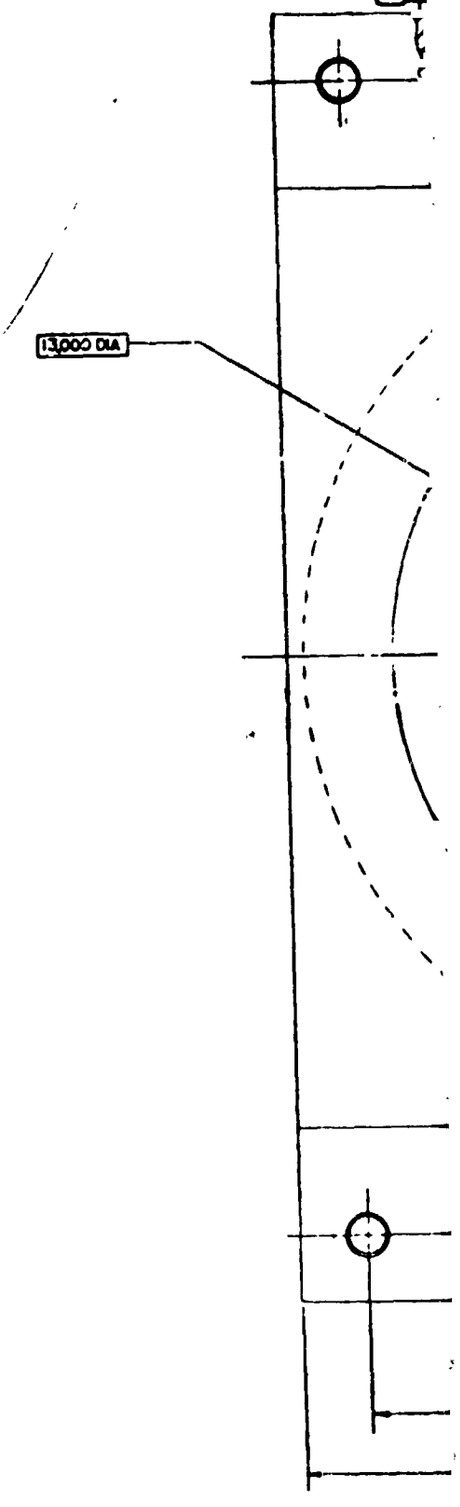

Y (2) (5) (6)

15 14 13 12 11

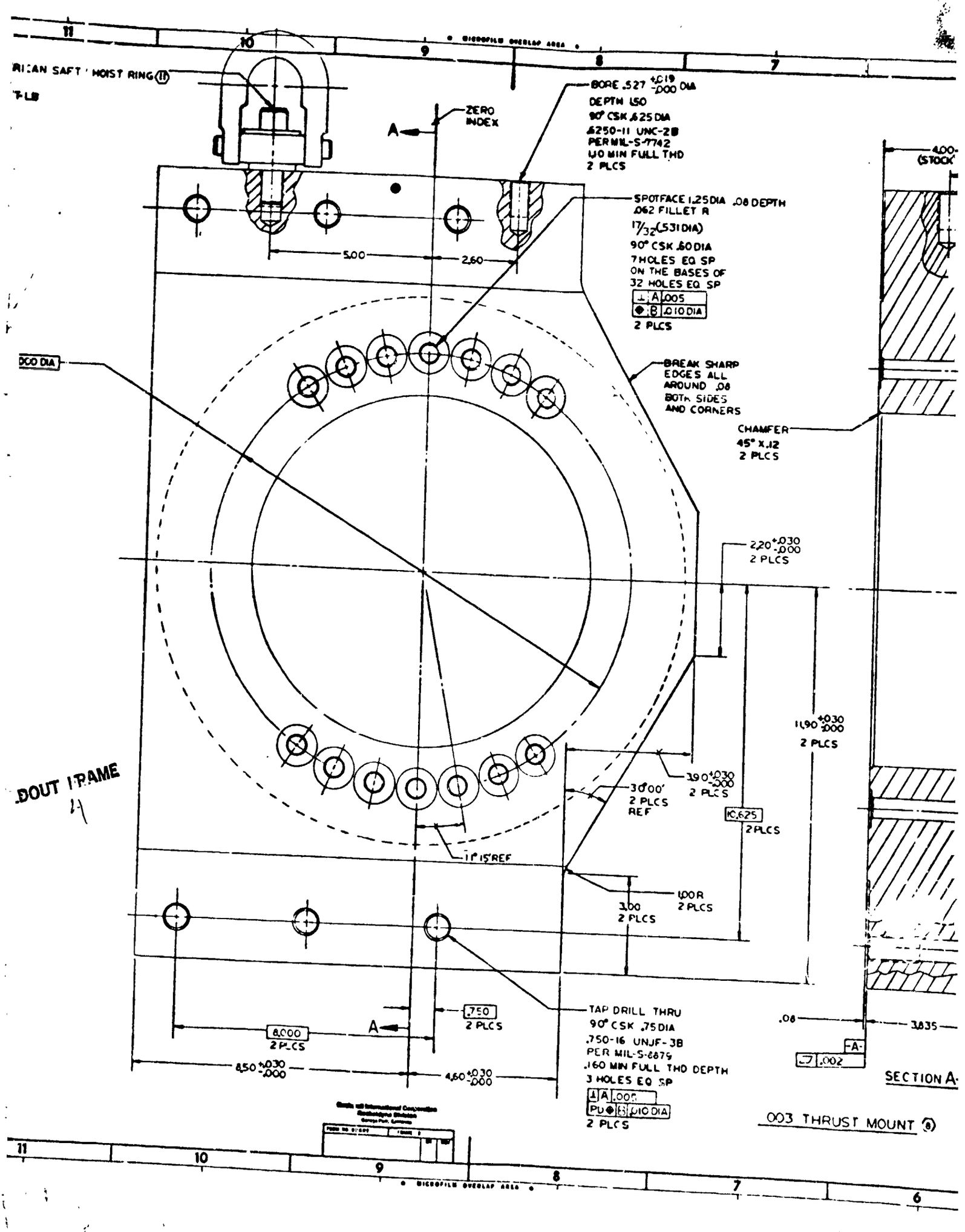
BORE .527 +.019 -.000 DIA
DEPTH 1.50
90° CSK .625 DIA
.6250-11 UNC-2B
PER MIL-S-7742
1.0 MIN FULL THD
2 PLCS
ZERO INDEX
A
SPOTFACE 1.25 DIA .08 DEPTH
.062 FILLET R
17/32 (.531 DIA)
90° CSK .60 DIA
7 HOLES EQ SP
ON THE BASES OF
32 HOLES EQ SP
⊥ A .005
⌖ B .010 DIA
2 PLCS
5.00
2.60
BREAK SHARP
EDGES ALL
AROUND .08
BOTH SIDES
AND CORNERS
CHAMFER
45° X .12
2 PLCS
4.00
(STOCK)
2.20 +.030 -.000
2 PLCS
11.90 +.030 -.000
2 PLCS
3.90 +.030 -.000
2 PLCS
30°00'
2 PLCS
REF
Ø.625
2 PLCS
11°15' REF
1.00 R
2 PLCS
3.00
2 PLCS
.750
2 PLCS
8.000
2 PLCS
8.50 +.030 -.000
4.60 +.030 -.000
TAP DRILL THRU
90° CSK .75 DIA
.750-16 UNJF-3B
PER MIL-S-8879
.160 MIN FULL THD DEPTH
3 HOLES EQ SP
⊥ A .005
PU ⌖ B .010 DIA
2 PLCS
.08
3.835
-A-
⊥ .002
SECTION A-
003 THRUST MOUNT 8
DOUT FRAME
11
10
9
8
7
6

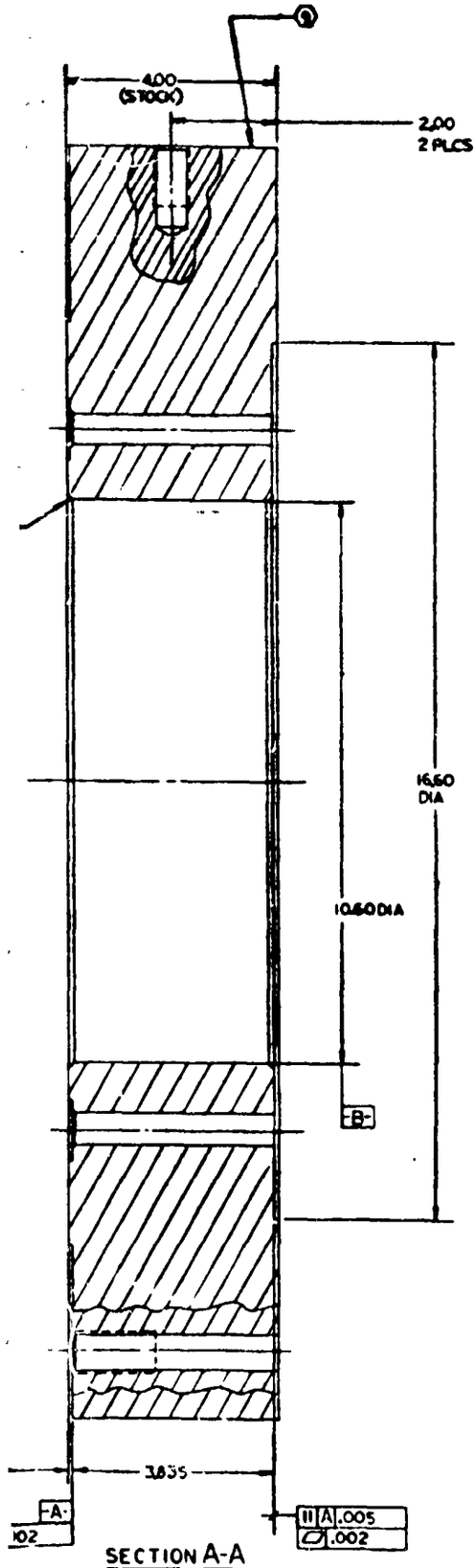

SECTION A-A

RUST MOUNT ⑨

:SOLDOUT FRAME

Figure 35. 40K Thrust Mour
Dome Modificat.

⑪ AMERICAN DRILL BUSHING.
2000 CAMFIELD AVE.,CITY OF COMMERCE, CAL.(727-1515)

⑩ PAINT PER RA0108-012 COLOR 15045 PER FED-STD-595.

⑨ IDENTIFY PER RA0104-008, IMPRESSION STAMP.

⑧ PHOSPHATE TREAT PER TT-C-490, METHOD IV, TYPE I (RA0109-002 TYPE II). ⑩

⑦ MATERIAL PROPERTIES
MIN YIELD 72000 PSI, MIN ULTIMATE TENSILE 90000 PSI.
MIN ELONGATION 12% IN 4D.

⑥ LEAK TEST WITH DRY NITROGEN(GN_2) AT 100±10 PSIG UNDER WATER. NO LEAKAGE ALLOWED. (5 MINUTES MIN).

⑤ PROOF PRESSURE TEST WITH DEIONIZED WATER AT 5400±100 PSIG. MAINTAIN PROOF PRESSURE FOR 2 MINUTES. REPEAT FOR A TOTAL OF 5 CYCLES IN A HAZARD TEST CELL.
CALCULATED BURST PRESSURE AT 70°F = 14,000 PSI.

④ WELD PER RA0107-027.

③ APPLY DRY FILM LUBRICATION TO THREADS PER RA0112-003, TYPE I.

② CLEAN PER RA0110-018.

① MACHINE PER RA0103-016.

75/76

DASH NO.	MATL	SIZE	SPECIFICAT.
-007	A286	MAKE FROM NAS1008-90H	
-005	321 PIPE	2 IPS SCH 160	ASTM A31
-003	TI-U.S. STEEL PLATE	NOTED	ASTM ASI
-001			

NOTED

NOTED

40K THF
AND LOX D

J 02602 A

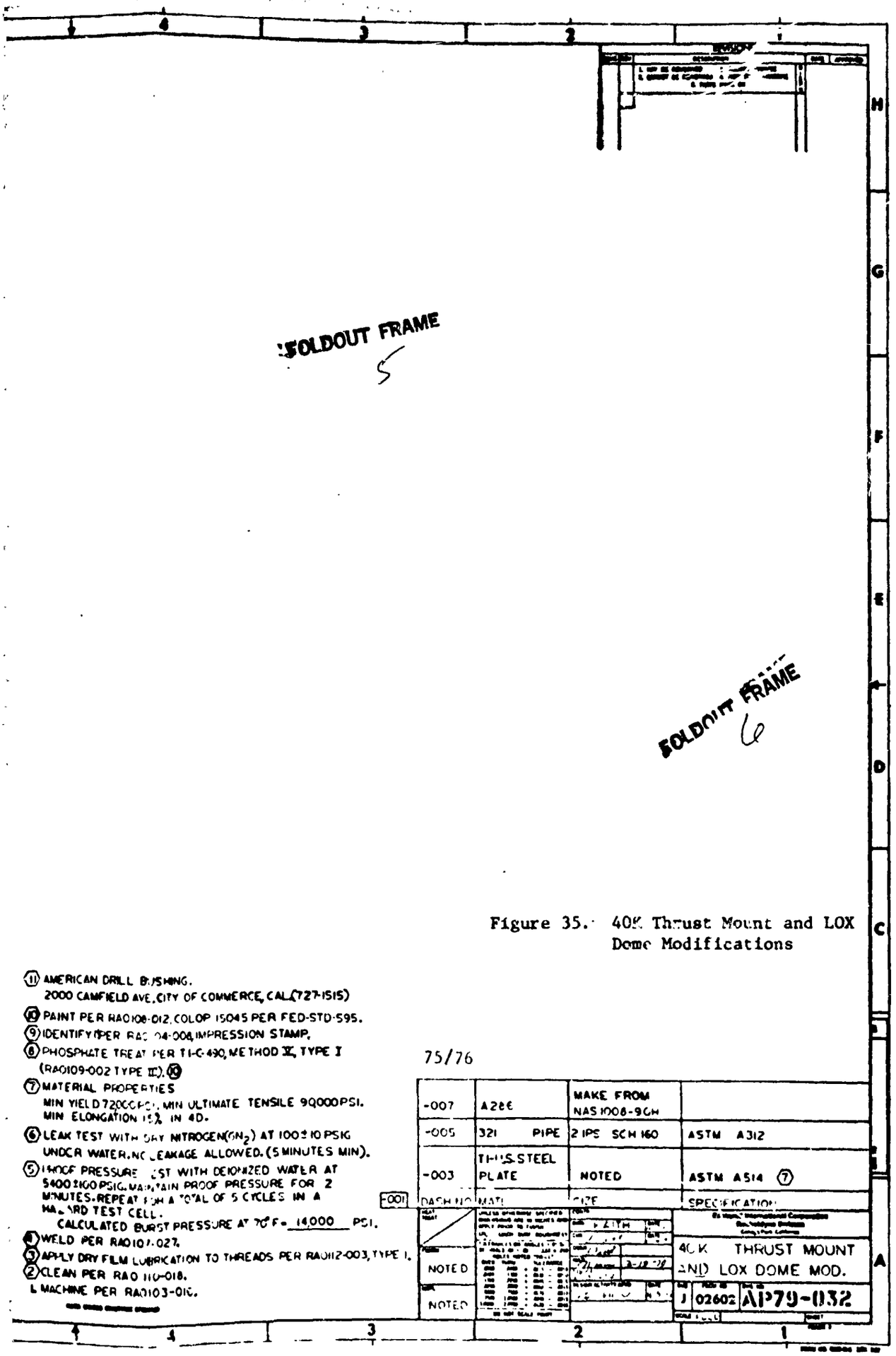

Figure 35. 40K Thrust Mount and LOX Dome Modifications

The injector has the capability to provide an acoustic absorber at its periphery by machining some material from the outer surface of the faceplate supporting ring as shown in Fig. 36. The cavity is tuned to 5400 Hz, with an open area measured approximately 10% of the injector face area. The predicted chamber first tangential mode is 5200 Hz. Slight detuning may occur if the gas temperature in the absorber exceeds 50% of the chamber equilibrium temperature. However, based on experience, absorber open area is a more significant parameter and 10% open area will provide adequate damping.

Fabrication Description

Fabrication of the faceplate assembly, the injector body assembly, the thrust mount, and the igniter tube, as well as the modification to the LOX dome, was accomplished by Rocketdyne. The oxidizer post assembly, the igniter post, and the igniter sleeve were purchase parts. The post brazing and final assembly was also completed by Rocketdyne.

Figure 37 is the faceplate assembly. The ring was rough machined, then the faceplate was EB welded into the ring. A welding backup ring was required. The backup ring was later removed during final machining. The piston ring sealing surface was ground to size.

Figures 38 and 39 show the injector body assembly. The fuel manifold and the 16 feed ports were machined prior to welding the assembly. The center cavity was machined after the welds were proof pressure tested. This sequence eliminated a proof pressure plate.

The hex on a Swageloc was removed, the Swageloc threaded into the body, then welded in place.

Figure 40 is the oxidizer post. The bores in the posts are gun drilled. The oxidizer posts are designed to extend above the upstream face of the body in case a leak seal braze cycle is required.

The completed injector assembly is shown in Fig. 41.

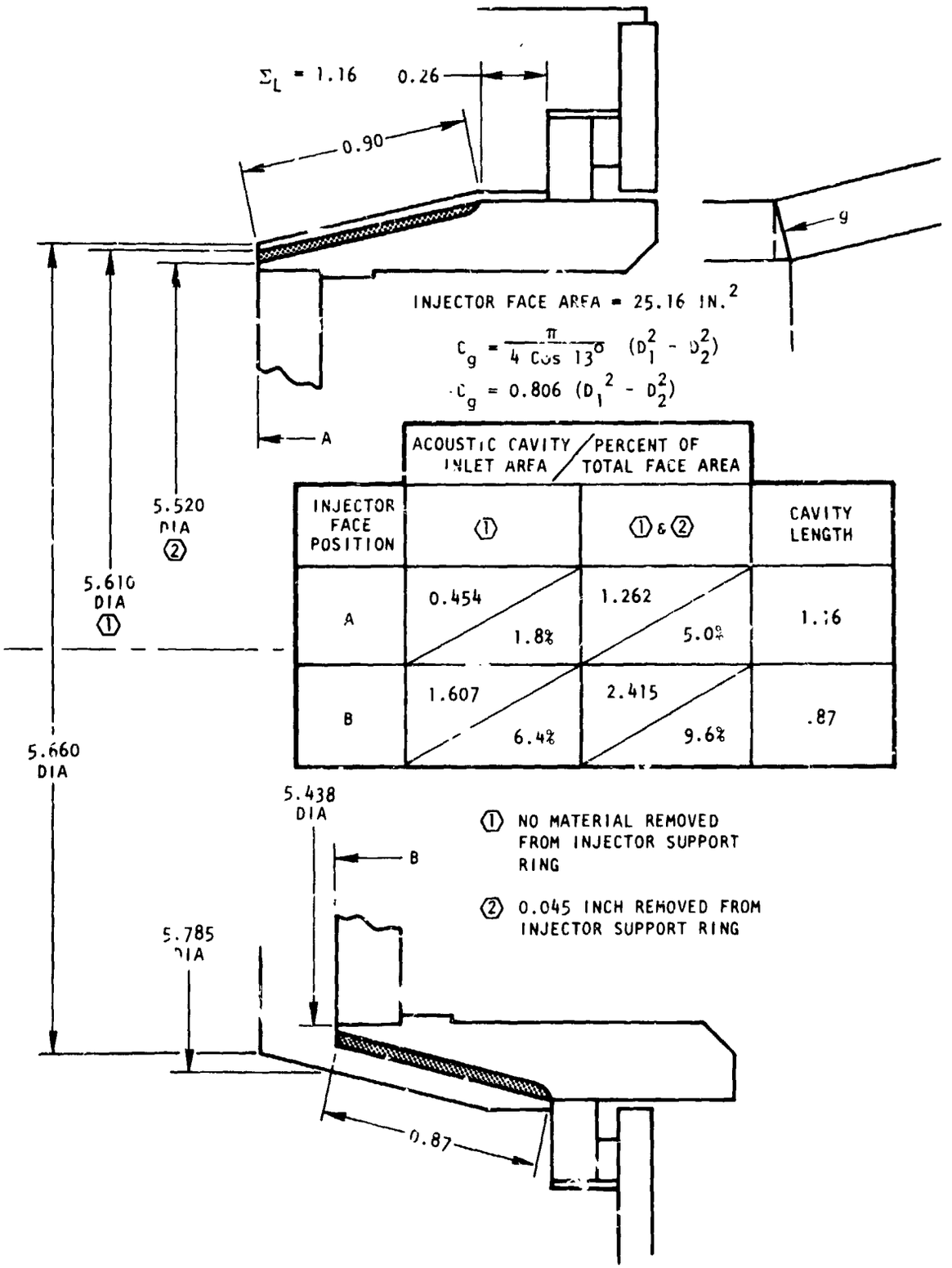

INJECTOR FACE POSITION	ACOUSTIC CAVITY / PERCENT OF INLET AREA / TOTAL FACE AREA ①	① & ②	CAVITY LENGTH
A	0.454 / 1.8%	1.262 / 5.0%	1.16
B	1.607 / 6.4%	2.415 / 9.6%	.87

Figure 36. Acoustic Absorber Capability

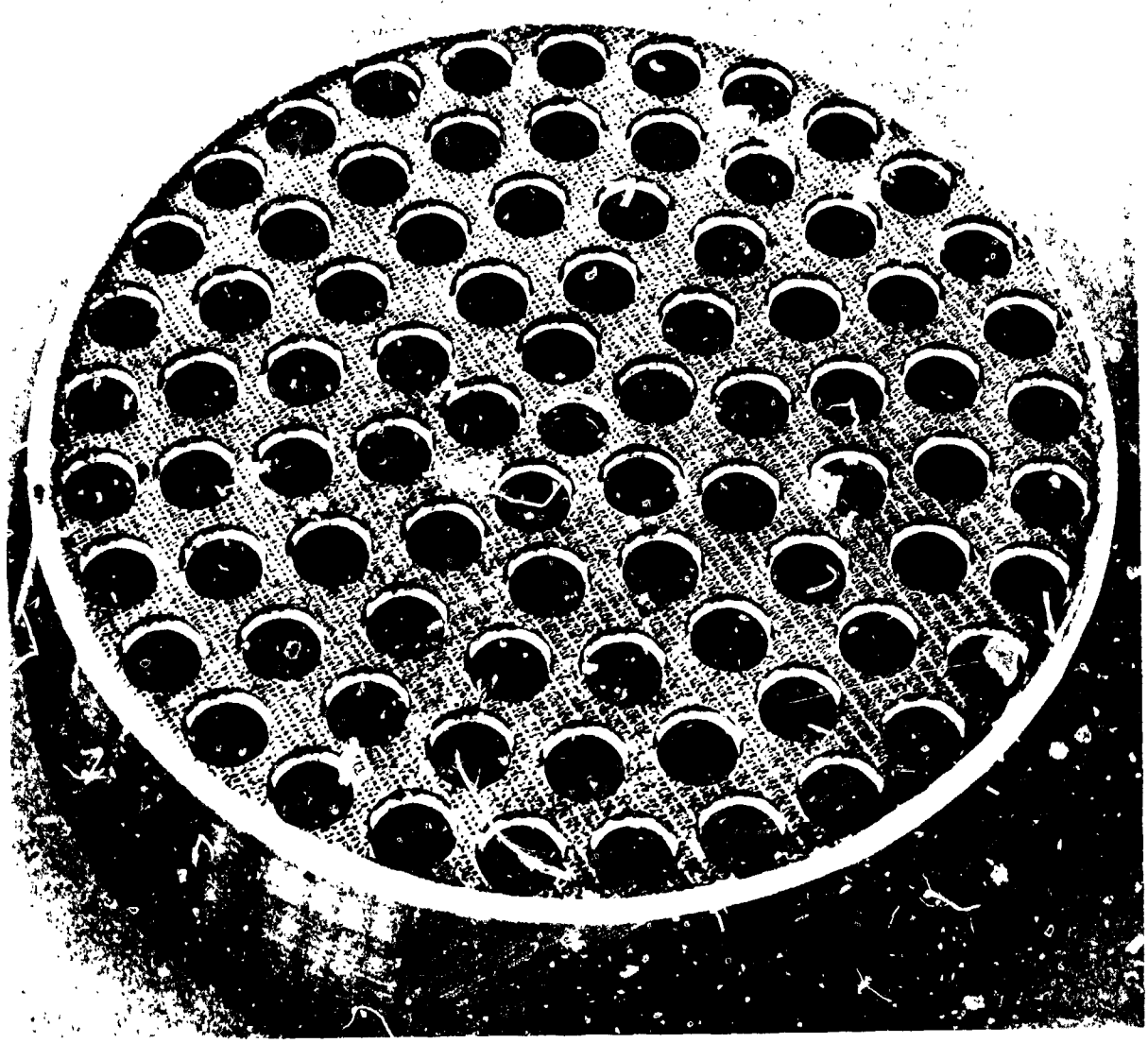

1XX42-8/10/79-C1G

Figure 37. Injector Face Assembly

1XX42-8/10/79-C1F

Figure 38. Injector Body (Rear View)

C-2

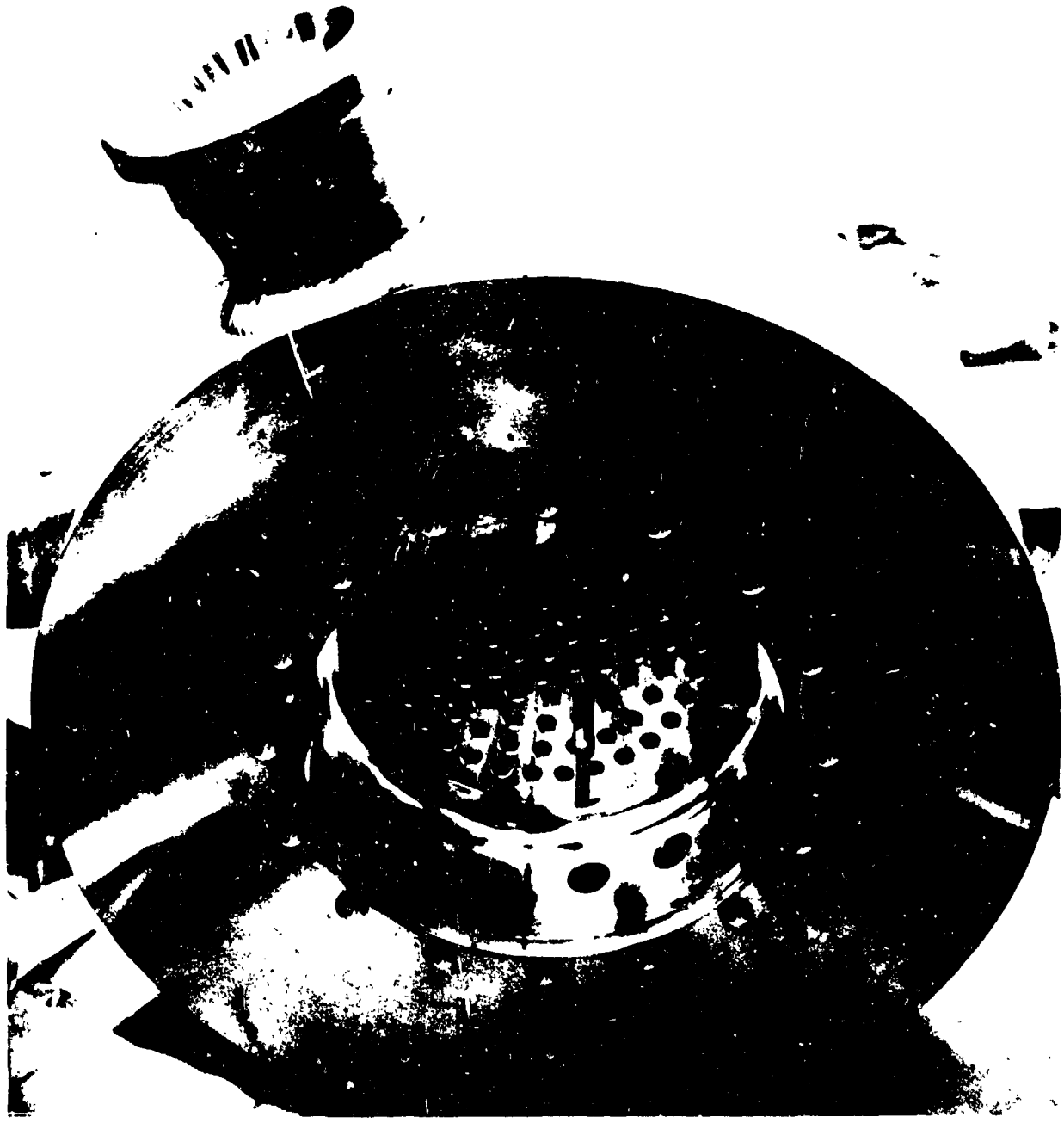

1XX42-8/10/79-C1E

Figure 39. Injector Body (Front View)

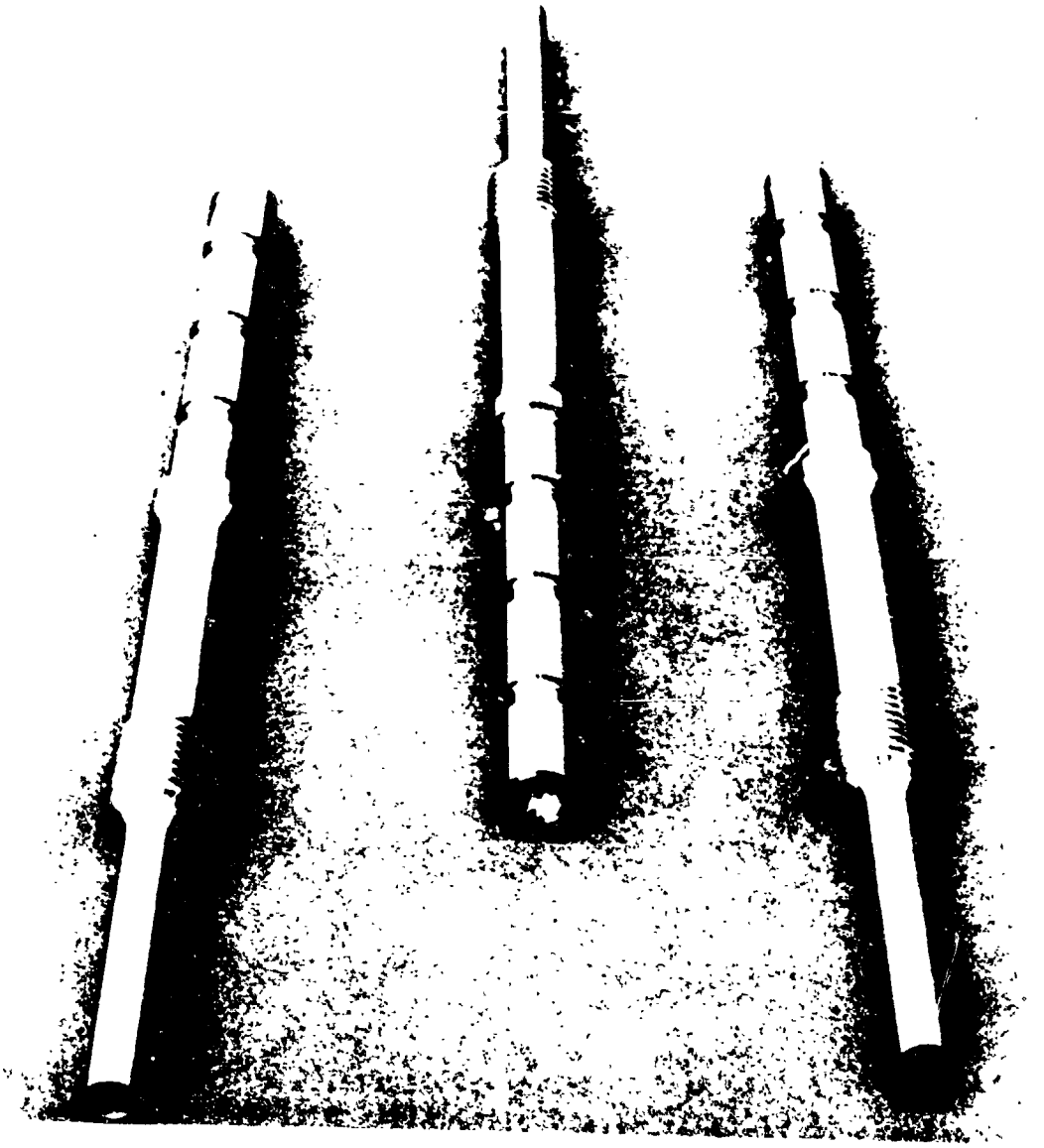

1XX42-8/10/79-C1D

Figure 40. Oxidizer Post

1XX45-11/2/79-C1B

Figure 4. Injector Assembly

SUMMARY

Based on the results of the Task I performance, stability, and heat transfer analysis, the coaxial injector concept was selected for the LOX/CH_4 application. In Task II the detailed design of the injector was accomplished and the injector was fabricated.

The injector has 82 coaxial elements. A ridgimesh face material was used to provide adequate face cooling and permit low operating face temperatures. The injector incorporates several unique features that permit easy changes in the injector operating parameters. The injector face can be moved in or out axially by adjusting the injector post sleeve height. In this way, the oxidizer post recess depth can be adjusted from zero to a depth equal to twice the oxidizer post diameter. In addition, the fuel annulus gap and, thus, the fuel injection velocity and ΔP, can be adjusted by changing the face nut. These features also will permit the easy repair or replacement of the injector parts in case of damage.

REFERENCES

1. Burick, R. J., Space Storage Propellant Performance Program Coaxial Injector Characterization, NASA CR-120936, October 1972.

2. R-7338, Space Storable Regenerative Cooling Investigation - Interim Report, NASA CR-72360, Rocketdyne Division, Rockwell International, 25 September 1968.

3. R-7475, Advanced Engine Aerospike Experimental Program - Interim Report, NAS8-20349, Rocketdyne Division, Rockwell International, 15 July 1968.